Supporting Information

Atroposelective Synthesis of Aldehydes via Alcohol Dehydrogenase Catalyzed Stereodivergent Desymmetrization

Mengjing Ye[a, b, #], Congcong Li[b, c, #], Dongguang Xiao[a], Ge Qu[b, c], Bo Yuan[b, c, *], Zhoutong Sun[b, c, *]

[a]School of Biological Engineering, Tianjin University of Science and Technology, Tianjin 300457, China

[b]Tianjin Institute of Industrial Biotechnology, Chinese Academy of Sciences, Tianjin 300308, China

[c]Key Laboratory of Engineering Biology for Low-Carbon Manufacturing, Chinese Academy of Sciences, 32 West 7th Avenue, Tianjin Airport Economic Area, Tianjin 300308, China

*Corresponding authors. Email addresses: yuanb@tib.cas.cn (B. Yuan); sunzht@tib.cas.cn (Z. Sun).

Table of Contents

1. General information

All chemicals were purchased from Sigma-Aldrich, Bide Pharmatech Ltd., Shanghai Macklin Biochemical Co., or Anhui Zesheng Technology Co., Ltd. and used without further purification unless otherwise stated.

HPLC analysis was performed on a Shimadzu system equipped with an LC-40B XR binary pump, SIL-40C autosampler unit, SPD-40V diode array detector, and CTO-40C temperature-controlled column oven.

NMR spectra were recorded on a Bruker AVANCE III 400 MHz NMR spectrometer (Bruker Biospin, Germany, 7.47 μs 90 pulses, 1.00 s relaxation delay and 16 scans) in $CDCl_3$, tetramethylsilane (TMS; δ = 0.00 ppm) was used as the internal standard for ^1H NMR. The solvent signal ($CDCl_3$, δ = 77.00 ppm) was used as an internal standard for ^{13}C NMR.

2. Preparation of alcohol dehydrogenases

2.1 General information of alcohol dehydrogenases

2.1.1 Gene information of alcohol dehydrogenases

Enzyme	PDB ID	Expression of gene	GenBank	Source	Ref
ADH-R1	/	NAD(P)-dependent short-chain alcohol dehydrogenase	WP_013688875.1	*Burkholderia gladioli*	1
ADH-R2	4BMS	*Ras*-ADH/ NADP-dependent alclohol dehydrogenase/short-chain dehydrogenase	EU485985.1	*Ralstonia sp.*	2
ADH-R3	4RF2	*R*-specific alcohol dehydrogenase	WP_054768785.1	*Lactobacillus kefiri*	3
ADH-R4	/	3-beta-hydroxysteroid dehydrogenase	KGO31568.1	*Oenococcus alcoholitolerans*	4
ADH-R5	/	alcohol dehydrogenase	WP_011241052.1	*Zymomonas mobilis*	5
ADH-R6	/	zinc-dependent alcohol dehydrogenase	WP_003252433.1	*Parageobacillus thermoglucosidasius*	6
ADH-R7	2D1Y	alcohol dehydrogenase	WP_011172461.1	*Thermus thermophilus*	7
ADH-R8	/	NAD-dependent alcohol dehydrogenase	WP_011158613.1	*Rhodopseudomonas palustris*	8
ADH-R9	/	*S*-(hydroxymethyl) glutathione dehydrogenase	WP_011425488.1	*Rhizobium etli*	9
ADH-R10	/	L-threonine dehydrogenase	WP_044345496.1	*Pseudomonas meliae*	10

Table S1. General information of alcohol dehydrogenases.

2.1.2 Protein sequence information of alcohol dehydrogenases

ADH-R1:
MSKRLEGKVALVTGGTSGIGLATAKDLAAQGARVIITGRRQAELDQAVAALGQGVR
GVRSDVTRSADLDALFETIRATEGRLDVLFTNAGGGSMAALGEISEQHFDDTFERNV
KAVVFTVQKALPLMPQGASIILNGSIAGSTGTQAFSIYGASKAAVRALARSWVLDLK

ERGIRVNVVSPGSTRTIGLAELGGDTQEGQDGLLAYLASLVPIGRLADPSEIAKVVSFL
ASDDSSFINGAEITADGGQAQV

ADH-R2:
MYRLLNKTAVITGGNSGIGLATAKRFVAEGAYVFIVGRRRKELEQAAAEIGRNVTAV
KADVTKLEDLDRLYAIVREQRGSIDVLFANSGAIEQKTLEEITPEHYDRTFDVNVRGL
IFTVQKALPLLRDGGSVILTSSVAGVLGLQAHDTYSAAKAAVRSLARTWTTELKGRSI
RVNAVSPGAIDTPIIENQVSTQEEADELRAKFAAATPLGRVGRPEELAAAVLFLASDD
SSYVAGIELFVDGGLTQV

ADH-R3:
MTDRLKGKVAIVTGGTLGIGLAIADKFVEEGAKVVITGRHADVGEKAAKSIGGTDVI
RFVQHDASDEAGWTKLFDTTEEAFGPVTTVVNNAGIAVSKSVEDTTTEEWRKLLSV
NLDGVFFGTRLGIQRMKNKGLGASIINMSSIEGFVGDPTLGAYNASKGAVRIMSKSA
ALDCALKDYDVRVNTVHPGYIKTPLVDDLEGAEEMMSQRTKTPMGHIGEPNDIAWI
CVYLASDESKFATGAEFVVDGGYTAQ

ADH-R4:
MVDRLKGKVAIVTGGTLGIGLSIVDLYLKEGAKVVFTGRRENVGKKAYQDLGSPKN
AKFVVHDAADEEGWKKLFADTIAEFGKVDILVNNAGIGVPGNVENTDYAQWRQTM
DVNLDGVYLGTHYGVINMKNPQSGDASIINMSSIEGLVGDPNLFAYNATKGALRIMS
KSAAIYCANQDYNLRINTIHPGYIKTPLVDKIQGAEEMMSQRTKTPMGHVGVPDDIG
WLAVYLGSEESKFATGAEFTVDGGYTAQ

ADH-R5:
MKAAVITKDHTIEVKDTKLRPLKYGEALLEMEYCGVCHTDLHVKNGDFGDETGRIT
GHEGIGIVKQVGEGVTSLKVGDRASVAWFFKGCGHCEYCVSGNETLCRNVENAGYT
VDGAMAEECIVVADYSVKVPDGLDPAVASSITCAGVTTYKAVKVSQIQPGQWLAIY
GLGGLGNLALQYAKNVFNAKVIAIDVNDEQLAFAKELGADMVINPKNEDAAKIIQE
KVGGAHATVVTAVAKSAFNSAVEAIRAGGRVVAVGLPPEKMDLSIPRLVLDGIEVLG
SLVGTREDLKEAFQFAAEGKVKPKVTKRKVEEINQIFDEMEHGKFTGRMVVDFTHH

ADH-R6:
MKAAVVEQFKEPLKIKEVEKPSISYGEVLVRIKACGVCHTDLHAAHGDWPVKPKLPL
IPGHEGVGIVEEVGPGVTHLKVGDRVGIPWLYSACGHCEYCLSGQETLCEHQENAGY
SVDGGYAEYCRAAADYVVKIPDNLSFEEAAPIFCAGVTTYKALKVTGTKPGEWVAI
YGIGGLGHVAVQYAKAMGLHVVAVDIGDEKLELAKELGADLVVNPAKENAAQFM
KEKVGGVHAAVVTAVSKPAFQSAYNSIRRGGTCVLVGLPPEEMPIPIFDTVLNGIKIIG
SIVGTRKDLQEALQFAAEGKVKTIIEVQPLEKINEVFDRMLKGEINGRVVLTLENNN

ADH-R7:
MGLFAGKGVLVTGGARGIGRAIAQAFAREGALVALCDLRPEGKEVAEAIGGAFFQV
DLEDERERVRFVEEAAYALGRVDVLVNNAAIAAPGSALTVRLPEWRRVLEVNLTAP
MHLSALAAREMRKVGGGAIVNVASVQGLFAEQENAAYNASKGGLVNLTRSLALDL

APLRIRVNAVAPGAIATEAVLEAIALSPDPERTRRDWEDLHALRRLGKPEEVAEAVLF
LASEKASFITGAILPVDGGMTASFMMAGRPV

ADH-R8:
MTQMRRQSLVKFDAPLCETIIDAPKPQGREVLVKIERCGLCHSDLHIQDGYADLGGG
KKLDTTRGMTLPFTLGHEIAGVVAEVGPDAPQDLIGTKKAVFPWIGCGKCRDCLAG
DENLCAKNRFLGVSIDGGFATHVLVPDAKYLLDYDPLPTNVAATLMCSGITAYGAL
KRLVDRPRQRNLLLIGLGGVGMMGLSLAQAMFKQPIAVADLSPAAREAALKNGAA
VAYDPSEPDVAKRIFKETDGGFDGVVDFAGNDKSMNFAVSTVARGGKIVVSGLMGG
QFSLPMVQWIYKRMTVEGFMVGTLEETKELLALARAGKVKPTPMKEEPMQDAQKW
IDQLRAGKVVGRIMLAN

ADH-R9:
MDVRAAVATQAGKPLEVMTVQLDGPKAGEVLVEVKATGICHTDDFTLSGADPEGLF
PAILGHEGAGIVVDVGPGVTSVKKGDHVIPLYTPECRECYSCTSRKTNLCTAIRATQG
QGVMPDGTSRFSIGKDKIHHYMGCSTFANYTVLPEIALAKINPDAPFDKVCYIGCGVT
TGIGAVINTAKVEVGSTAIVFGLGGIGLNVLQGLRLAGADMIIGVDINPDRKAWGEKF
GMTHFVNPKEVGDDIVPYLVNMTKRGGDLIGGADYTFDCTGNTKVMRQALEASHR
GWGKSVIIGVAGAGQEISTRPFQLVTGRNWMGTAFGGARGRTDVPKIVDWYMQGKI
QIDPMITHTMPLEDINTGFELMHKGESIRGVVVY

ADH-R10:
MISTFFIPAVNIIGTGCIDEAMLAIRKYGFLKALIVTDAGLAKAGVASQVAGLLVEQGI
DSVVYDGAKPNPTIANVENGLALLRERQCDFVISLGGGSPHDCAKGIALCASNGGHIS
DYEGVDRSAKPQLPLIAINTTAGTASEMTRFCIITDEARHVKMAIIDRNVTPLLSVNDP
NMMIAMPKSLTAATGMDALTHAIEAYVSTAANPITDACALQAMALIANNLRDAFTN
GANITARENMAYAQFLAGMAFNNASLGYVHAMAHQLGGFYDLPHGVCNAVLLPH
VQRFNASVSAARLTDVAHAMGCNIRGLSPQEGAQAAIEAIRALSAAVEIPAGLAVLG
VKEEDFPILATNALKDACGLTNPRRADFEQIQEIFRQAM

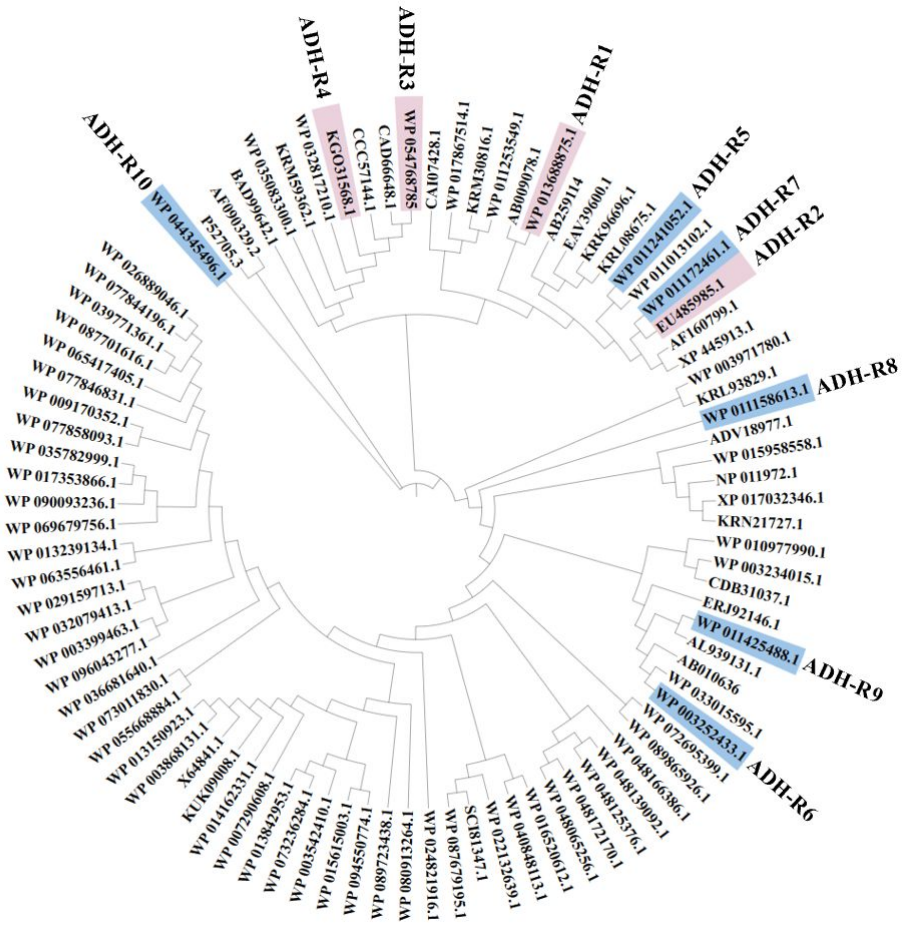

Figure S1. Phylogenetic analysis of alcohol dehydrogenases. The evolutionary tree was constructed in MEGA11.

2.2 Heterologous expression of alcohol dehydrogenases

2.2.1 Screening of enzyme library

Colonies were picked and incubated in 700 μL LB medium containing kanamycin (50 μg mL^{-1})/ampicillin (100 μg mL^{-1}), shaken in a 96-well plate at 180 rpm and cultured at 37 °C for 12 hours. Then, 300 μL of TB medium was added to a 96-well plate, and IPTG and kanamycin/ampicillin were added to make the final concentrations of 0.2 mM and 50 μg mL^{-1} /100 μg mL^{-1} respectively (TB medium, IPTG and antibiotics were pre-mixed and sub-packed), and the protein was cultured at 30 °C at 800 rpm for 16 h. The cell precipitate was collected and washed. The cell pellets were harvested and washed with 400 μL of 50 mM, pH 7.4 potassium phosphate buffer and centrifuged for 10 min with 4000 rpm at 4 °C. Then, 6 U mL^{-1} DNase I and 1 mg mL^{-1} lysozyme, 10 mM dialdehyde, 20 mM glucose, 2.5 mg mL^{-1} GDH, 1 mM $NADP^+$ and 5% DMSO were added to the 96-well plate and reacted at 30 °C at 800 rpm

for 24 hours. The remaining substrates and products were extracted with MTBE and analyzed by HPLC.

2.2.2 Heterologous expression and purification of alcohol dehydrogenase

The seed solution was streaked on an agar plate supplemented with kanamycin (50 μg mL^{-1})/ampicillin (100 μg mL^{-1}) for heterologous expression. Single colonies were picked and inoculated to LB broth cultures containing kanamycin (50 μg mL^{-1})/ampicillin (100 μg mL^{-1}) and incubate for 8 hours (37 °C, 220 rpm). The seed culture was then inoculated into 1 L of LB medium (1% v/v) containing kanamycin (50 μg mL^{-1}) / ampicillin (100 μg mL^{-1}). Cultures were incubated at 37 °C, 220 rpm, until OD_{600} reached 0.6-0.8, then induced by IPTG (0.1 mM). Further incubation was performed at 20 °C, 220 rpm. The cells were harvested by centrifugation (4000 rpm, 20 min, 4 °C), the supernatant was discarded, and cells were washed with NaPi buffer (50 mM, pH 7.4) and then disrupted by a sonicator (35% power, 3.0 sec pulse on, 4.0 sec pulse off, 15 min). The cells were then centrifuged, and the supernatant was obtained as the cell-free extract (CFE), which was stored at -80 °C until further use.

Protein purification was accomplished with AKTA pure equipped with a 5 mL His Trap ™ FF column pre-equilibrated with washing buffer. After loading with crude extract, the column was washed with 5 column volumes (CV) of washing buffer followed by protein elution with 3 CV of elute buffer. Subsequently, the collected protein samples were dialyzed into desalted solution at 4 ℃ for 12 hours, and then transferred to a flexible dialysis tube (10 kDa cut-off value). After SDS-PAGE analysis, protein samples were divided into equal parts and frozen in liquid nitrogen before storage at -80℃.

Buffer	Composition
Washing buffer	25 mM PBS, 30 mM iminazole, pH 7.4
Elute buffer	25 mM PBS, 500 mM iminazole, pH 7.4
Desalination solution	25 mM PBS, 5% glycerol , pH 7.4

Table S2. Buffer compositions used for protein purification.

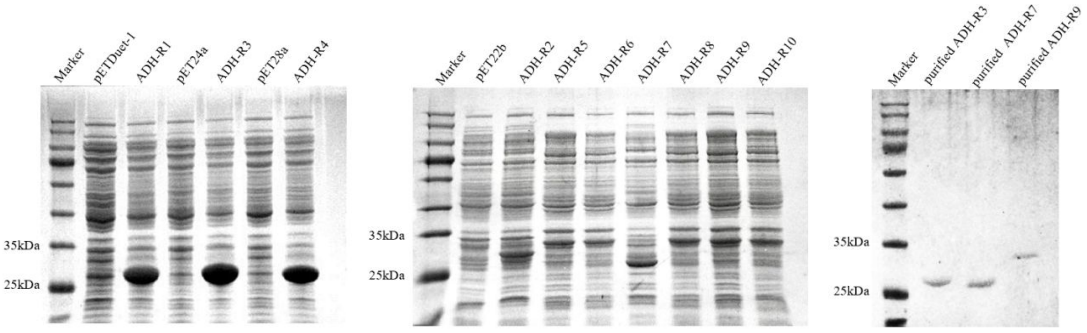

Figure S2. SDS-Page of crude and purified alcohol dehydrogenases. (Content of target enzymes: ADH-R1: 25.69%, ADH-R2: 10.65%, ADH-R3: 36.96%, ADH-R4: 28.29%, ADH-R5: 9.68%, ADH-R6: 10.71%, ADH-R7: 13.57%, ADH-R8: 9.90%, ADH-R9: 8.02%, ADH-R10: 9.77%, analyzed and estimated by Image J.)

3. Procedures for molecular docking simulations

The 3D structure of the substrate molecules were built and optimized using PyMOL.[11] Semi-flexible docking was performed using the Lamarckian Genetic Algorithm (LGA) implemented in AutoDock 4.2. In this docking approach, the receptor protein was considered rigid while the substrate molecules were allowed to be flexible. Each substrate was individually docked into the active site of ADH, and the low-energy substrate structures that satisfied the attacking criteria were selected to generate the complex structures. To visualize the results of molecular docking, Discovery Studio Visualizer[12] was employed to create a 2D interaction diagram that demonstrates the interactions between the protein and the small molecules.

In the case of (*R*)-**2h** and (*S*)-**2k**, the selectivity of ADH-R7, R9, and R10 are reversed due to change of interactions between the substrates and key residues of the activity pocket. For example, as shown in Figure S3, when **1h** and **1k** are docked into the activity site of R9, key interactions between **1h** and H62, M136, Y88, and between **1k** and C169, A319 are identified, which all contribute significantly to change of binding poses and final configuration of the products.

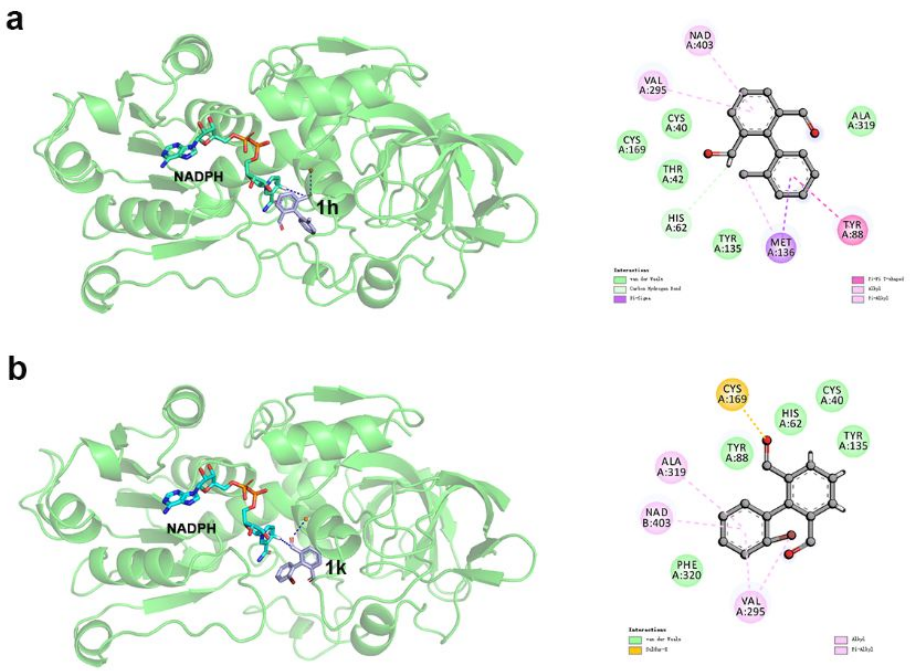

Figure S3. Docking models of (a) **1h** and (b) **1k** at ADH-R9.

4. Procedures for alcohol dehydrogenases catalyzed desymmetrization of biaryl dialdehydes

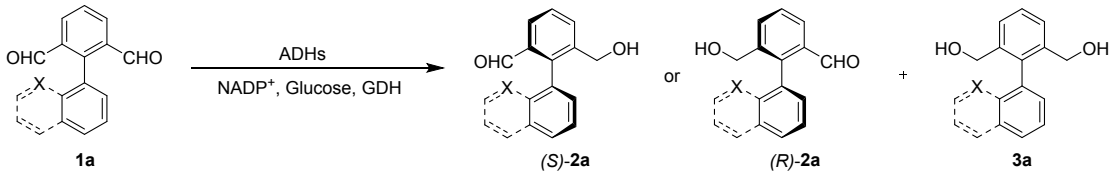

1a *(S)*-**2a** *(R)*-**2a** **3a**

For analytical scale reactions, the dialdehyde was dissolved in DMSO (400 mM stock solution). Subsequently, 10 mM **1a**, 1 mM $NADP^+$, 20 mM glucose, 2.5 mg mL^{-1} GDH, ADHs (0.1 g mL^{-1} whole cell with 6 U mL^{-1} DNase I and 1 mg mL^{-1} lysozyme) were added to a 2 mL Eppendorf tube with DMSO (5% v/v) in NaPi buffer (pH 7.4, 50 mM) to reach 1 mL final volume, and then incubated at 30 °C, 800 rpm. At intervals, aliquots were taken, extracted with tert-butyl methyl ether (extraction ratio = 1:2), dried over anhydrous sodium sulfate, and the organic phase was analyzed by high performance liquid chromatography (HPLC).

For upscaled reactions, the dialdehyde was dissolved in DMSO (400 mM stock solution). Subsequently, 10 mM **1a**, 1 mM $NADP^+$, 20 mM glucose, 2.5 mg mL^{-1} GDH, ADHs (100 mL crude enzyme) were added to a 500 mL round bottom flask with DMSO (5% v/v) in NaPi buffer (pH 7.4, 50 mM) to reach a 200 mL final volume, and then incubated at 30 °C, 800 rpm. We used HPLC to detect the reaction regularly and found that the conversion rate approached 90% when the reaction lasted for 6 hours. The mixture was extracted with ethyl acetate (400 mL, 3 times), the organic phases were combined, saturated NaCl was added and then extracted with ethyl acetate again. Dried over Na_2SO_4 and evaporated under reduced pressure. Flash column chromatography was performed to obtain monoaldehyde product (PE: EA=2:1).

The absolute configuration of the monoaldehyde product **2a** was determined by comparing the elution orders of the HPLC peaks for **2a** (Figure S19) with reference to previous reports,[13] where same HPLC conditions were employed (Chiralpak® AD-H, eluents: n-hexane/i-PrOH = 90:10).

5. Supplementary figures

conv/ %	1	2	3	4	5	6	7	8	9	10	11	12
A	6	12	16	0	6	37	**65 (R1)**	20	57	11	**74 (R2)**	63
B	33	**78 (R5)**	**84 (R6)**	**79 (R7)**	**78 (R8)**	**81 (R9)**	32	**78(R10)**	56	33	48	6
C	11	13	9	9	9	**32 (R3)**	12	4	4	9	8	13
D	10	7	12	6	13	12	7	8	10	8	6	8
E	9	13	6	10	14	8	10	6	5	8	4	6
F	**96 (R4)**	10	10	17	9	11	10	8	6	11	7	11
G	6	14	15	17	14	10	18	14	8	13	10	9
H	18	7	7	13	10	10	9	11	30	12	23	28

Table S3. A heatmap representative of ADHs screen of **1a** for conversions (%, determined by HPLC). A deeper red color represents a higher conversion. Reaction conditions: **1a** (10 mM), DMSO (5 %), $NADP^+$ (1 mM), glucose (20 mM) and GDH (2.5 mg mL^{-1}), ADHs (0.1 g mL^{-1} whole cell), DNase I (6 U mL^{-1}) and lysozyme (1 mg mL^{-1}), in phosphate buffer (50 mM), 30 °C, 24 h, 800 rpm, final volume: 0.5 mL (A1: blank; A2: pET22b; A3: pET28a; C4: pET24a).

ee / %	1	2	3	4	5	6	7	8	9	10	11	12
A	99 *(R)*	99 *(R)*	99 *(R)*	0	93 *(S)*	92 *(S)*	55 *(R)*	57 *(S)*	81 *(S)*	67 *(S)*	96 *(R)*	87 *(S)*
B	95 *(R)*	86 *(S)*	94 *(S)*	92 *(S)*	93 *(S)*	95 *(S)*	96 *(R)*	92 *(S)*	75 *(S)*	18 *(S)*	74 *(S)*	84 *(S)*
C	92 *(S)*	90 *(S)*	91 *(S)*	91 *(S)*	93 *(S)*	41 *(R)*	40 *(S)*	78 *(S)*	78 *(S)*	50 *(S)*	50 *(S)*	96 *(S)*
D	92 *(S)*	90 *(S)*	94 *(S)*	89 *(S)*	94 *(S)*	95 *(S)*	89 *(S)*	91 *(S)*	95 *(S)*	91 *(S)*	88 *(S)*	90 *(S)*
E	70 *(S)*	93 *(S)*	88 *(S)*	68 *(S)*	94 *(S)*	91 *(S)*	92 *(S)*	87 *(S)*	90 *(S)*	92 *(S)*	80 *(S)*	86 *(S)*
F	96 *(R)*	10 *(R)*	10 *(R)*	17 *(R)*	9 *(R)*	11 *(R)*	10 *(R)*	8 *(R)*	6 *(R)*	11 *(R)*	7 *(R)*	11 *(R)*
G	6 *(R)*	14 *(R)*	15 *(R)*	17 *(R)*	14 *(R)*	10 *(R)*	18 *(R)*	14 *(R)*	8 *(R)*	13 *(R)*	10 *(R)*	9 *(R)*
H	18 *(R)*	7 *(R)*	7 *(R)*	3 *(R)*	10 *(R)*	10 *(R)*	9 *(R)*	11 *(R)*	30 *(R)*	12 *(R)*	23 *(R)*	28 *(R)*

Table S4. A heatmap representative of ADHs screen of **1a** for *ee* (%, determined by HPLC). A deeper red color represents a higher *ee*. Reaction conditions: **1a** (10 mM), DMSO (5 %), $NADP^+$ (1 mM), glucose (20 mM) and GDH (2.5 mg mL^{-1}), ADHs (0.1 g mL^{-1} whole cell), DNase I (6 U mL^{-1}) and lysozyme (1 mg mL^{-1}), in phosphate buffer (50 mM), 30 °C, 24 h, 800 rpm, final volume: 0.5 mL.

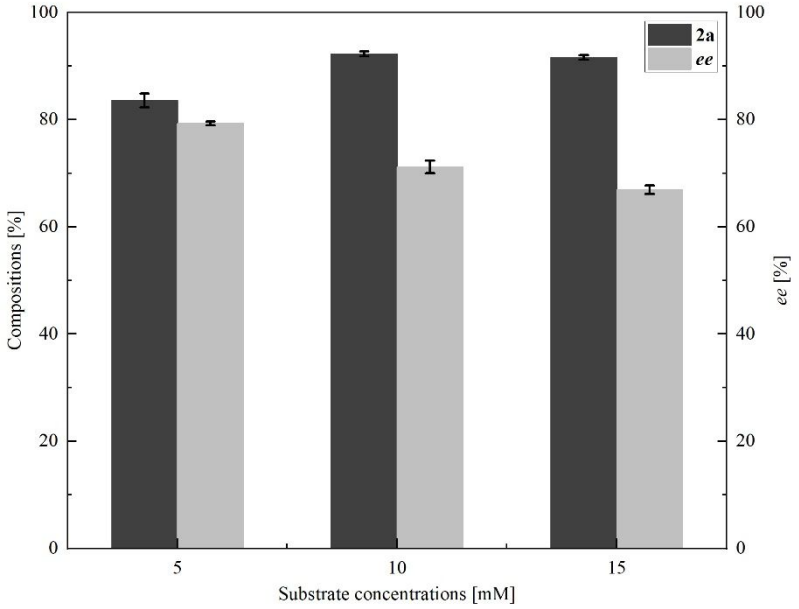

Figure S4. The reduction of **1a** catalyzed by ADH-R1 under various substrate concentrations. Reaction conditions: **1a** (5 mM -15 mM), DMSO (5 %), ADH-R1 (0.1 g mL^{-1} whole cell with 6 U mL^{-1} DNase I and 1 mg mL^{-1} lysozyme), $NADP^+$ (1 mM), glucose (20 mM) and GDH (2.5 mg mL^{-1}), in phosphate buffer (50 mM), 30 °C, 2 h, 800 rpm, final volume: 1.0 mL.

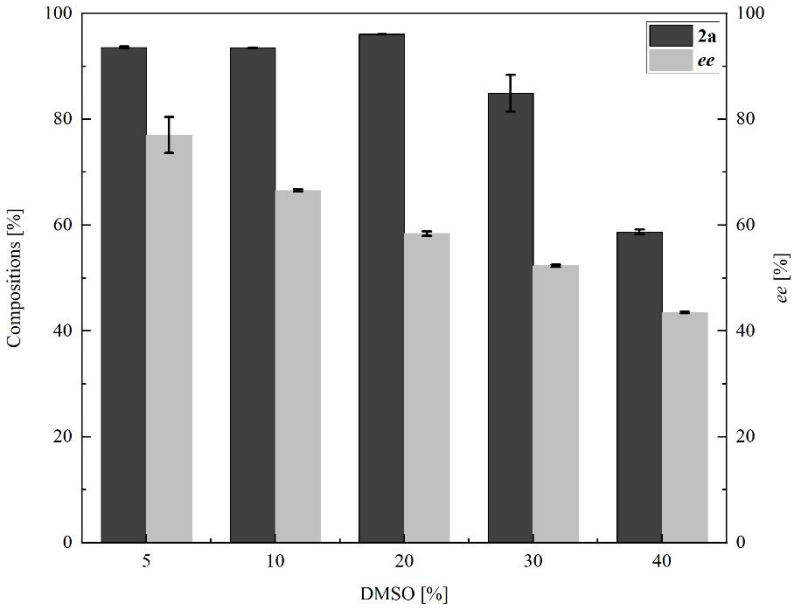

Figure S5. The reduction of 1a catalyzed by ADH-R1 under various DMSO. Reaction conditions: **1a** (10 mM), DMSO (5 % - 40 %), ADH-R1 (0.1 g mL^{-1} whole cell with 6 U mL^{-1} DNase I and 1 mg mL^{-1} lysozyme), $NADP^+$ (1 mM), glucose (20 mM) and GDH (2.5 mg mL^{-1}), in phosphate buffer (50 mM), 30 °C, 2 h, 800 rpm, final volume: 1.0 mL.

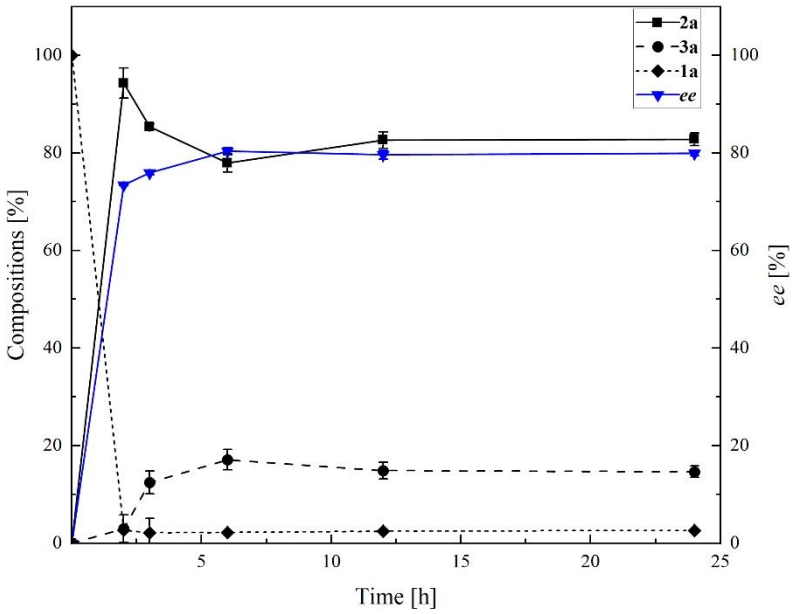

Figure S6. Time-course profiles for the reduction of **1a** catalyzed by ADH-R1. Reaction conditions: **1a** (10 mM), DMSO (5 %), ADH-R1 (0.1 g mL^{-1} whole cell with 6 U mL^{-1} DNase I and 1 mg mL^{-1} lysozyme), $NADP^+$ (1 mM), glucose (20 mM) and GDH (2.5 mg mL^{-1}), in phosphate buffer (50 mM), 30 °C, 800 rpm, final volume: 1.0 mL.

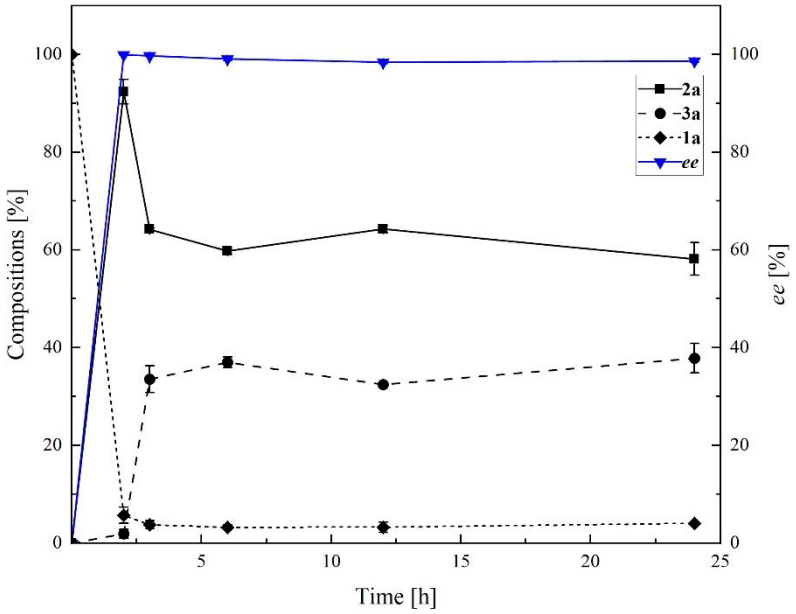

Figure S7. Time-course profiles for the reduction of **1a** catalyzed by ADH-R2. Reaction conditions: **1a** (10 mM), DMSO (5 %), ADH-R2 (0.1 g mL^{-1} whole cell with 6 U mL^{-1} DNase I and 1 mg mL^{-1} lysozyme), $NADP^+$ (1 mM), glucose (20 mM) and GDH (2.5 mg mL^{-1}), in phosphate buffer (50 mM), 30 °C, 800 rpm, final volume: 1.0 mL.

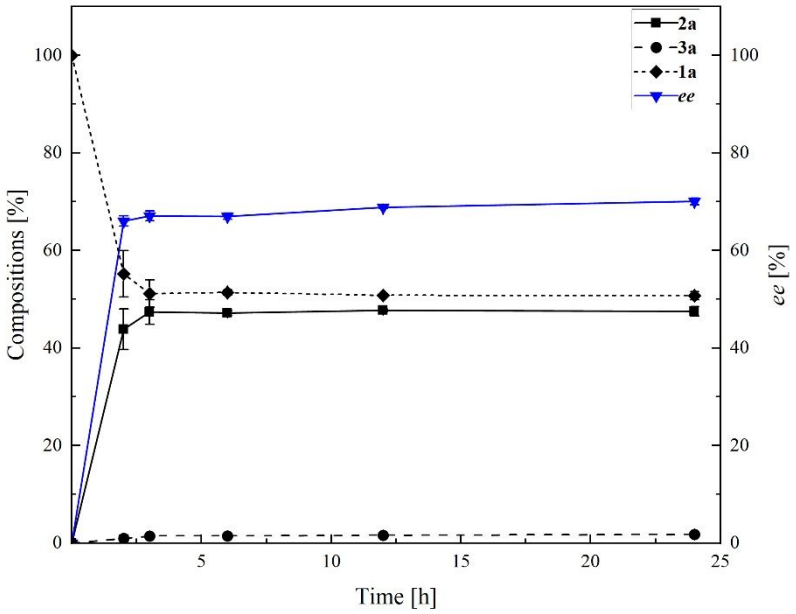

Figure S8. Time-course profiles for the reduction of **1a** catalyzed by ADH-R3. Reaction conditions: **1a** (10 mM), DMSO (5 %), ADH-R3 (0.1 g mL^{-1} whole cell with 6 U mL^{-1} DNase I and 1 mg mL^{-1} lysozyme), $NADP^+$ (1 mM), glucose (20 mM) and GDH (2.5 mg mL^{-1}), in phosphate buffer (50 mM), 30 °C, 800 rpm, final volume: 1.0 mL.

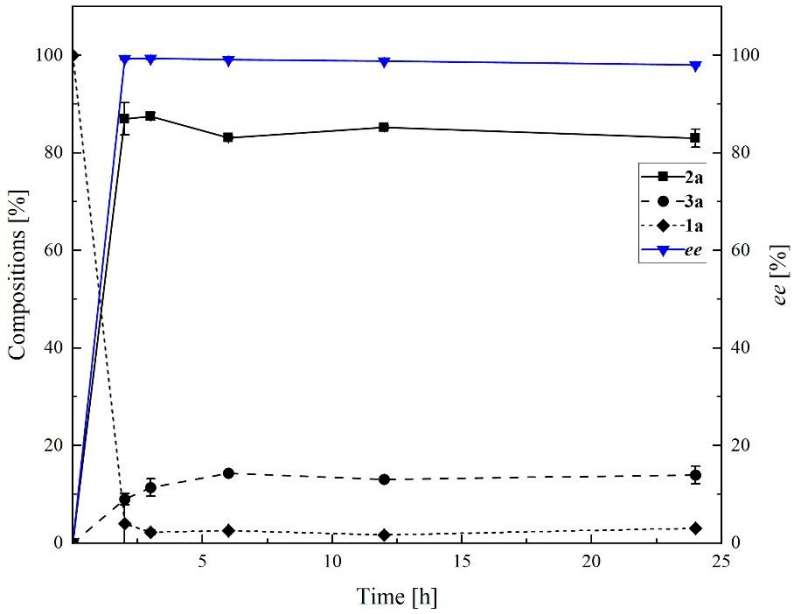

Figure S9. Time-course profiles for the reduction of **1a** catalyzed by ADH-R4. Reaction conditions: **1a** (10 mM), DMSO (5 %), ADH-R4 (0.1 g mL^{-1} whole cell with 6 U mL^{-1} DNase I and 1 mg mL^{-1} lysozyme), $NADP^+$ (1 mM), glucose (20 mM) and GDH (2.5 mg mL^{-1}), in phosphate buffer (50 mM), 30 °C, 800 rpm, final volume: 1.0 mL.

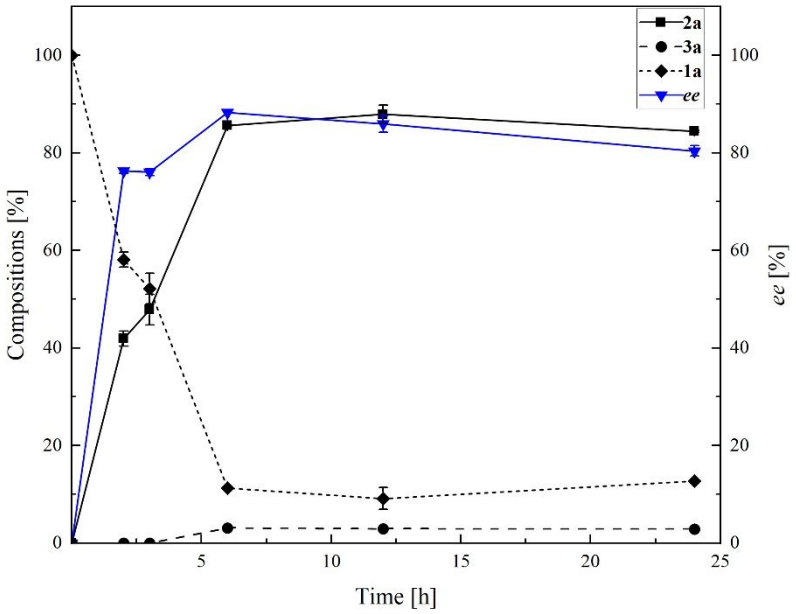

Figure S10. Time-course profiles for the reduction of **1a** catalyzed by ADH-R5. Reaction conditions: **1a** (10 mM), DMSO (5 %), ADH-R5 (0.1 g mL^{-1} whole cell with 6 U mL^{-1} DNase I and 1 mg mL^{-1} lysozyme), $NADP^+$ (1 mM), glucose (20 mM) and GDH (2.5 mg mL^{-1}), in phosphate buffer (50 mM), 30 °C, 800 rpm, final volume: 1.0 mL.

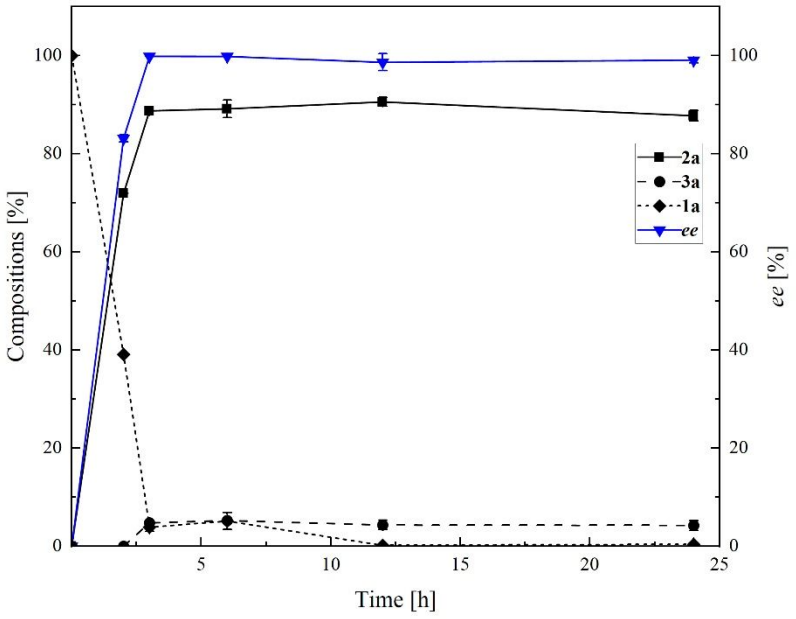

Figure S11. Time-course profiles for the reduction of **1a** catalyzed by ADH-R6. Reaction conditions: **1a** (10 mM), DMSO (5 %), ADH-R6 (0.1 g mL^{-1} whole cell with 6 U mL^{-1} DNase I and 1 mg mL^{-1} lysozyme), $NADP^+$ (1 mM), glucose (20 mM) and GDH (2.5 mg mL^{-1}), in phosphate buffer (50 mM), 30 °C, 800 rpm, final volume: 1.0 mL.

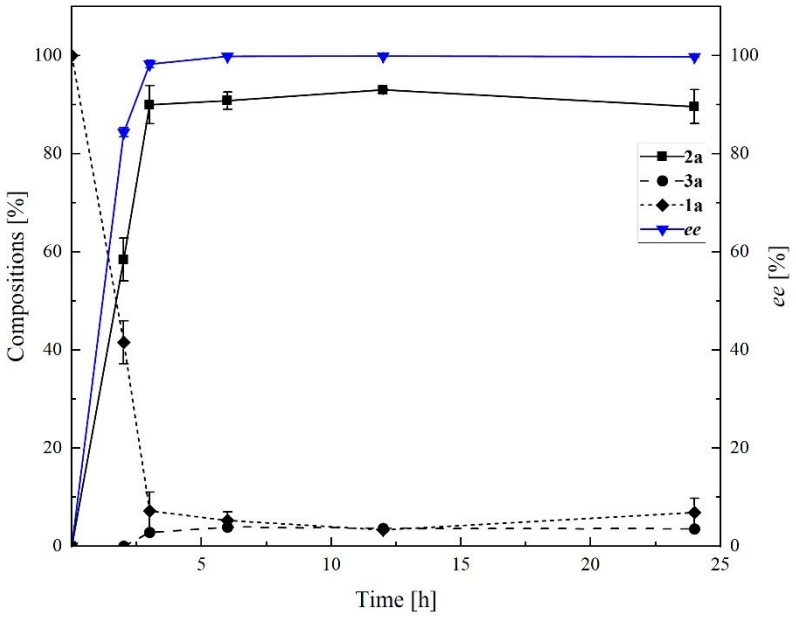

Figure S12. Time-course profiles for the reduction of **1a** catalyzed by ADH-R7. Reaction conditions: **1a** (10 mM), DMSO (5 %), ADH-R7 (0.1 g mL^{-1} whole cell with 6 U mL^{-1} DNase I and 1 mg mL^{-1} lysozyme), $NADP^+$ (1 mM), glucose (20 mM) and GDH (2.5 mg mL^{-1}), in phosphate buffer (50 mM), 30 °C, 800 rpm, final volume: 1.0 mL.

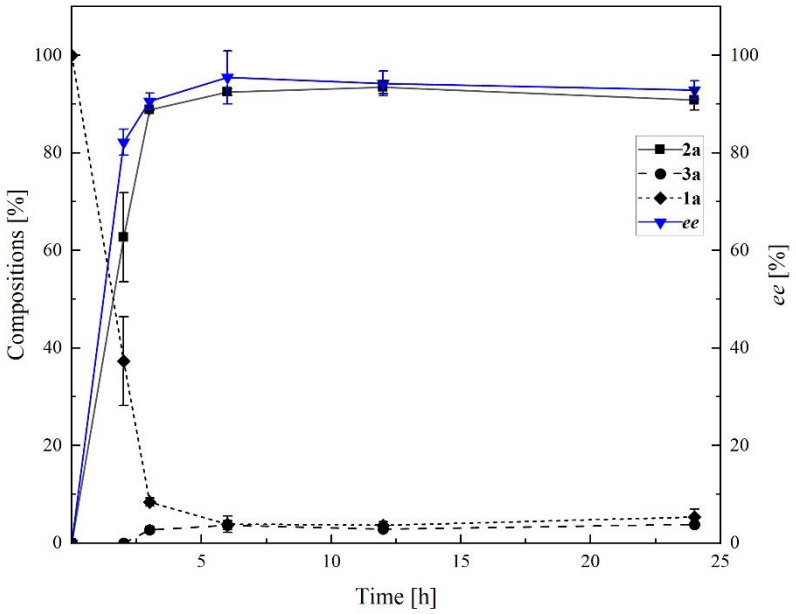

Figure S13. Time-course profiles for the reduction of **1a** catalyzed by ADH-R8. Reaction conditions: **1a** (10 mM), DMSO (5 %), ADH-R8 (0.1 g mL^{-1} whole cell with 6 U mL^{-1} DNase I and 1 mg mL^{-1} lysozyme), $NADP^+$ (1 mM), glucose (20 mM) and GDH (2.5 mg mL^{-1}), in phosphate buffer (50 mM), 30 °C, 800 rpm, final volume: 1.0 mL.

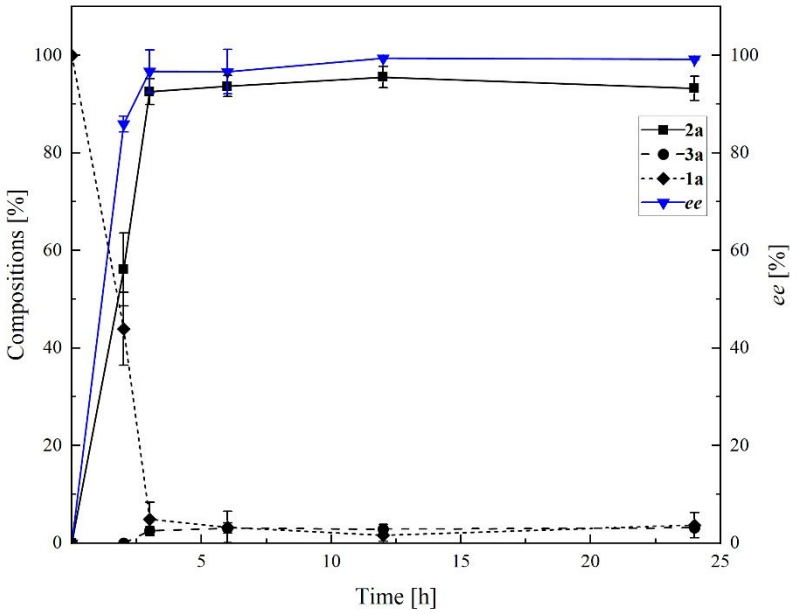

Figure S14. Time-course profiles for the reduction of **1a** catalyzed by ADH-R9. Reaction conditions: **1a** (10 mM), DMSO (5 %), ADH-R9 (0.1 g mL^{-1} whole cell with 6 U mL^{-1} DNase I and 1 mg mL^{-1} lysozyme), $NADP^+$ (1 mM), glucose (20 mM) and GDH (2.5 mg mL^{-1}), in phosphate buffer (50 mM), 30 °C, 800 rpm, final volume: 1.0 mL.

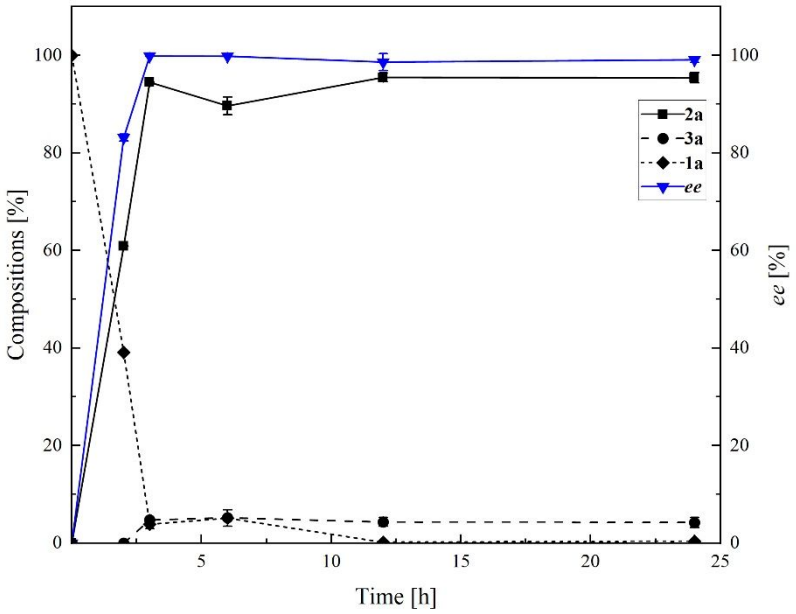

Figure S15. Time-course profiles for the reduction of **1a** catalyzed by ADH-R10. Reaction conditions: **1a** (10 mM), DMSO (5 %), ADH-R10 (0.1 g mL^{-1} whole cell with 6 U mL^{-1} DNase I and 1 mg mL^{-1} lysozyme), $NADP^+$ (1 mM), glucose (20 mM) and GDH (2.5 mg mL^{-1}), in phosphate buffer (50 mM), 30 °C, 800 rpm, final volume: 1.0 mL.

Entry	Enzyme	Diol [%]	ee [%]	Configuration of **2a**
1	R1	34.9%±0.9	55.4%±1.5	*S*
2	R2	72.9%±0.0	91.5%±2.0	*S*
3	R4	58.6%±1.3	97.2%±0.6	*S*
4	R7	20.6%±0.6	56.8%±1.1	*R*
5	R9	20.6%±0.6	51.8%±3.2	*R*
6	R10	14.1%±0.4	40.2%±3.8	*R*

Table S5. The reduction of *rac*-**2a** catalyzed by ADHs. Reaction conditions: *rac*-**2a** (10 mM), DMSO (5 %), ADHs (0.1 g mL^{-1} whole cell with 6 U mL^{-1} DNase I and 1 mg mL^{-1} lysozyme), $NADP^+$ (1 mM), glucose (20 mM) and GDH (2.5 mg mL^{-1}), in phosphate buffer (50 mM), 30 °C, 24 h, 800 rpm, final volume: 1.0 mL.

6. Synthesis of biaryl substrates 1a-m

General procedures for the synthesis of substrates **1a-m.**[14]

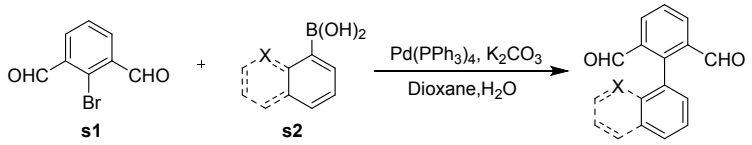

A 250 mL round-bottomed flask was filled with 2-bromobenzaldehyde **s1** (5.0 mmol), boronic acid **s2** (11.5 mmol), K_2CO_3 (34.5 mmol) and $Pd(PPh_3)_4$ (0.09 mmol), and was evacuated and charged with nitrogen three times. Then degassed 1,4- dioxane (5.6 mL) and water (7.5 mL) were added and heated at 95 °C for 3 days in nitrogen atmosphere. After cooling to room temperature, the mixture was poured into water and extracted with dichloromethane for three times. The organic layer was washed with brine and dried over anhydrous $MgSO_4$. The solvent was removed under vacuum. The residue was purified by silica gel column chromatography (PE: EA = 4:1 to 1:9) and washed with ethanol to obtain the compound.

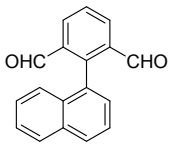

2-(naphthalen-1-yl) isophthalaldehyde (**1a**): 1196 mg, 92% isolated yield, yellow oil.

^{1}H NMR (400 MHz, Chloroform-*d*) δ 9.56 (s, 2H), 8.38 (d, *J* = 7.7 Hz, 2H), 8.04 (dd, *J* = 19.4, 8.3 Hz, 2H), 7.79 (t, *J* = 7.8 Hz, 1H), 7.69 – 7.45 (m, 4H), 7.33 (d, *J* = 8.3 Hz, 1H). **^{13}C NMR** (101 MHz, $CDCl_3$) δ 190.78, 146.61, 135.60, 133.36, 133.28, 132.59, 130.09, 129.73, 129.38, 128.89, 128.70, 127.67, 126.84, 125.67, 124.96.

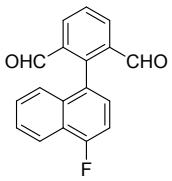

2-(4-fluoronaphthalen-1-yl) isophthalaldehyde (**1b**): 1001 mg, 72% isolated yield, yellow solid.

^{1}H NMR (400 MHz, Chloroform-*d*) δ 9.58 (s, 2H), 8.38 (d, *J* = 7.7 Hz, 2H), 8.29 (d, *J* = 8.4 Hz, 1H), 7.81 (t, *J* = 7.9 Hz, 1H), 7.67 (t, *J* = 7.7 Hz, 1H), 7.59 – 7.52 (m, 1H), 7.51 – 7.42 (m, 1H), 7.39 – 7.30 (m, 2H). **^{13}C NMR** (101 MHz, $CDCl_3$) δ 190.51, 145.66, 135.77, 134.72, 132.79, 129.19, 129.11, 128.66, 127.19, 126.07, 125.66, 121.43, 121.38, 109.02, 108.81.

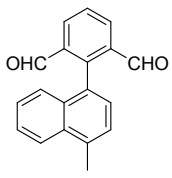

2-(4-methylnaphthalen-1-yl) isophthalaldehyde (**1c**): 1028 mg, 75% isolated yield, white solid.

^{1}H NMR (400 MHz, Chloroform-*d*) δ 9.57 (s, 2H), 8.37 (d, *J* = 7.8 Hz, 2H), 8.17 (d, *J* = 8.3 Hz, 1H), 7.78 (t, *J* = 7.8 Hz, 1H), 7.63 (t, *J* = 7.6 Hz, 1H), 7.48 (s, 2H), 7.40 (d, *J* = 7.0 Hz, 1H), 7.34 (d, *J* = 8.4 Hz, 1H), 2.85 (s, 3H). **^{13}C NMR** (101 MHz, $CDCl_3$) δ 190.96, 146.99, 136.41, 135.73, 133.44, 132.50, 129.20, 128.74, 128.20, 127.21, 126.61, 126.37, 125.74, 124.88, 19.67.

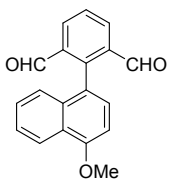

2-(4-methoxynaphthalen-1-yl) isophthalaldehyde (**1d**): 1349 mg, 93% isolated yield, light green solid.

^{1}H NMR (400 MHz, Chloroform-*d*) δ 9.61 (s, 2H), 8.44 (d, *J* = 8.4 Hz, 1H), 8.36 (d, *J* = 6.5 Hz, 2H), 7.76 (t, *J* = 7.6 Hz, 1H), 7.57 (t, *J* = 7.6 Hz, 1H), 7.50 (t, *J* = 7.6 Hz, 1H), 7.40 (d, *J* = 7.7

Hz, 1H), 7.27 (s, 1H), 6.98 (d, *J* = 7.8 Hz, 1H), 4.14 (s, 3H). **^{13}C NMR** (101 MHz, $CDCl_3$) δ 191.18, 156.57, 146.89, 136.03, 134.30, 132.53, 129.81, 128.64, 128.09, 126.08, 125.47, 125.39, 122.77, 121.80, 103.00, 55.80.

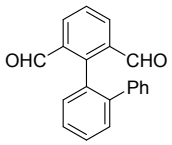

[1,1':2',1"-terphenyl]-2,6-dicarbaldehyde (**1e**): 815 mg, 57% isolated yield, white solid.

^{1}H NMR (400 MHz, Chloroform-*d*) δ 9.86 (s, 2H), 8.13 (d, *J* = 7.8 Hz, 2H), 7.65 (t, *J* = 8.1 Hz, 1H), 7.56 (q, *J* = 7.7 Hz, 3H), 7.43 (d, *J* = 7.2 Hz, 1H), 7.18 (s, 3H), 7.01 (s, 2H). **^{13}C NMR** (101 MHz, $CDCl_3$) δ 190.70, 147.62, 142.84, 139.63, 134.62, 132.61, 131.89, 131.07, 130.36, 129.76, 129.38, 128.42, 128.35, 127.46, 127.39.

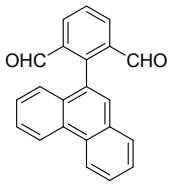

2-(phenanthren-9-yl) isophthalaldehyde (**1f**): 1039 mg, 67% isolated yield, light orange solids.

^{1}H NMR (400 MHz, Chloroform-*d*) δ 9.69 (s, 2H), 8.85 (dd, *J* = 18.0, 8.4 Hz, 2H), 8.41 (d, *J* = 9.5 Hz, 2H), 7.94 (d, *J* = 7.8 Hz, 1H), 7.88 – 7.70 (m, 5H), 7.58 (t, *J* = 7.6 Hz, 1H), 7.39 (d, *J* = 8.2 Hz, 1H). **^{13}C NMR** (101 MHz, $CDCl_3$) δ 190.78, 146.52, 135.79, 132.65, 132.30, 130.76, 130.64, 130.51, 130.25, 128.99, 128.93, 127.98, 127.81, 127.65, 127.62, 126.91, 123.38, 122.83.

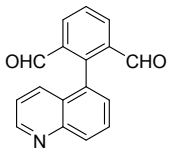

2-(quinolin-5-yl) isophthalaldehyde (**1g**): 1005 mg, 77% isolated yield, white solid.

^{1}H NMR (400 MHz, Chloroform-*d*) δ 9.58 (s, 2H), 9.04 (d, *J* = 5.9 Hz, 1H), 8.38 (dd, *J* = 13.1, 8.1 Hz, 3H), 7.90 (t, *J* = 7.8 Hz, 1H), 7.84 (t, *J* = 8.1 Hz, 1H), 7.70 (d, *J* = 8.4 Hz, 2H), 7.63 (d, *J* = 7.1 Hz, 1H), 7.43 (dd, *J* = 8.6, 4.2 Hz, 1H). **^{13}C NMR** (101 MHz, $CDCl_3$) δ 190.13, 151.17, 147.82, 144.64, 135.66, 133.71, 133.02, 132.20, 132.10, 132.03, 131.15, 130.64, 129.72, 129.40, 128.70, 128.55, 128.50, 122.45.

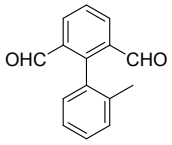

2'-methyl-[1,1'-biphenyl]-2,6-dicarbaldehyde (**1h**): 997 mg, 89% isolated yield, white solid.

^{1}H NMR (400 MHz, Chloroform-*d*) δ 9.73 (s, 2H), 8.30 (d, *J* = 10.3 Hz, 2H), 7.71 (t, *J* = 7.7 Hz, 1H), 7.46 (t, *J* = 7.4 Hz, 1H), 7.42 – 7.33 (m, 2H), 7.27 (d, *J* = 7.3 Hz, 1H), 2.09 (s, 3H). **^{13}C NMR** (101 MHz, $CDCl_3$) δ 190.93, 147.98, 136.87, 134.58, 132.73, 132.20, 130.69, 130.39, 129.39, 128.54, 126.07, 20.47.

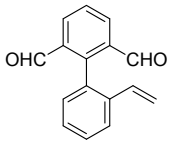

2'-vinyl-[1,1'-biphenyl]-2,6-dicarbaldehyde (**1i**): 1086 mg, 92% isolated yield, yellow solid.

^{1}H NMR (400 MHz, Chloroform-*d*) δ 9.72 (s, 2H), 8.30 (d, *J* = 9.4 Hz, 2H), 7.85 – 7.66 (m, 2H), 7.56 (d, *J* = 7.3 Hz, 1H), 7.44 (t, *J* = 7.5 Hz, 1H), 7.31 (s, 1H), 6.31 (dd, *J* = 17.6, 10.9 Hz, 1H), 5.71 (d, *J* = 17.1 Hz, 1H), 5.23 (d, *J* = 10.9 Hz, 1H). **^{13}C NMR** (101 MHz, $CDCl_3$) δ 190.80, 146.96, 137.91, 134.90, 133.89, 132.68, 131.30, 130.97, 129.64, 128.74, 127.77, 125.73, 117.70.

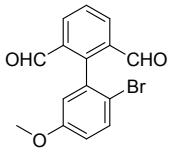

2'-bromo-5'-methoxy-[1,1'-biphenyl]-2,6-dicarbaldehyde (**1j**): 623mg, 69% isolated yield, yellow solid.

^{1}H NMR (400 MHz, Chloroform-*d*) δ 9.78 (s, 2H), 8.32 (d, *J* = 7.7 Hz, 2H), 7.75 (t, *J* = 7.8 Hz, 1H), 7.67 (d, *J* = 8.9 Hz, 1H), 6.99 (d, *J* = 8.9 Hz, 1H), 6.92 (s, 1H), 3.86 (s, 3H). **^{13}C NMR** (101 MHz, $CDCl_3$) δ 190.26, 158.88, 146.60, 134.75, 134.30, 133.72, 132.79, 129.19, 117.90, 116.70, 114.67, 55.72.

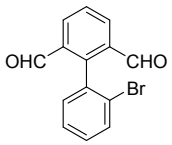

2'-bromo-[1,1'-biphenyl]-2,6-dicarbaldehyde (**1k**): 1181 mg, 82% isolated yield, yellow solid.

^{1}H NMR (400 MHz, Chloroform-*d*) δ 9.75 (s, 2H), 8.31 (d, *J* = 10.4 Hz, 2H), 7.83 – 7.72 (m, 2H), 7.52 (t, *J* = 6.7 Hz, 1H), 7.42 (dd, *J* = 21.1, 8.6 Hz, 2H). **^{13}C NMR** (101 MHz, $CDCl_3$) δ

190.94, 190.21, 146.58, 137.66, 135.53, 134.40, 134.03, 133.07, 132.93, 132.24, 130.88, 130.48, 129.21, 128.93, 127.60, 126.81, 124.56, 124.37.

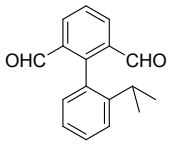

2'-isopropyl-[1,1'-biphenyl]-2,6-dicarbaldehyde (**1l**): 1072 mg, 85% isolated yield, white solid.

^{1}H NMR (400 MHz, Chloroform-*d*) δ 9.76 (s, 2H), 8.30 (d, *J* = 7.7 Hz, 2H), 7.71 (t, *J* = 7.7 Hz, 1H), 7.53 (d, *J* = 6.8 Hz, 2H), 7.38 – 7.31 (m, 1H), 7.22 (d, *J* = 7.6 Hz, 1H), 1.12 (d, *J* = 6.8 Hz, 6H). **^{13}C NMR** (101 MHz, $CDCl_3$) δ 190.86, 147.97, 147.84, 134.93, 132.57, 130.82, 130.49, 129.84, 128.46, 126.02, 125.82, 30.62, 23.70.

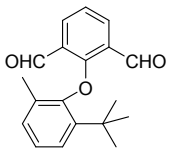

2-(2-(tert-butyl)-6-methylphenoxy) isophthalaldehyde (**1m)**: yellow solid.

^{1}H NMR (400 MHz, Chloroform-*d*) δ 10.01 (s, 2H), 8.12 (d, *J* = 7.7 Hz, 2H), 7.38 (d, *J* = 7.8 Hz, 1H), 7.26 (d, *J* = 7.8 Hz, 1H), 7.18 (t, *J* = 7.7 Hz, 1H), 7.10 (d, *J* = 7.7 Hz, 1H), 1.96 (s, 3H), 1.48 (s, 9H). **^{13}C NMR** (101 MHz, $CDCl_3$) δ 187.94, 161.12, 155.77, 140.88, 135.36, 131.47, 127.66, 127.10, 126.47, 126.09, 122.68, 35.32, 30.38, 17.82.

7. Synthesis of monoaldehyde substrates 2a-m

General procedures for the synthesis of substrates **2a-m**.

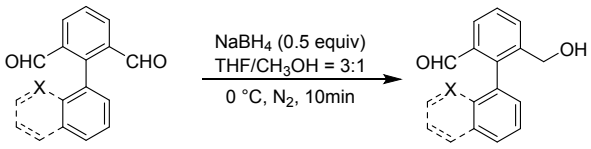

In a flame-dried flask, dialdehyde (0.2 mmol), $NaBH_4$ (0.1 mmol), dried THF/CH_3OH = 3:1 (2.0 ml) and magnetons were charged. The reaction mixture was stirred at 0 °C for 10 minutes in nitrogen atmosphere. The reaction mixture was then quenched with water and extracted with CH_2Cl_2 (3×10 ml). Dry anhydrous Na_2SO_4, evaporate solvent to obtain residue, and purify with silica gel column chromatography (PE: EA = 4:1 to 1:9) to obtain monoaldehyde product.

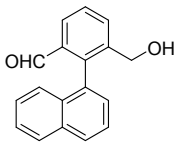

3-(hydroxymethyl)-2-(naphthalen-1-yl) benzaldehyde (**2a**): 44 mg, 84% isolated yield, yellow oil.

^{1}H NMR (400 MHz, Chloroform-*d*) δ 9.48 (s, 1H), 8.07 (d, *J* = 7.8 Hz, 1H), 7.97 (q, *J* = 7.8 Hz, 3H), 7.66 (t, *J* = 7.7 Hz, 1H), 7.62 – 7.52 (m, 2H), 7.43 (t, *J* = 8.4 Hz, 2H), 7.30 (d, *J* = 5.6 Hz, 1H), 4.41 – 4.28 (m, 2H). **^{13}C NMR** (101 MHz, Chloroform-*d*) δ 192.13, 142.13, 140.85, 135.01, 133.48, 133.10, 132.81, 132.65, 129.47, 128.95, 128.66, 128.62, 128.09, 127.86, 127.15, 126.54, 126.38, 125.47, 125.22, 62.29. **HRMS** calcd. for $C_{18}H_{14}O_2Na$ 285.0891 $[M+Na]^+$, found 285.0897.

(*S*)-3-(hydroxymethyl)-2-(naphthalen-1-yl) benzaldehyde: $[\alpha]_D^{19}$ = -33.6 (c = 0.75, CH_2Cl_2).

(*R*)-3-(hydroxymethyl)-2-(naphthalen-1-yl) benzaldehyde: $[\alpha]_D^{19}$ = +34.6(c = 0.75, CH_2Cl_2).

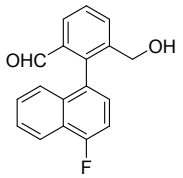

2-(4-fluoronaphthalen-1-yl)-3-(hydroxymethyl) benzaldehyde (**2b**): 52 mg, 92% isolated yield, yellow solid.

^{1}H NMR (400 MHz, Chloroform-*d*) δ 9.50 (s, 1H), 8.25 (d, *J* = 8.4 Hz, 1H), 8.07 (d, *J* = 7.7 Hz, 1H), 7.96 (d, *J* = 7.5 Hz, 1H), 7.65 (dt, *J* = 21.0, 7.6 Hz, 2H), 7.50 (t, *J* = 7.6 Hz, 1H), 7.36 (t, *J* = 6.3 Hz, 1H), 7.29 (d, *J* = 7.0 Hz, 2H), 4.34 (q, *J* = 13.5 Hz, 2H). **^{13}C NMR** (101 MHz, Chloroform-*d*) δ 191.87, 160.28, 157.75, 141.28, 141.04, 135.20, 134.01, 133.13, 128.86, 128.10, 127.89, 127.80, 126.86, 126.60, 125.51, 125.48, 121.27, 121.22, 109.11, 108.91, 62.20. **HRMS** calcd. for $C_{18}H_{14}O_2F$ 281.0978 $[M+H]^+$, found 281.0987.

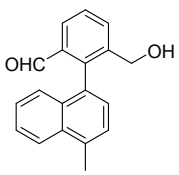

3-(hydroxymethyl)-2-(4-methylnaphthalen-1-yl) benzaldehyde (**2c**): 50 mg, 90% isolated yield, yellow oil.

^{1}H NMR (400 MHz, Chloroform-*d*) δ 9.49 (s, 1H), 8.13 (d, *J* = 8.2 Hz, 1H), 8.06 (d, *J* = 7.3 Hz, 1H), 7.93 (d, *J* = 7.2 Hz, 1H), 7.61 (dt, *J* = 21.9, 7.2 Hz, 2H), 7.43 (d, *J* = 7.1 Hz, 2H), 7.30 (d, *J* = 6.4 Hz, 2H), 4.34 (q, *J* = 13.5 Hz, 2H), 2.82 (s, 3H). **^{13}C NMR** (101 MHz, Chloroform-*d*) δ 192.26, 142.51, 140.97, 135.48, 135.15, 133.08, 132.70, 132.67, 130.93, 128.54, 127.84, 126.72, 126.33, 126.11, 125.99, 124.79, 62.42, 19.61. **HRMS** calcd. for $C_{19}H_{16}O_2Na$ 299.1048 $[M+Na]^+$, found 299.1048.

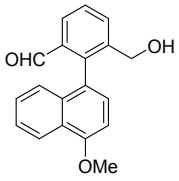

3-(hydroxymethyl)-2-(4-methoxynaphthalen-1-yl) benzaldehyde (**2d**): 52 mg, 89% isolated yield, yellow oil.

^{1}H NMR (400 MHz, Chloroform-*d*) δ 9.54 (s, 1H), 8.48 – 8.38 (m, 1H), 8.13 – 8.02 (m, 1H), 7.97 – 7.91 (m, 1H), 7.72 – 7.61 (m, 1H), 7.55 (t, *J* = 7.5 Hz, 1H), 7.45 (t, *J* = 7.5 Hz, 1H), 7.32 (d, *J* = 9.8 Hz, 1H), 7.24 (d, *J* = 8.2 Hz, 1H), 6.94 (d, *J* = 7.7 Hz, 1H), 4.44 – 4.32 (m, 2H), 4.12 (s, 3H). **^{13}C NMR** (101 MHz, Chloroform-*d*) δ 192.45, 155.96, 142.41, 141.32, 135.49, 133.54, 133.09, 128.49, 128.28, 127.60, 126.34, 125.80, 125.57, 125.26, 124.58, 122.64, 103.17, 62.49, 55.70. **HRMS** calcd. for $C_{19}H_{16}O_3Na$ 315.0997 $[M+Na]^+$, found 315.0994.

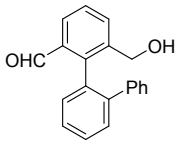

6-(hydroxymethyl)-[1,1':2',1''-terphenyl]-2-carbaldehyde (**2e**): 54 mg, 93% isolated yield, yellow oil:

^{1}H NMR (400 MHz, Chloroform-*d*) δ 9.82 (s, 1H), 7.88 (d, *J* = 7.8 Hz, 1H), 7.73 (d, *J* = 7.7 Hz, 1H), 7.57 (s, 1H), 7.48 (d, *J* = 5.4 Hz, 2H), 7.35 – 7.29 (m, 2H), 7.20 (s, 3H), 7.08 (s, 2H), 4.49 – 4.28 (m, 2H). **^{13}C NMR** (101 MHz, Chloroform-*d*) δ 192.20, 143.06, 141.72, 140.19, 139.82, 134.34, 133.26, 131.22, 130.35, 129.31, 129.21, 129.05, 128.24, 127.44, 127.24, 126.64, 62.32, 29.75. **HRMS** calcd. for $C_{20}H_{16}O_2Na$ 311.1048 $[M+Na]^+$, found 311.1049.

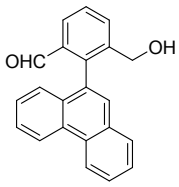

3-(hydroxymethyl)-2-(phenanthren-9-yl) benzaldehyde (**2f**): 48 mg, 77% isolated yield, yellow oil.

^{1}H NMR (400 MHz, Chloroform-*d*) δ 9.62 (s, 1H), 8.82 (dd, *J* = 14.2, 8.4 Hz, 2H), 8.16 – 8.07 (m, 1H), 7.99 (d, *J* = 7.4 Hz, 1H), 7.92 (d, *J* = 7.6 Hz, 1H), 7.83 – 7.65 (m, 5H), 7.54 (t, *J* = 7.4 Hz, 1H), 7.39 – 7.34 (m, 1H), 4.52 – 4.33 (m, 2H). **^{13}C NMR** (101 MHz, Chloroform-*d*) δ 192.12, 140.97, 135.18, 133.16, 131.69, 131.53, 130.92, 130.44, 129.19, 128.83, 128.76, 127.51, 127.47, 127.37, 127.31, 126.49, 123.27, 122.76, 62.29, 29.74. **HRMS** calcd. for $C_{20}H_{16}O_2Na$ 311.1048 $[M+Na]^+$, found 311.1038.

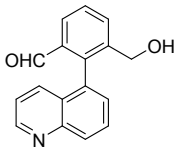

3-(hydroxymethyl)-2-(quinolin-5-yl) benzaldehyde (**2g**): 46mg, 87% isolated yield, yellow oil.

^{1}H NMR (400 MHz, Chloroform-*d*) δ 9.48 (d, *J* = 2.6 Hz, 1H), 8.94 (t, *J* = 5.1 Hz, 1H), 8.23 (t, *J* = 7.6 Hz, 1H), 8.07 (d, *J* = 7.8 Hz, 1H), 8.00 (d, *J* = 7.6 Hz, 1H), 7.83 (td, *J* = 7.9, 7.5, 3.5 Hz, 1H), 7.70 – 7.64 (m, 2H), 7.51 (d, *J* = 7.3 Hz, 1H), 7.35 (dt, *J* = 8.1, 3.8 Hz, 1H), 4.44 – 4.23 (m, 2H). **^{13}C NMR** (101 MHz, Chloroform-*d*) δ 191.49, 150.76, 147.89, 141.03, 140.32, 135.06, 133.97, 133.44, 133.25, 132.15, 132.05, 130.07, 129.10, 128.94, 128.64, 128.54, 127.92, 126.82, 121.94, 61.97. **HRMS** calcd. for $C_{17}H_{14}NO_2$ 264.1025 $[M+H]^+$, found 264.1027.

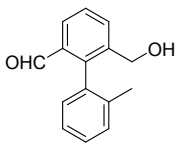

6-(hydroxymethyl)-2'-methyl-[1,1'-biphenyl]-2-carbaldehyde (**2h**): 38mg, 85% isolated yield, yellow oil.

^{1}H NMR (400 MHz, Chloroform-*d*) δ 9.64 (s, 1H), 8.00 (d, *J* = 7.7 Hz, 1H), 7.88 (d, *J* = 7.4 Hz, 1H), 7.58 (t, *J* = 7.6 Hz, 1H), 7.36 (td, *J* = 17.6, 16.1, 8.1 Hz, 3H), 7.18 (d, *J* = 7.2 Hz, 1H), 4.48 – 4.34 (m, 2H), 2.03 (s, 3H). **^{13}C NMR** (101 MHz, Chloroform-*d*) δ 192.25, 143.63, 139.74, 136.42, 134.85, 133.97, 133.21, 130.33, 129.70, 128.66, 128.27, 126.43, 126.08, 62.42, 20.15. **HRMS** calcd. for $C_{15}H_{14}O_2Na$ 249.0891 $[M+Na]^+$, found 249.0885.

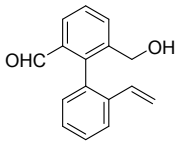

6-(hydroxymethyl)-2'-vinyl-[1,1'-biphenyl]-2-carbaldehyde (**2i**): 42 mg, 89% isolated yield, yellow oil.

^{1}H NMR (400 MHz, Chloroform-*d*) δ 9.64 (s, 1H), 8.05 – 7.98 (m, 1H), 7.89 (d, *J* = 7.6 Hz, 1H), 7.74 (d, *J* = 7.8 Hz, 1H), 7.60 (t, *J* = 7.6 Hz, 1H), 7.49 (t, *J* = 7.6 Hz, 1H), 7.40 (t, *J* = 7.4 Hz, 1H), 7.22 (d, *J* = 7.5 Hz, 1H), 6.38 – 6.23 (m, 1H), 5.70 (d, *J* = 17.5 Hz, 1H), 5.23 – 5.13 (m, 1H), 4.42 (s, 2H). **^{13}C NMR** (101 MHz, Chloroform-*d*) δ 192.07, 142.60, 140.18, 136.86, 134.32, 134.18, 133.81, 133.14, 130.36, 128.90, 128.52, 127.87, 126.48, 125.49, 116.60, 62.47. **HRMS** calcd. for $C_{16}H_{15}O_2$ 239.1072 $[M+H]^+$, found 239.1078.

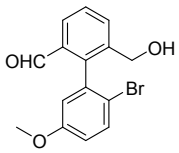

2'-bromo-6-(hydroxymethyl)-5'-methoxy-[1,1'-biphenyl]-2-carbaldehyde (**2j**): 59 mg, 92% isolated yield, yellow oil.

^{1}H NMR (400 MHz, Chloroform-*d*) δ 9.69 (s, 1H), 8.01 (d, *J* = 7.7 Hz, 1H), 7.92 (d, *J* = 7.5 Hz, 1H), 7.63 (t, *J* = 7.3 Hz, 2H), 6.92 (d, *J* = 8.8 Hz, 1H), 6.85 (s, 1H), 4.50 (t, *J* = 12.6 Hz, 2H), 3.83 (s, 3H). **^{13}C NMR** (101 MHz, Chloroform-*d*) δ 191.55, 158.95, 142.47, 139.68, 137.31, 133.72, 133.58, 133.26, 128.96, 126.72, 117.00, 116.05, 114.36, 62.27, 55.65. **HRMS** calcd. for $C_{15}H_{14}O_3Br$ 321.0126 $[M+H]^+$, found 321.0121.

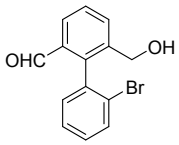

2'-bromo-6-(hydroxymethyl)-[1,1'-biphenyl]-2-carbaldehyde (**2k**): 52 mg, 89% isolated yield, yellow oil.

^{1}H NMR (400 MHz, Chloroform-*d*) δ 9.67 (s, 1H), 8.01 (d, *J* = 7.7 Hz, 1H), 7.92 (d, *J* = 7.6 Hz, 1H), 7.76 (d, *J* = 8.0 Hz, 1H), 7.67 – 7.61 (m, 1H), 7.47 (t, *J* = 7.4 Hz, 1H), 7.37 (t, *J* = 8.2 Hz, 1H), 7.32 (s, 1H), 4.46 (q, *J* = 13.4 Hz, 2H). **^{13}C NMR** (101 MHz, Chloroform-*d*) δ 191.50, 142.51, 139.77, 136.56, 133.83, 133.25, 132.95, 131.50, 130.18, 128.97, 127.63, 126.90, 124.06, 62.32. **HRMS** calcd. for $C_{14}H_{12}O_2Br$ 291.0021 $[M+H]^+$, found 291.0028.

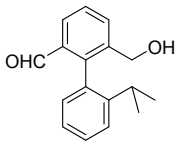

6-(hydroxymethyl)-2'-isopropyl-[1,1'-biphenyl]-2-carbaldehyde (**2l**): 42 mg, 83%isolated yield, yellow oil.

^{1}H NMR (400 MHz, Chloroform-*d*) δ 9.67 (s, 1H), 8.00 (d, *J* = 7.7 Hz, 1H), 7.92 – 7.87 (m, 1H), 7.61 – 7.55 (m, 1H), 7.48 (d, *J* = 4.4 Hz, 2H), 7.30 (s, 1H), 7.13 (d, *J* = 7.5 Hz, 1H), 4.44 (q, *J* = 13.4 Hz, 2H), 2.55 (p, *J* = 6.8 Hz, 1H), 1.17 (d, *J* = 6.8 Hz, 3H), 1.05 (d, *J* = 6.7 Hz, 3H). **^{13}C NMR** (101 MHz, Chloroform-*d*) δ 192.27, 147.24, 143.46, 140.09, 134.35, 133.37, 132.95, 129.72, 129.14, 128.21, 126.28, 126.00, 125.86, 62.39, 30.29, 24.12, 23.57. **HRMS** calcd. for $C_{17}H_{18}O_2Na$ 277.1204 $[M+H]^+$, found 277.1205.

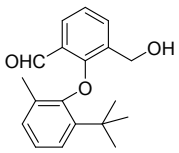

2-(2-(tert-butyl)-6-methylphenoxy)-3-(hydroxymethyl) benzaldehyde (**2m**): 42 mg, 71% isolated yield, yellow solid.

^{1}H NMR (400 MHz, Chloroform-*d*) δ 9.62 (s, 1H), 7.79 (t, *J* = 7.3 Hz, 2H), 7.34 (d, *J* = 7.6 Hz, 1H), 7.23 – 7.16 (m, 1H), 7.12 (t, *J* = 7.7 Hz, 1H), 7.05 (d, *J* = 7.7 Hz, 1H), 4.80 (s, 2H), 1.89 (s, 3H), 1.48 (d, *J* = 2.2 Hz, 9H). **^{13}C NMR** (101 MHz, Chloroform-*d*) δ 188.66, 156.78, 155.83, 140.50, 134.61, 131.33, 131.14, 128.66, 127.70, 126.12, 125.21, 122.66, 60.84, 35.31, 30.42, 17.68. **HRMS** calcd. for $C_{19}H_{22}O_3Na$ 321.1467 $[M+Na]^+$, found 321.1465.

8. Procedures for derivatization reactions

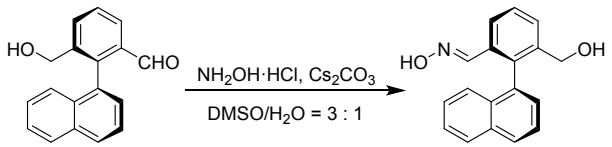

(*R*)-**2a** 4a

(*R*)-**2a** (0.2 mmol), $NH_2OH·HCl$ (0.24 mmol) and Cs_2CO_3 (0.24 mmol) were stirred in a 3:1 mixture of DMSO-H_2O (2 ml) at 100 °C for 7 hours under air. After the reaction was completed, the reaction mixture was cooled to room temperature and treated with water (2 mL). The resulting mixture was extracted with ethyl acetate (3×5 ml). Dry (Na_2SO_4) and evaporate the solvent to obtain the residue, which was purified by silica gel column (PE: EA= 1: 10) to obtain the reaction product (yield: 86%, 97% *ee*).

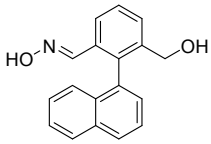

3-(hydroxymethyl)-2-(naphthalen-1-yl) benzaldehyde oxime (**4a**): 48 mg, 86% isolated yield, yellow oil.

^{1}H NMR (400 MHz, Chloroform-*d*) δ 7.96 (d, *J* = 8.3 Hz, 3H), 7.71 (d, *J* = 7.6 Hz, 1H), 7.61 – 7.49 (m, 4H), 7.41 (t, *J* = 7.5 Hz, 1H), 7.34 (d, *J* = 7.0 Hz, 1H), 7.28 (s, 1H), 4.33 – 4.21 (m, 2H). **^{13}C NMR** (101 MHz, Chloroform-*d*) δ 149.10, 140.34, 138.54, 134.29, 133.66, 132.24, 131.33, 129.12, 128.68, 128.55, 128.48, 127.74, 126.93, 126.40, 125.42, 124.68, 63.00. **HRMS** calcd. for $C_{18}H_{16}NO_2$ 278.1181 $[M+H]^+$, found 278.1186.

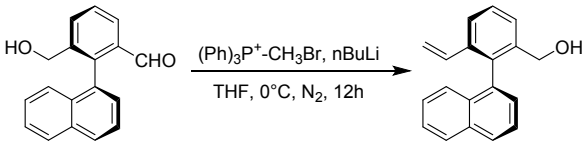

(*R*)-**2a** 5a

In a flame-dried flask, a flame-dried screw-cap reaction tube with Teflon coating was installed. To a magnetic stirring bar, methyl triphenylphosphonium bromide (0.22 mmol) and anhydrous tetrahydrofuran (1 mL) were added, and 2.5 mmol mL^{-1} nBuLi (0.22 mmol) in hexane was added ， the mixture was stirred at 0 °C for 30 minutes. Then, tetrahydrofuran solution (1 mL) dissolved in 2a (0.2 mmol) was added dropwise and stirred at 0 °C for 12 hours. After monitoring the completion of the reaction, the reaction mixture was quenched with water and extracted with CH_2Cl_2 (3×10 mL). Dry (Na_2SO_4) and evaporate the solvent to obtain the

residue, which was purified by silica gel column chromatography (PE： EA = 5∶1) to obtain the reaction product (yield: 83%, 95% *ee*).

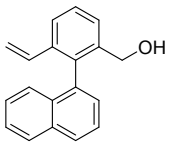

(2-(naphthalen-1-yl)-3-vinylphenyl) methanol (**5a**): 43 mg, 83% isolated yield, white solid.

^{1}H NMR (400 MHz, Chloroform-*d*) δ 7.95 (dd, *J* = 8.4, 4.2 Hz, 2H), 7.74 (d, *J* = 7.8 Hz, 1H), 7.55 (dt, *J* = 24.5, 7.5 Hz, 4H), 7.40 (t, *J* = 7.6 Hz, 1H), 7.37 – 7.31 (m, 2H), 6.19 (dd, *J* = 17.5, 11.0 Hz, 1H), 5.66 (d, *J* = 17.5 Hz, 1H), 4.99 (d, *J* = 11.0 Hz, 1H), 4.32 – 4.19 (m, 2H). **^{13}C NMR** (101 MHz, Chloroform-*d*) δ 139.98, 137.30, 137.27, 136.02, 135.00, 133.64, 132.29, 128.41, 128.24, 128.08, 127.52, 127.04, 126.57, 126.18, 125.67, 125.50, 124.16, 114.84, 63.40. **HRMS** calcd. for $C_{19}H_{16}ONa$ 283.1099 $[M+H]^+$, found 283.1105.

9. HPLC chromatogram

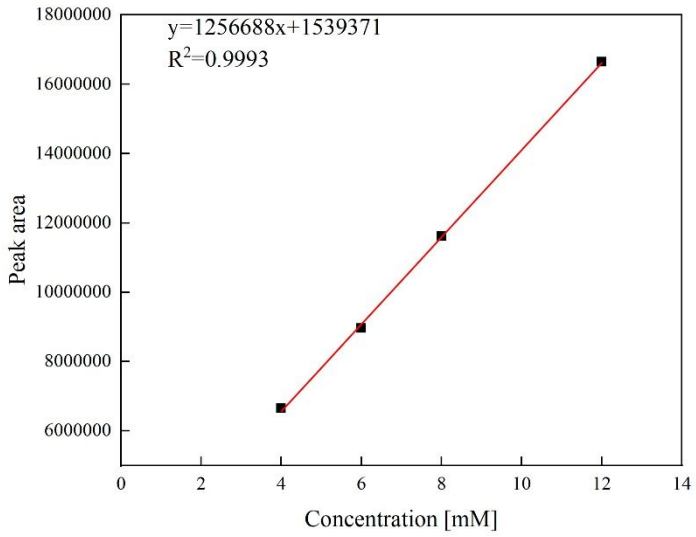

Figure S16. Standard curve for the model substrate *rac*-**2a**.

Samples with various concentrations of *rac*-**2a** with phosphate buffer containing 5% DMSO were run by HPLC. The yields of all target products (**2a~m**) were calculated according to the standard curve of the corresponding products.

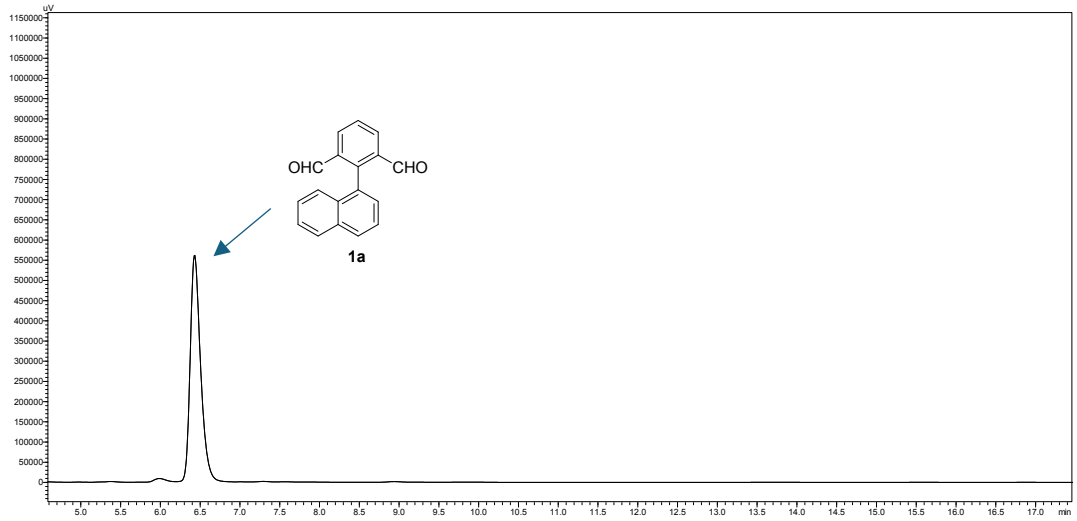

Figure S17. HPLC standards for **1a** (Chiralpak® AD-H, eluents: n-hexane/i-PrOH = 90/10, 254 nm, 30 °C, flow rate: 1.0 mL/min，retention time [min] for **1a**: 6.43).

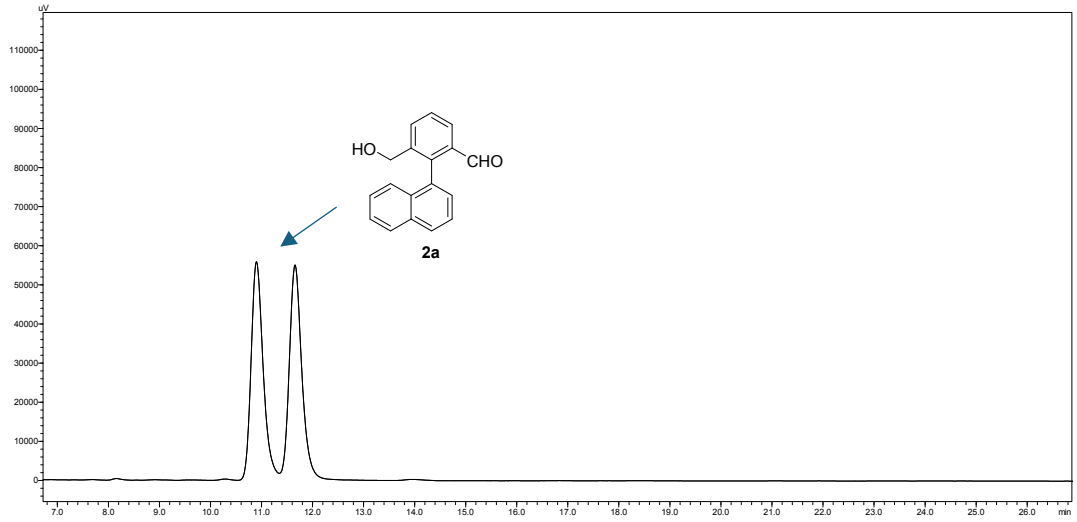

Figure S18. HPLC standards for *rac*-**2a** (Chiralpak® AD-H, eluents: n-hexane/i-PrOH = 90/10, 254 nm, 30 °C, flow rate: 1.0 mL/min，retention time [min] for *rac*-**2a**: 10.901/11.656).

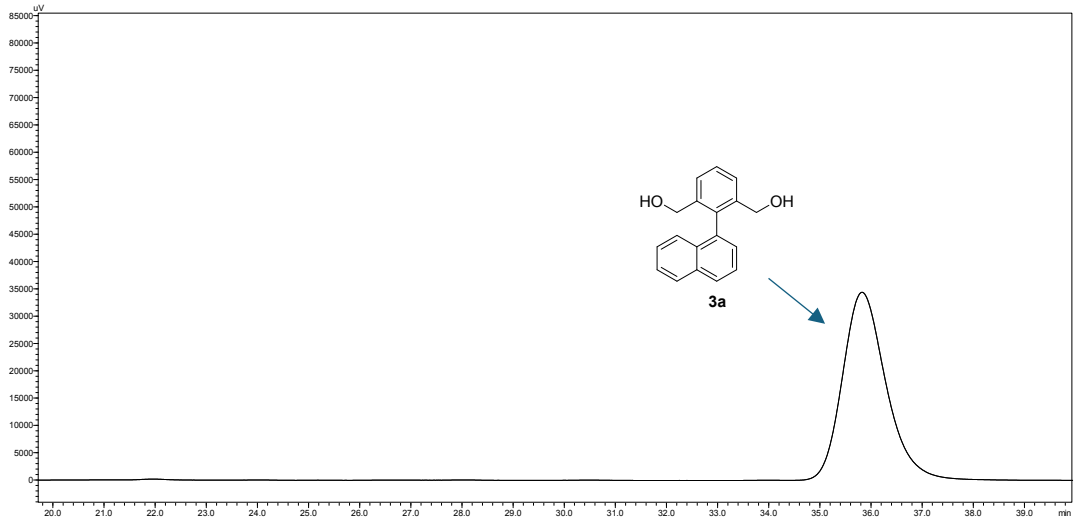

Figure S19. HPLC standards for **3a** (Chiralpak® AD-H, eluents: n-hexane/i-PrOH = 90/10, 254 nm, 30 °C, flow rate: 1.0 mL/min，retention time [min] for **3a**: 35.825).

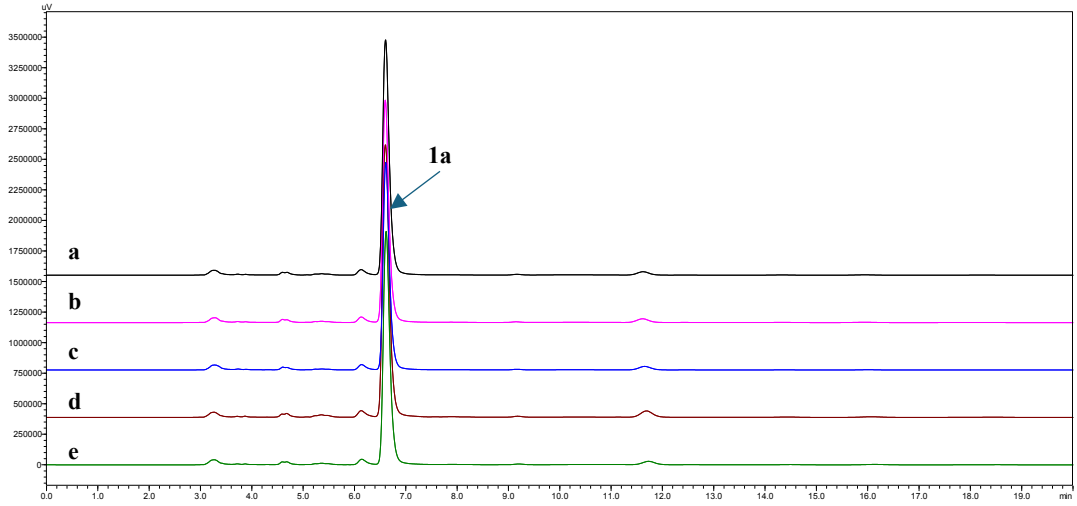

Figure S20. HPLC chromatograms of 3-(hydroxymethyl)-2-(naphthalen-1-yl) benzaldehyde (**2a**) produced by empty plasmid reactions (**a**: blank; **b**: pETDuet-1; **c**: pET22b; **d**: pET24a; **e**: pET28a).

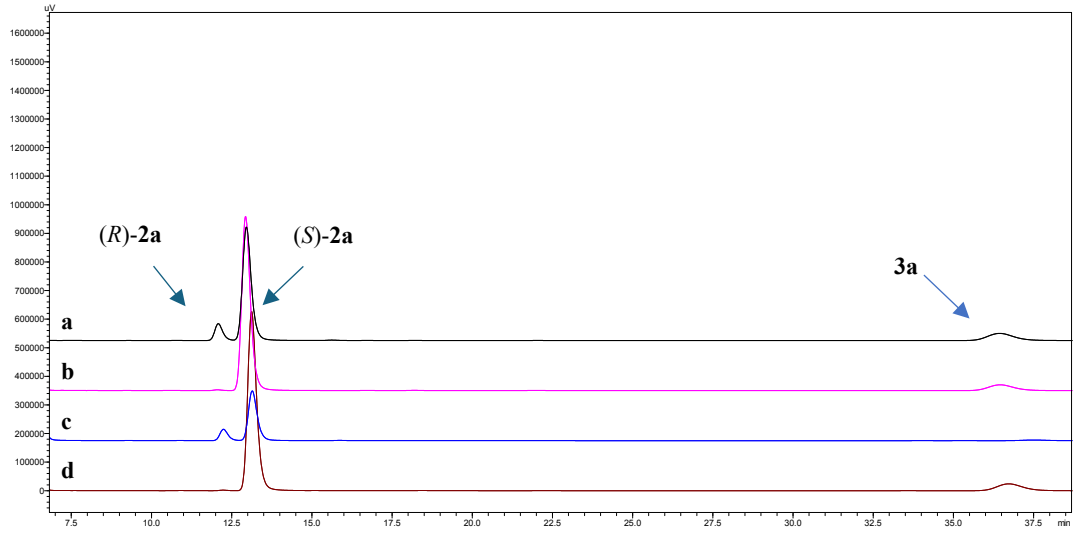

Figure S21. HPLC chromatograms of 3-(hydroxymethyl)-2-(naphthalen-1-yl) benzaldehyde (**2a**) produced by ADHs-catalyzed reactions (**a**: ADH-R1; **b**: ADH-R2; **c**: ADH-R3; **d**: ADH-R4).

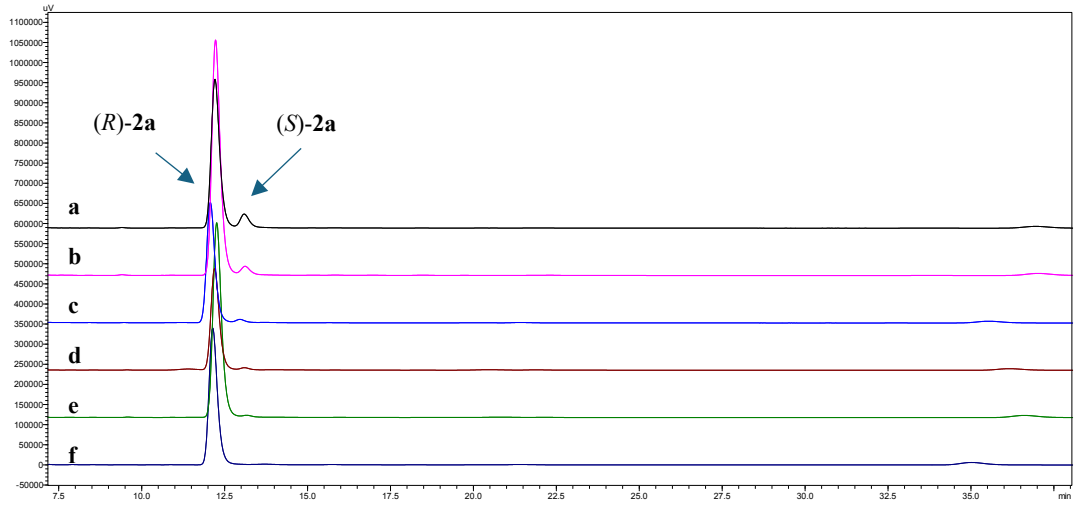

Figure S22. HPLC chromatograms of 3-(hydroxymethyl)-2-(naphthalen-1-yl) benzaldehyde (**2a**) produced by ADHs-catalyzed reactions (**a**: ADH-R5; **b**: ADH-R6; **c**: ADH-R7; **d**: ADH-R8; **e**: ADH-R9; **f**: ADH-R10).

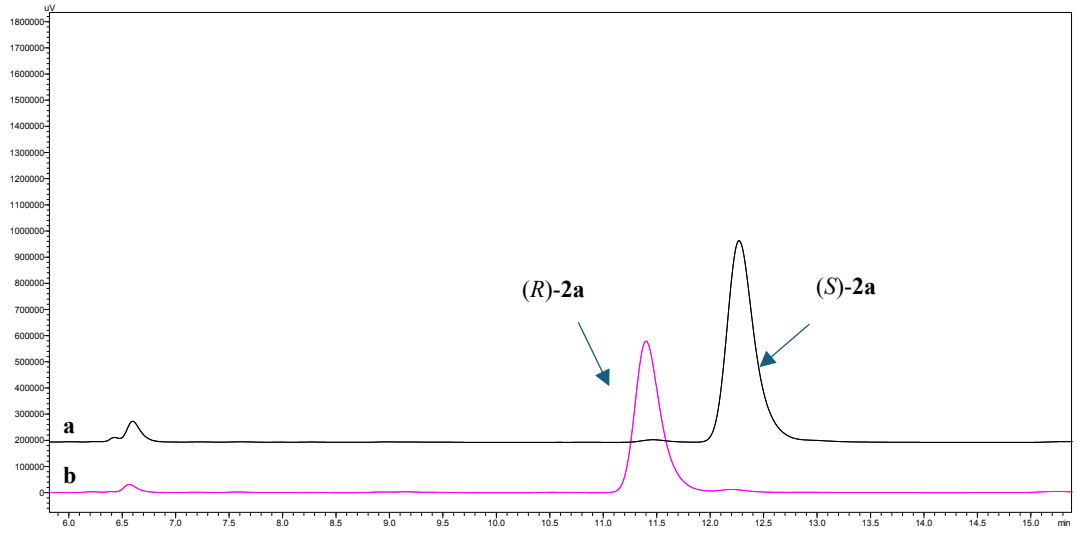

Figure S23. HPLC chromatograms of 3-(hydroxymethyl)-2-(naphthalen-1-yl) benzaldehyde (**2a**) produced by ADHs-catalyzed for upscaled reactions (**a**: ADH-R4; **b**: ADH-R10).

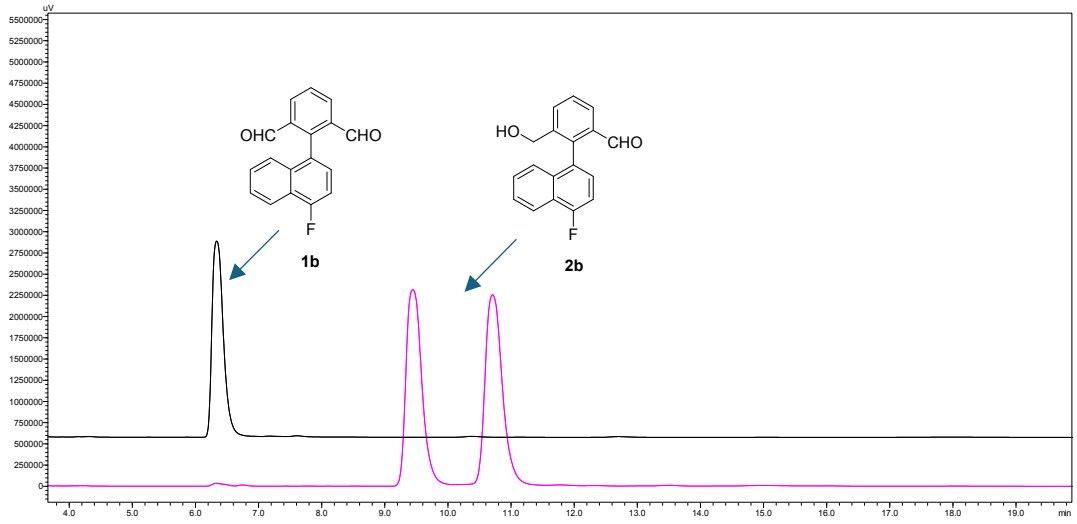

Figure S24. HPLC standards for **1b**-**2b** (Chiralpak® AD-H, eluents: n-hexane/i-PrOH = 90/10, 254 nm, 30 °C, flow rate: 1.0 mL/min, retention time [min] for **1b**: 6.336 and **2b**: 9.443/10.707).

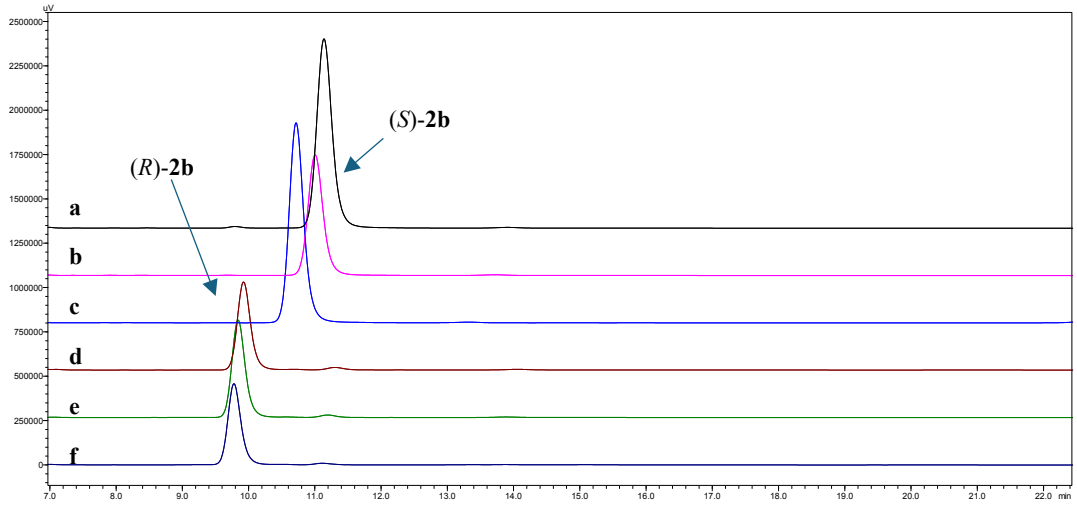

Figure S25. HPLC chromatograms of 2-(4-fluoronaphthalen-1-yl)-3-(hydroxymethyl) benzaldehyde (**2b**) produced by ADHs-catalyzed reactions, 24 h (**a**: ADH-R1; **b**: ADH-R2; **c**: ADH-R4; **d**: ADH-R7; **e**: ADH-R9; **f**: ADH-R10).

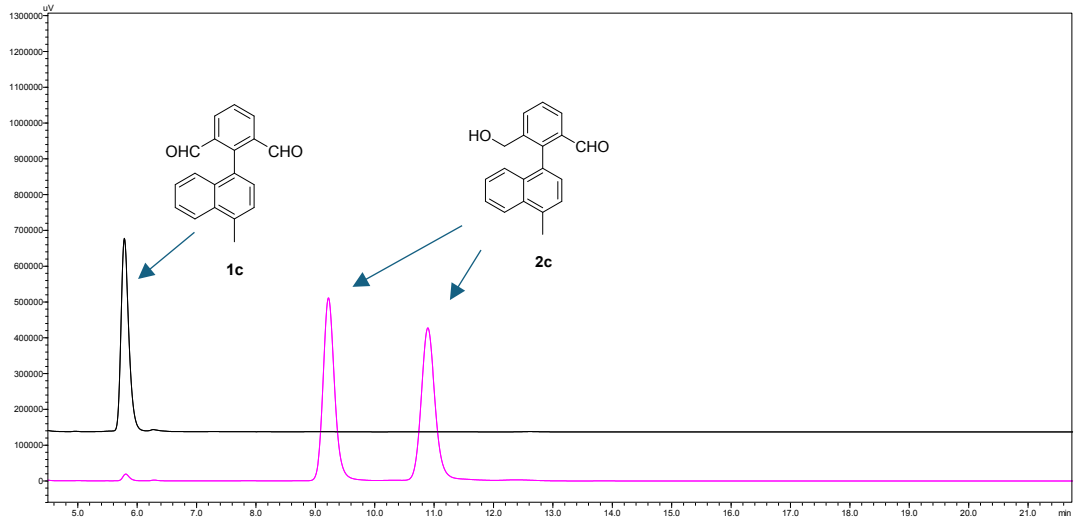

Figure S26. HPLC standards for **1c**-**2c** (Chiralpak® AD-H, eluents: n-hexane/i-PrOH = 90/10, 254 nm, 30 °C, flow rate: 1.0 mL/min，retention time [min] for **1c**: 5.784 and **2c**: 9.221/10.893).

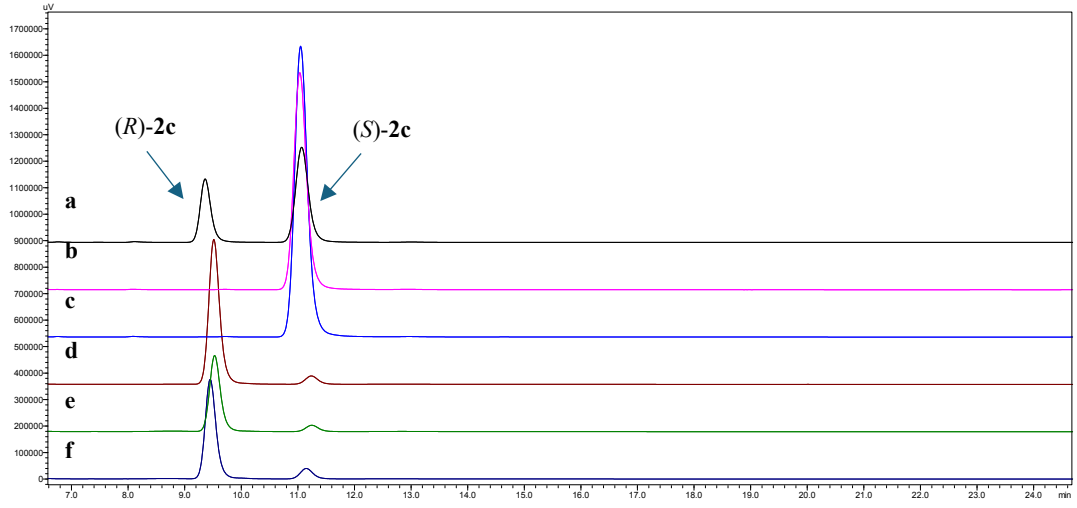

Figure S27. HPLC chromatograms of 3-(hydroxymethyl)-2-(4-methylnaphthalen-1-yl) benzaldehyde (**2c**) produced by ADHs-catalyzed reactions, 24 h (**a**: ADH-R1; **b**: ADH-R2; **c**: ADH-R4; **d**: ADH-R7; **e**: ADH-R9; **f**: ADH-R10).

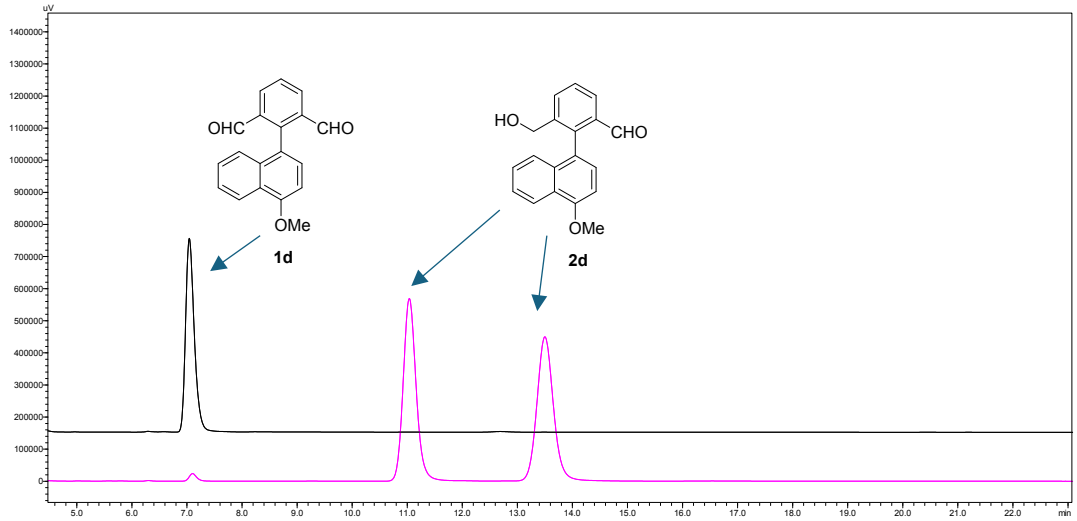

Figure S28. HPLC standards for **1d**-**2d** (Chiralpak® AD-H, eluents: n-hexane/i-PrOH = 90/10, 254 nm, 30 °C, flow rate: 1.0 mL/min，retention time [min] for **1d**: 7.042 and **2d**: 11.038/13.500).

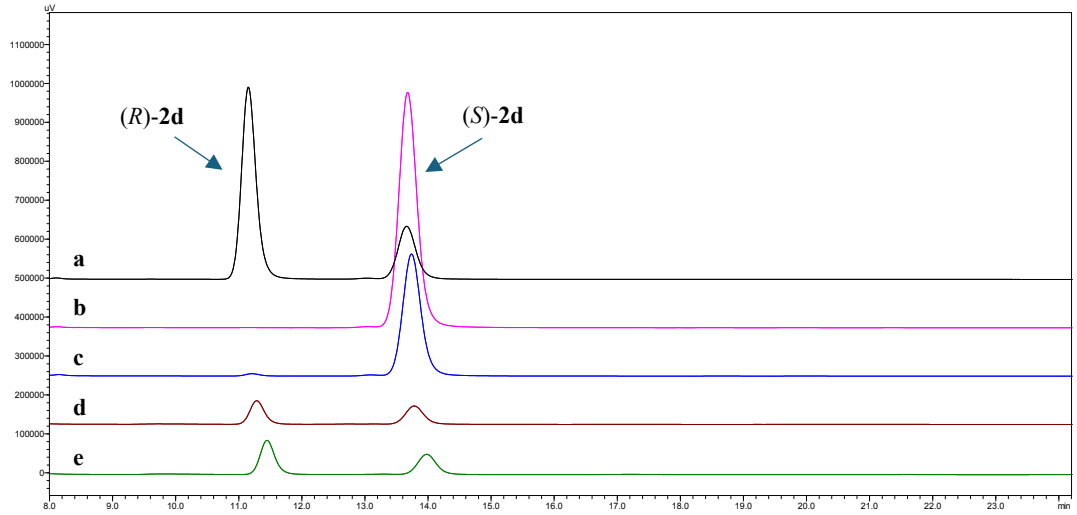

Figure S29. HPLC chromatograms of 3-(hydroxymethyl)-2-(4-methoxynaphthalen-1-yl) benzaldehyde (**2d**) produced by ADHs-catalyzed reactions, 24 h (**a**: ADH-R1; **b**: ADH-R2; **c**: ADH-R4; **d**: ADH-R7; **e**: ADH-R9).

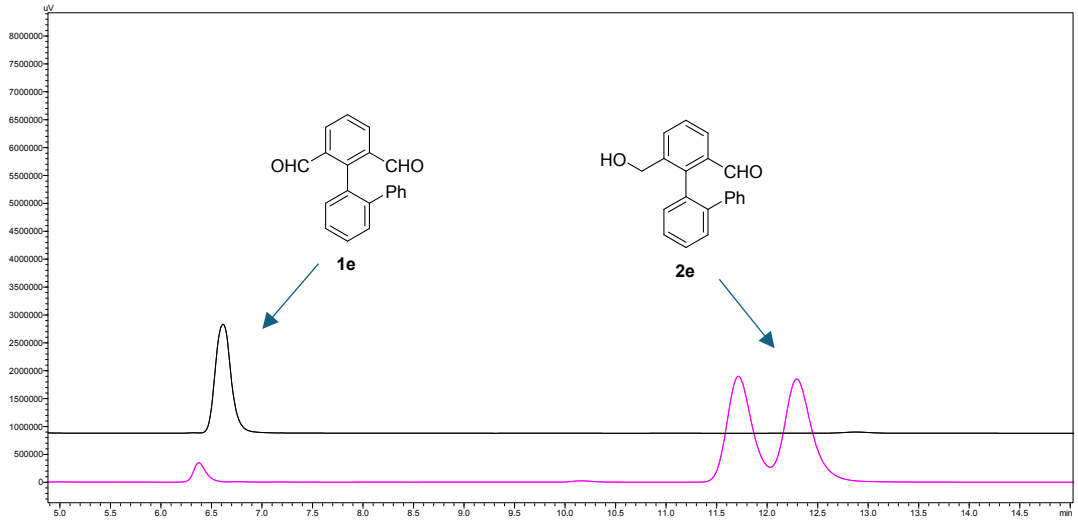

Figure S30. HPLC standards for **1e**-**2e** (Chiralpak® AD-H, eluents: n-hexane/i-PrOH = 90/10, 254 nm, 30 °C, flow rate: 1.0 mL/min，retention time [min] for **1e**: 7.570 and **2e**: 11.715/12.293).

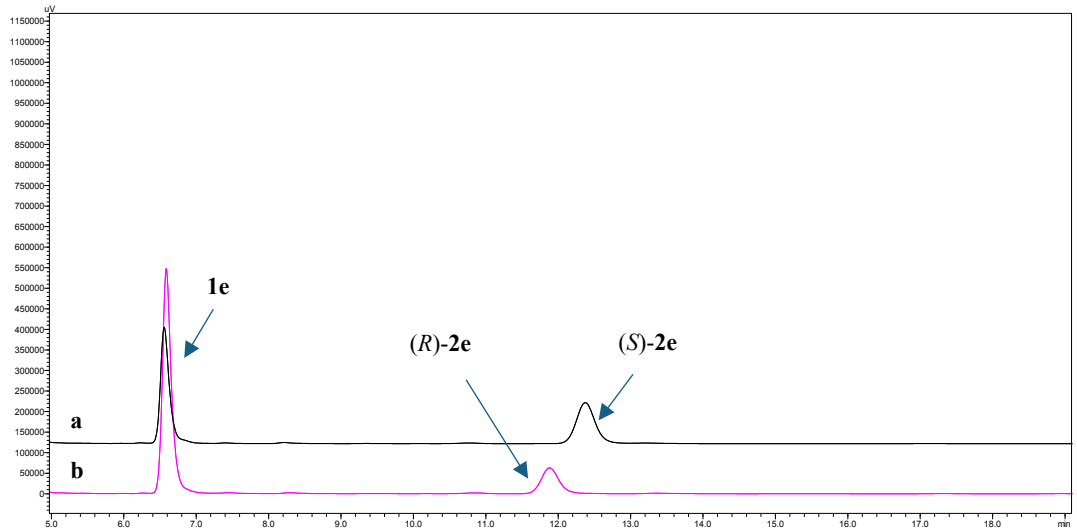

Figure S31. HPLC chromatograms of 6-(hydroxymethyl)-[1,1':2',1"-terphenyl]-2-carbaldehyde (**2e**) produced by ADHs-catalyzed reactions, 24 h (**a**: ADH-R2; **b**: ADH-R4).

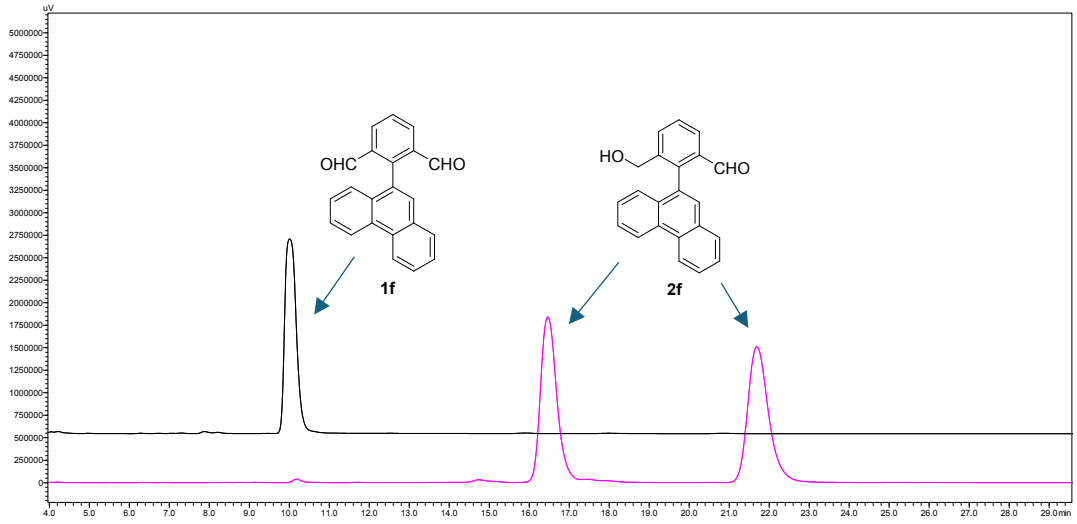

Figure S32. HPLC standards for **1f-2f** (Chiralpak® AD-H, eluents: n-hexane/i-PrOH = 90/10, 254 nm, 30 °C, flow rate: 1.0 mL/min，retention time [min] for **1f**: 10.009 and **2f**: 16.463/21.691).

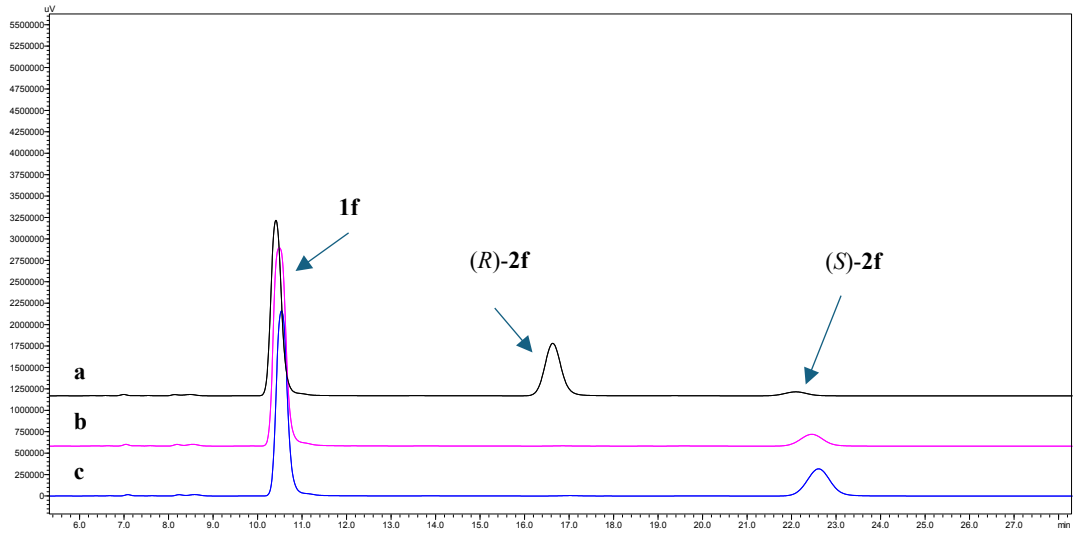

Figure S33. HPLC chromatograms of 3-(hydroxymethyl)-2-(phenanthren-9-yl) benzaldehyde (**2f**) produced by ADHs-catalyzed reactions, 24 h (**a**: ADH-R1; **b**: ADH-R2; **c**: ADH-R4).

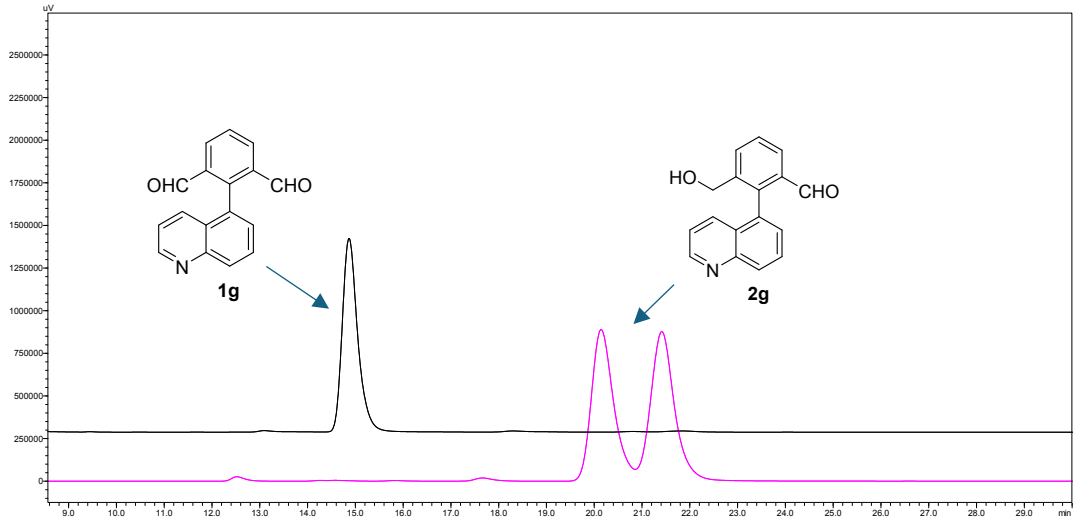

Figure S34. HPLC standards for **1g**-**2g** (Chiralpak® AD-H, eluents: n-hexane/i-PrOH = 90/10, 254 nm, 30 °C, flow rate: 1.0 mL/min, retention time [min] for **1g**: 14.869 and **2g**: 20.144/21.413).

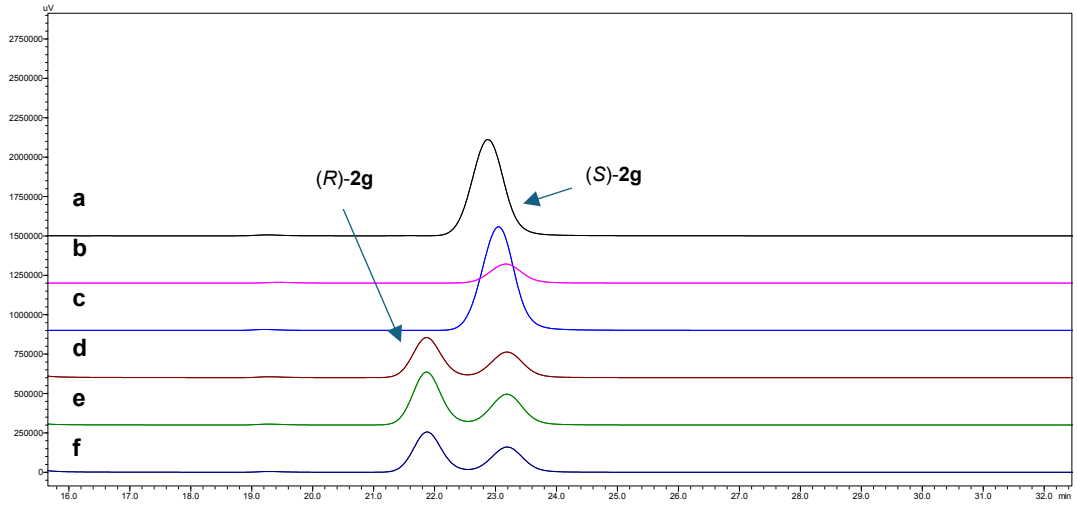

Figure S35. HPLC chromatograms of 3-(hydroxymethyl)-2-(quinolin-5-yl) benzaldehyde (**2g**) produced by ADHs-catalyzed reactions, 24 h (**a**: ADH-R1; **b**: ADH-R2; **c**: ADH-R4; **d**: ADH-R7; **e**: ADH-R9; **f**: ADH-R10).

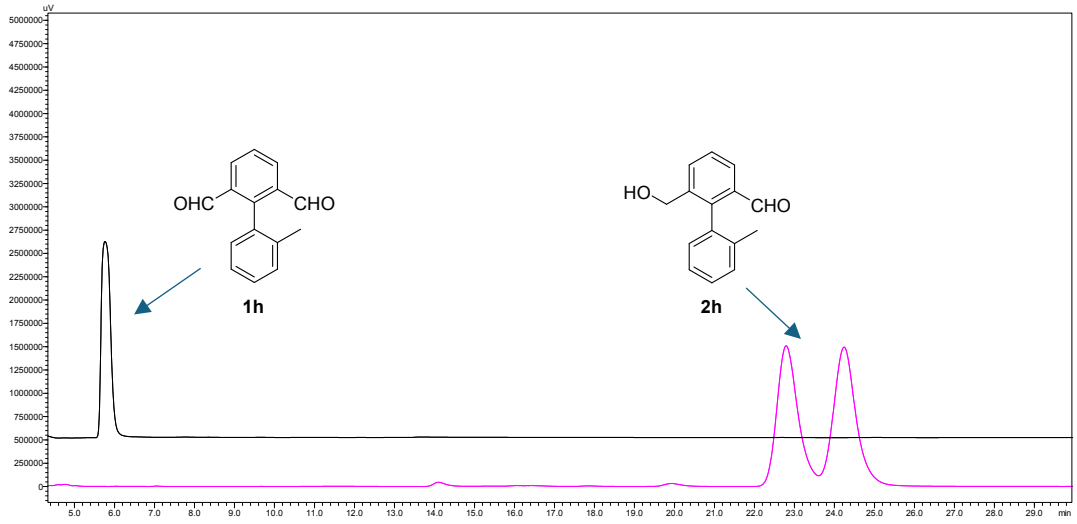

Figure S36. HPLC standards for **1h**-**2h** (Chiralpak® AD-H, eluents: n-hexane/i-PrOH = 98/2, 254 nm, 30 °C, flow rate: 1.0 mL/min，retention time [min] for **1h**: 5.764 and **2h**: 23.278/24.759).

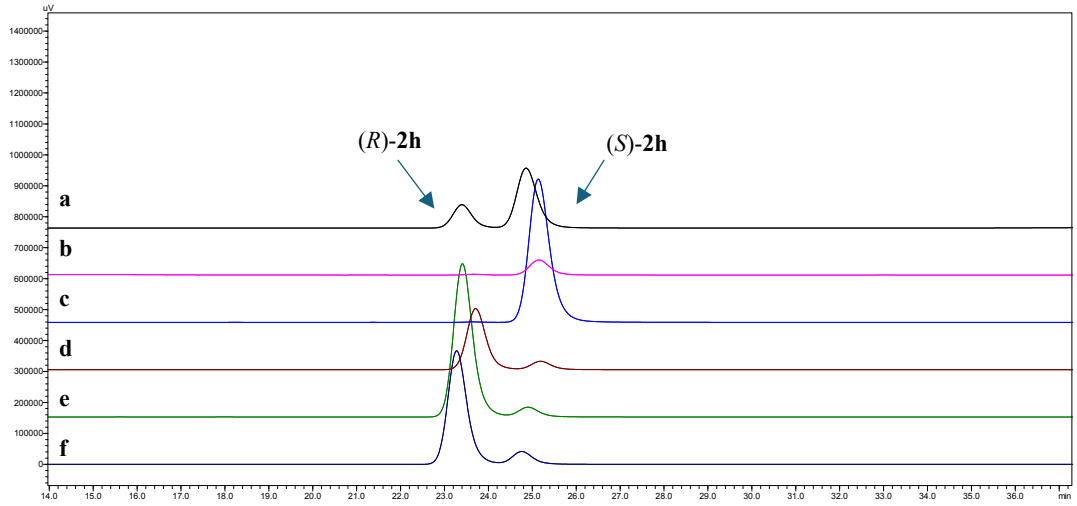

Figure S37. HPLC chromatograms of 6-(hydroxymethyl)-2'-methyl-[1,1'-biphenyl]-2-carbaldehyde (**2h**) produced by ADHs-catalyzed reactions, 24 h (**a**: ADH-R1; **b**: ADH-R2; **c**: ADH-R4; **d**: ADH-R7; **e**: ADH-R9; **f**: ADH-R10).

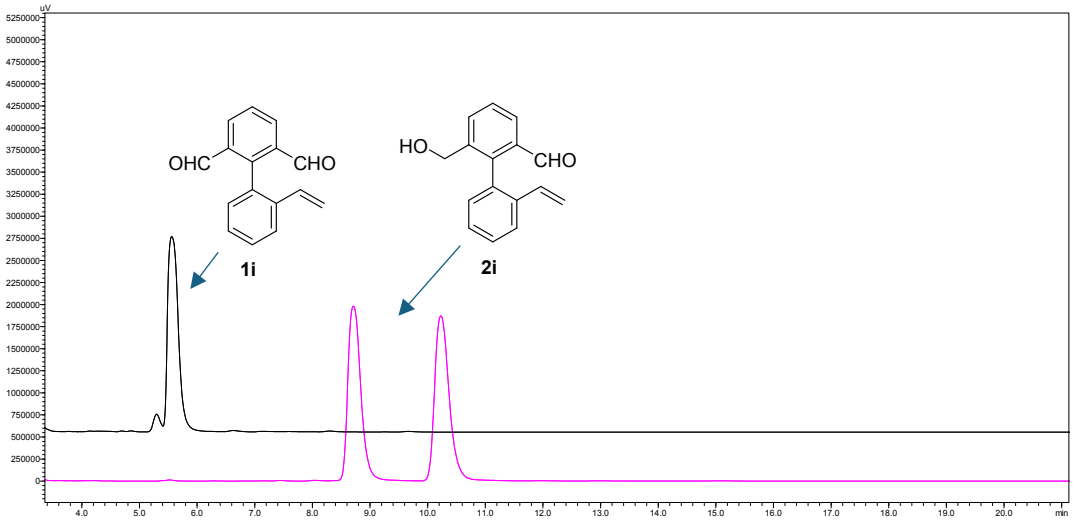

Figure S38. HPLC standards for **1i-2i** (Chiralpak® AD-H, eluents: n-hexane/i-PrOH = 90/10, 254 nm, 30 °C, flow rate: 1.0 mL/min，retention time [min] for **1i**: 5.560 and **2i**: 8.712/10.228).

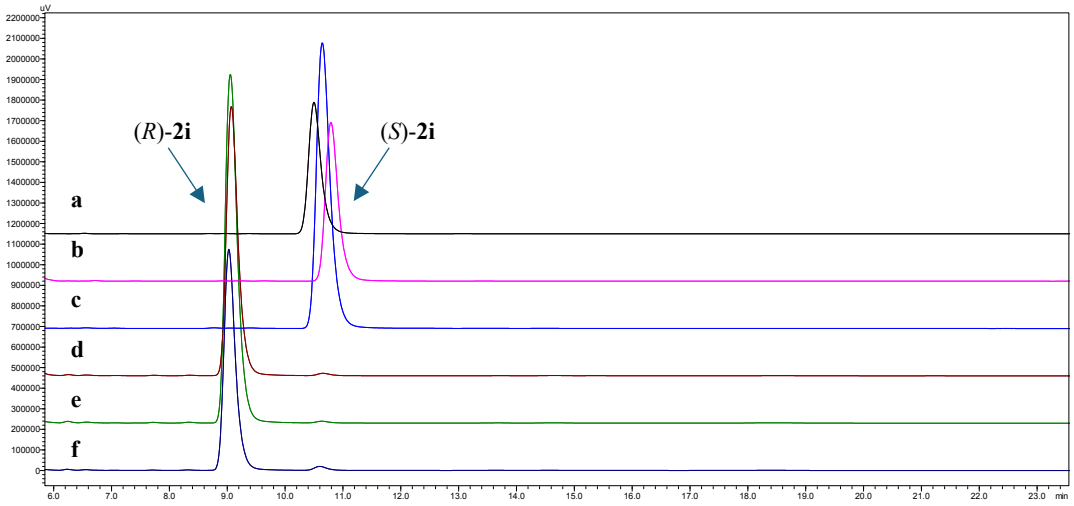

Figure S39. HPLC chromatograms of 6-(hydroxymethyl)-2'-vinyl-[1,1'-biphenyl]-2-carbaldehyde (**2i**) produced by ADHs-catalyzed reactions, 24 h (**a**: ADH-R1; **b**: ADH-R2; **c**: ADH-R4; **d**: ADH-R7; **e**: ADH-R9; **f**: ADH-R10).

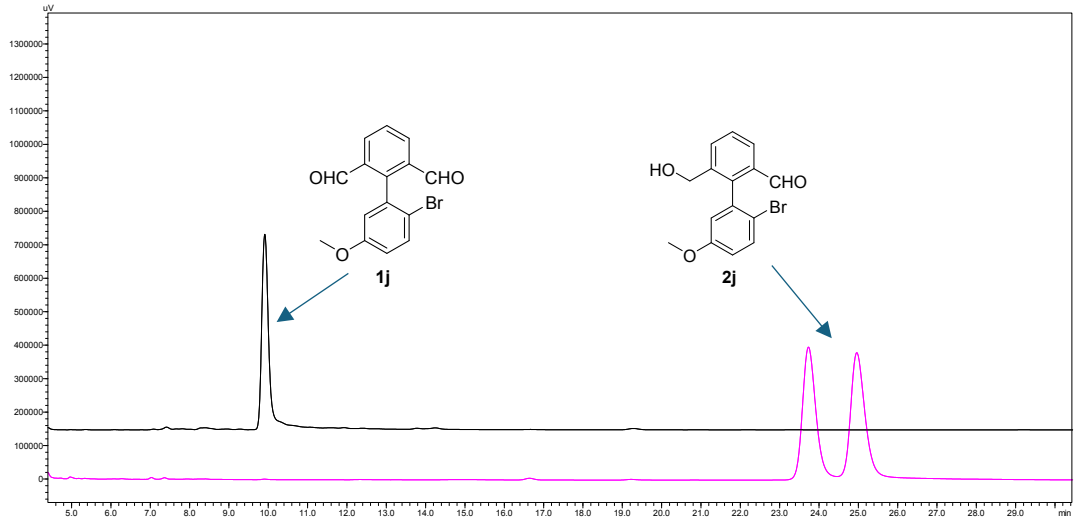

Figure S40. HPLC standards for **1j**-**2j** (Chiralpak® IA-3, eluents: n-hexane/i-PrOH = 95/5, 254 nm, 30 °C, flow rate: 1.0 mL/min，retention time [min] for **1j**: 9.912 and **2j**: 23.733/24.961).

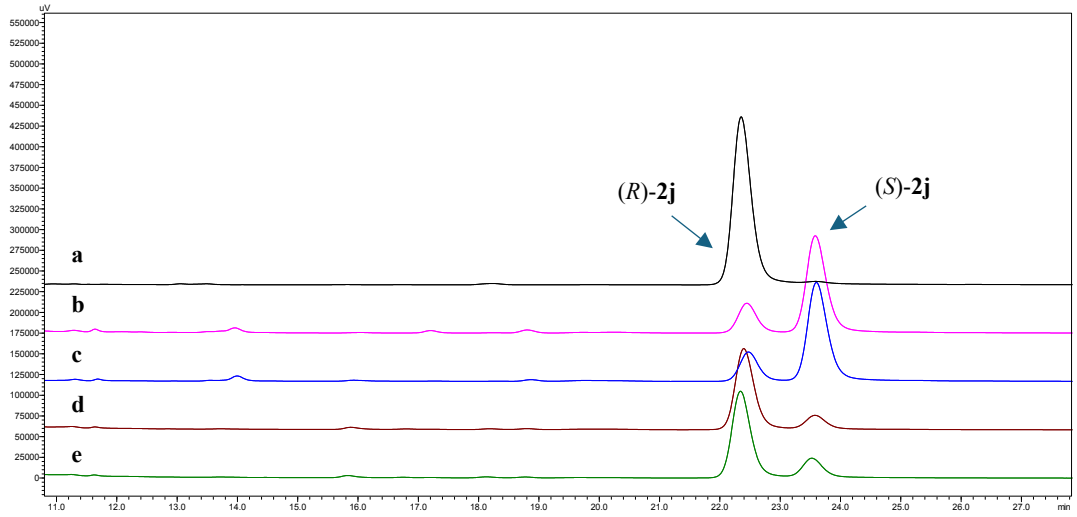

Figure S41. HPLC chromatograms of 2'-bromo-6-(hydroxymethyl)-5'-methoxy-[1,1'-biphenyl]-2-carbaldehyde (**2j**) produced by ADHs-catalyzed reactions, 24 h (**a**: ADH-R1; **b**: ADH-R2; **c**: ADH-R4; **d**: ADH-R9; **e**: ADH-R10).

.

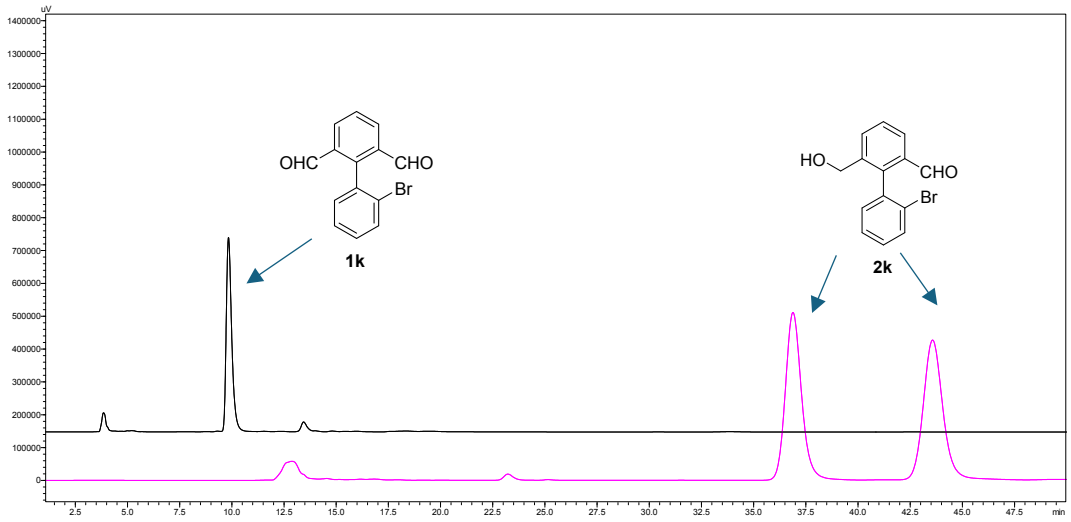

Figure S42. HPLC standards for **1k**-**2k** (Chiralpak® AD-H, eluents: n-hexane/i-PrOH = 98/2, 254 nm, 30 °C, flow rate: 1.0 mL/min，retention time [min] for **1k**: 8.721 and **2k**: 35.608/41.851).

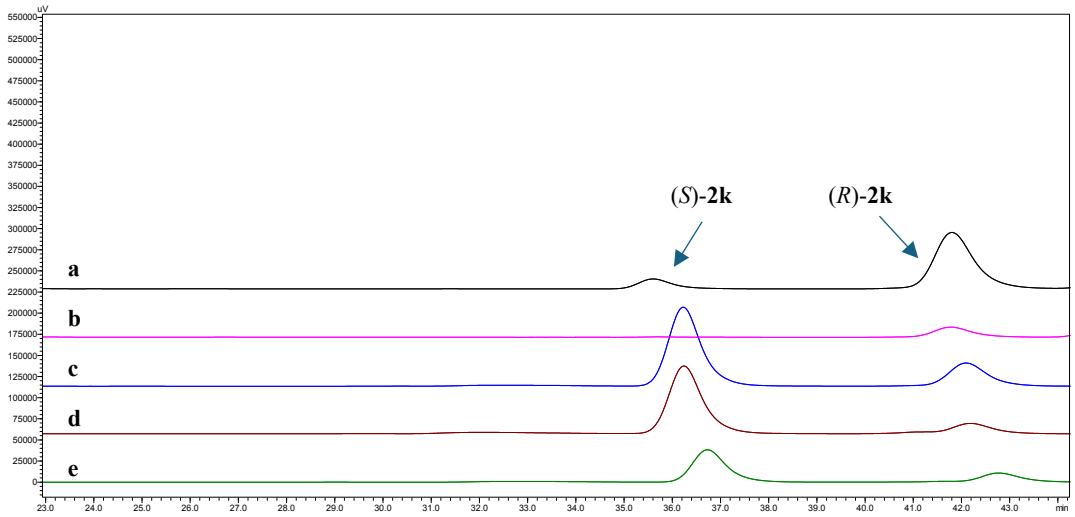

Figure S43. HPLC chromatograms of 2'-bromo-6-(hydroxymethyl)-[1,1'-biphenyl]-2-carbaldehyde (**2k**) produced by ADHs-catalyzed reactions, 24 h (**a**: ADH-R1; **b**: ADH-R2; **c**: ADH-R7; **d**: ADH-R9; **e**: ADH-R10).

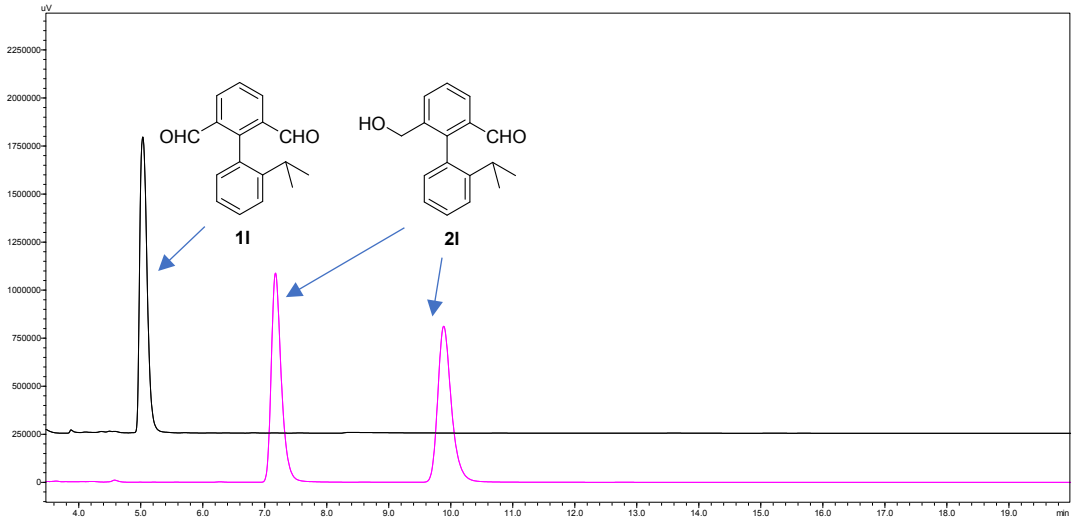

Figure S44. HPLC standards for **1l-2l** (Chiralpak® AD-H, eluents: n-hexane/i-PrOH = 90/10, 254 nm, 30 °C, flow rate: 1.0 mL/min，retention time [min] for **1l**: 5.033 and **2l**: 7.173/9.886).

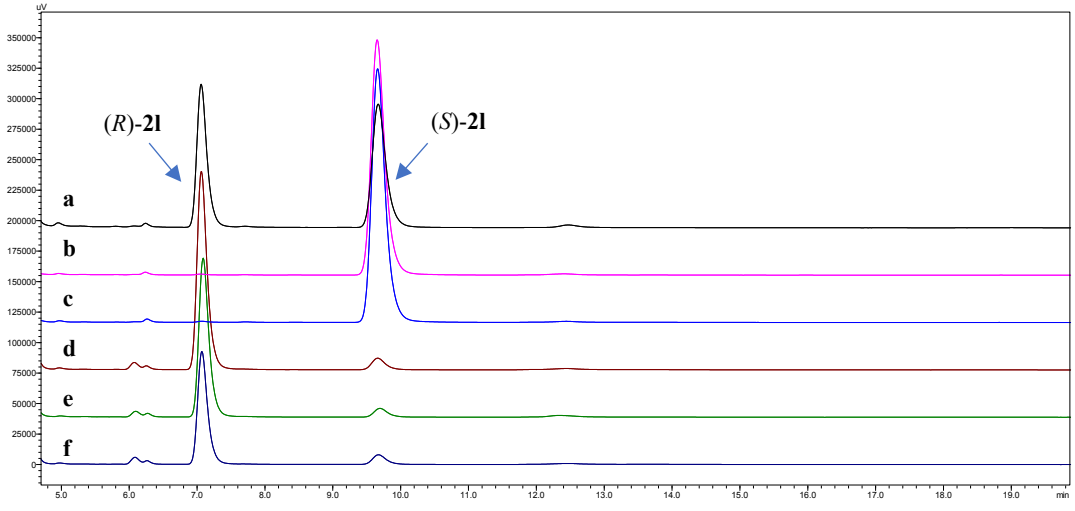

Figure S45. HPLC chromatograms of 6-(hydroxymethyl)-2'-isopropyl-[1,1'-biphenyl]-2-carbaldehyde (**2l**) produced by ADHs-catalyzed reactions, 24 h (**a**: ADH-R1; **b**: ADH-R2; **c**: ADH-R4; **d**: ADH-R7; **e**: ADH-R9; **f**: ADH-R10).

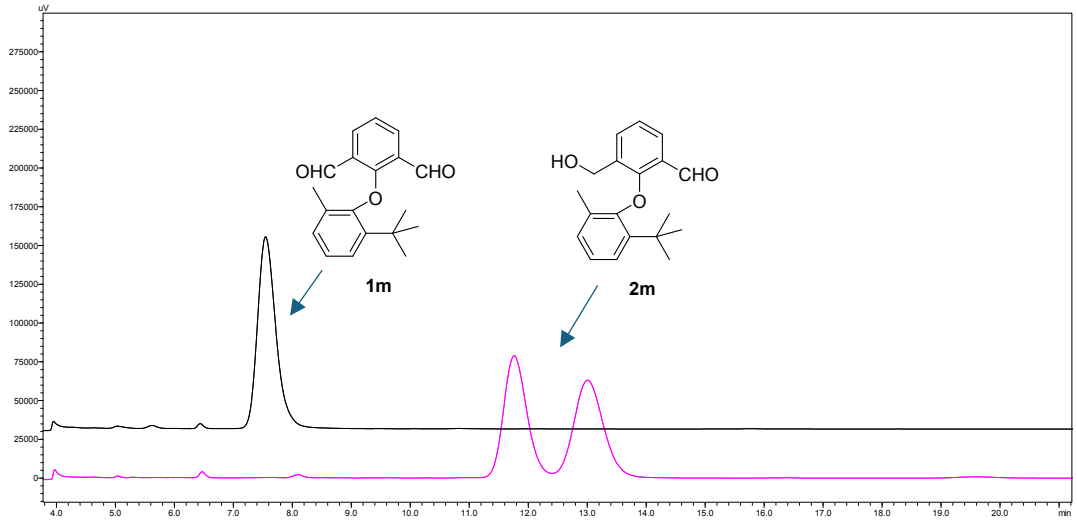

Figure S46. HPLC standards for **1m**-**2m** (Chiralcel® OJ-H, eluents: n-hexane/i-PrOH = 97/3, 254 nm, 30 °C, flow rate: 1.0 mL/min，retention time [min] for **1l**: 7.547 and **2l**: 11.762/13.007).

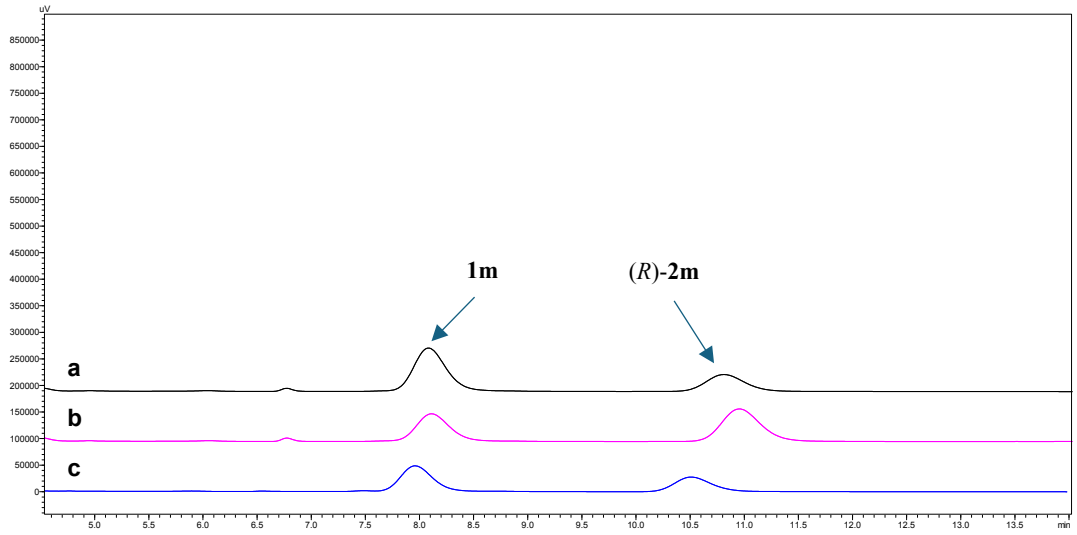

Figure S47. HPLC chromatograms of 2-(2-(tert-butyl)-6-methylphenoxy)-3-(hydroxymethyl) benzaldehyde (**2m**) produced by ADHs-catalyzed reactions, 24 h (**a**: ADH-R7; **b**: ADH-R9; **c**: ADH-R10).

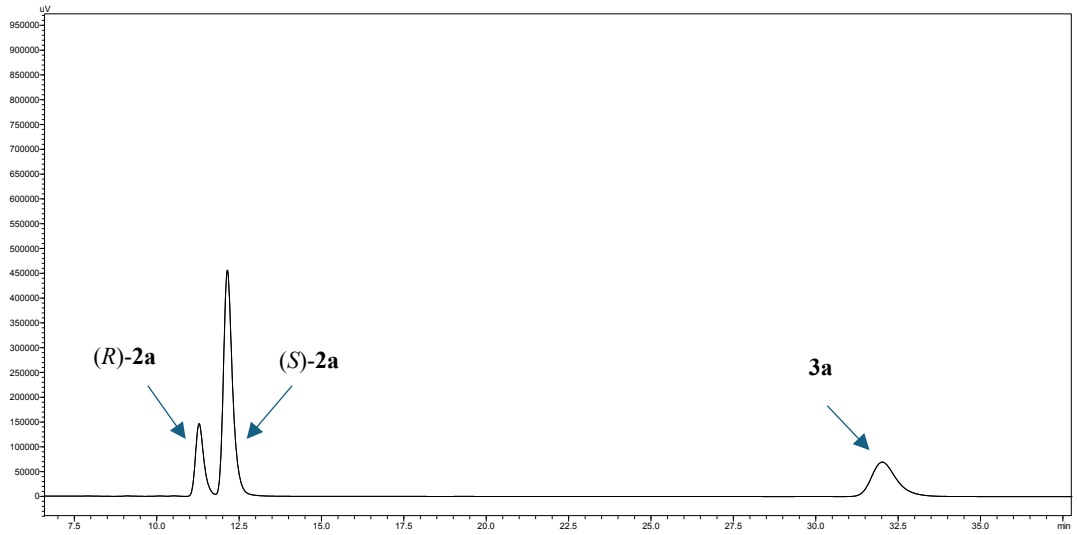

Figure S48. HPLC chromatograms of 3-(hydroxymethyl)-2-(naphthalen-1-yl) benzaldehyde (**3a**) produced by ADH-R1-catalyzed reaction, 24 h.

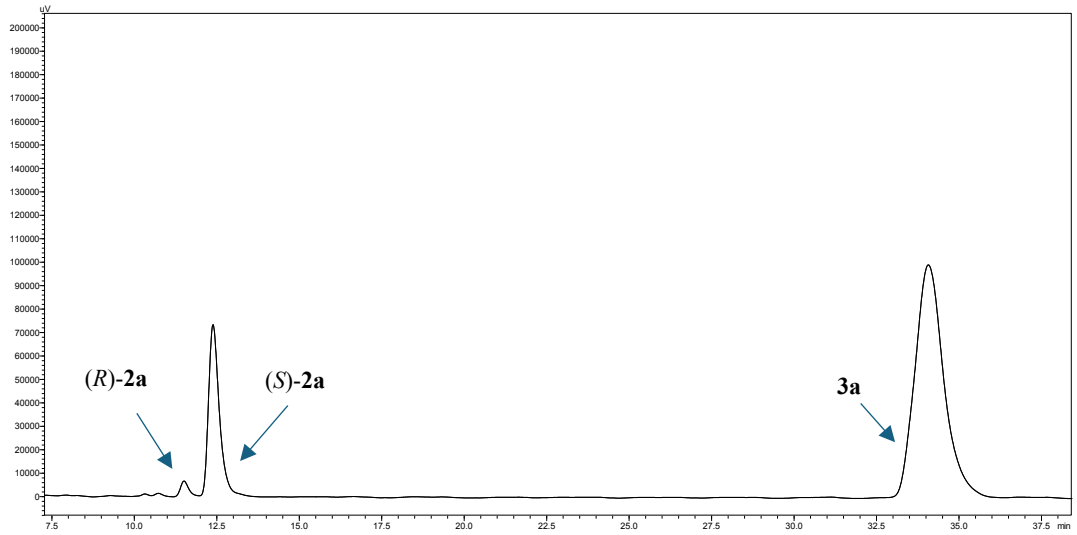

Figure S49. HPLC chromatograms of 3-(hydroxymethyl)-2-(naphthalen-1-yl) benzaldehyde (**3a**) produced by ADH-R2-catalyzed reaction, 24 h.

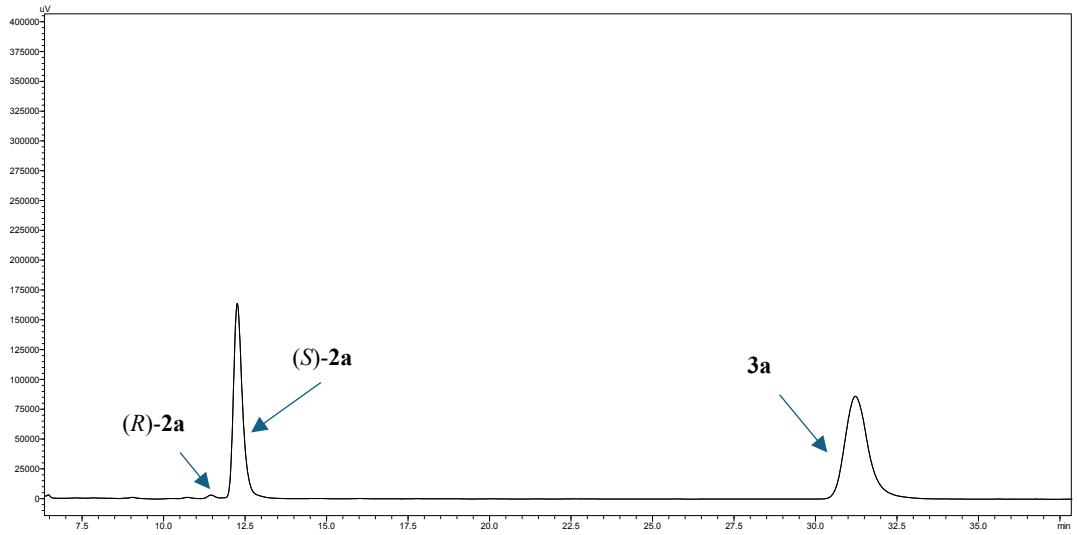

Figure S50. HPLC chromatograms of 3-(hydroxymethyl)-2-(naphthalen-1-yl) benzaldehyde (**3a**) produced by ADH-R4-catalyzed reaction, 24 h.

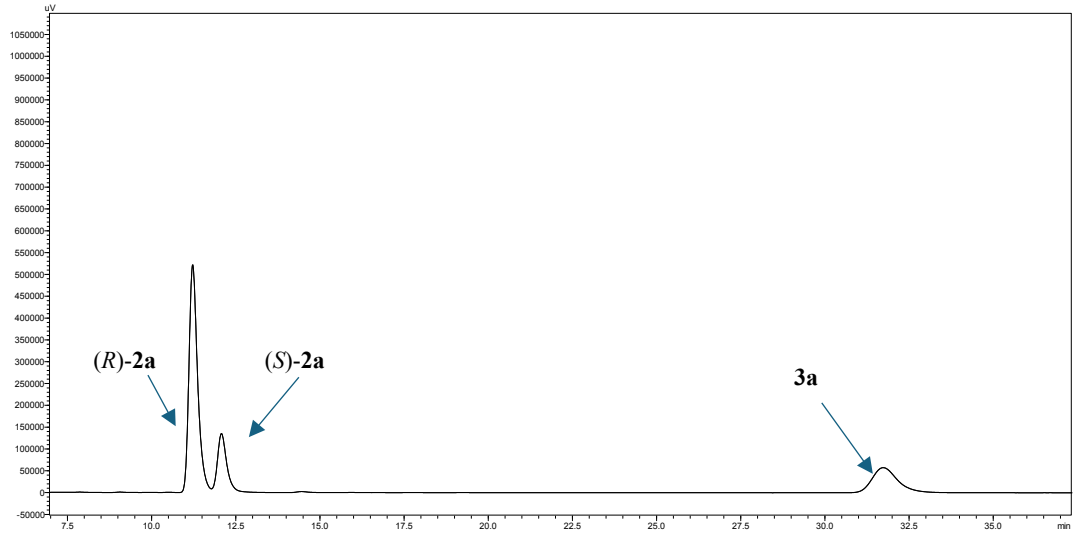

Figure S51. HPLC chromatograms of 3-(hydroxymethyl)-2-(naphthalen-1-yl) benzaldehyde (**3a**) produced by ADH-R7-catalyzed reaction, 24 h.

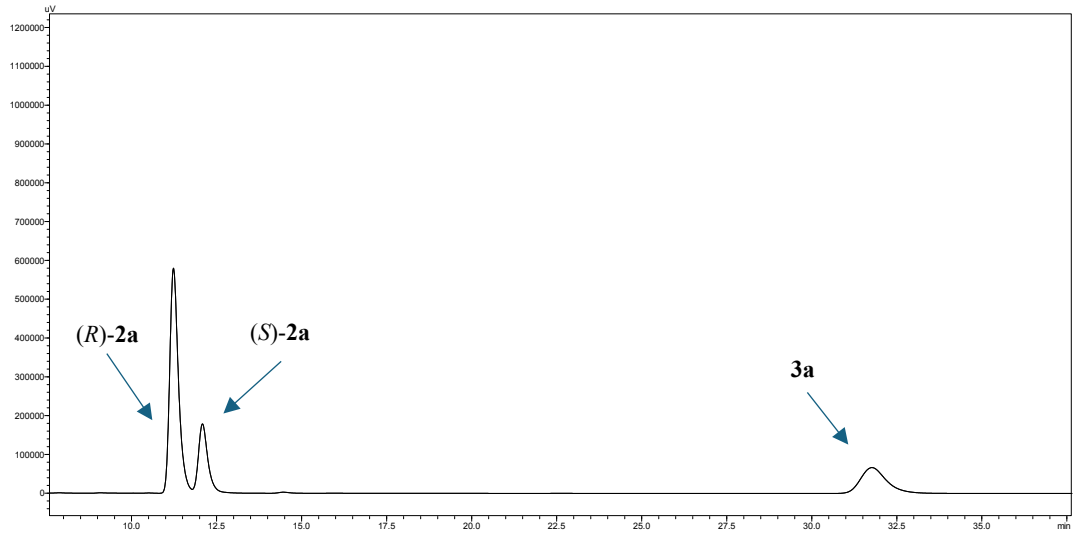

Figure S52. HPLC chromatograms of 3-(hydroxymethyl)-2-(naphthalen-1-yl) benzaldehyde (**3a**) produced by ADH-R9-catalyzed reaction, 24 h.

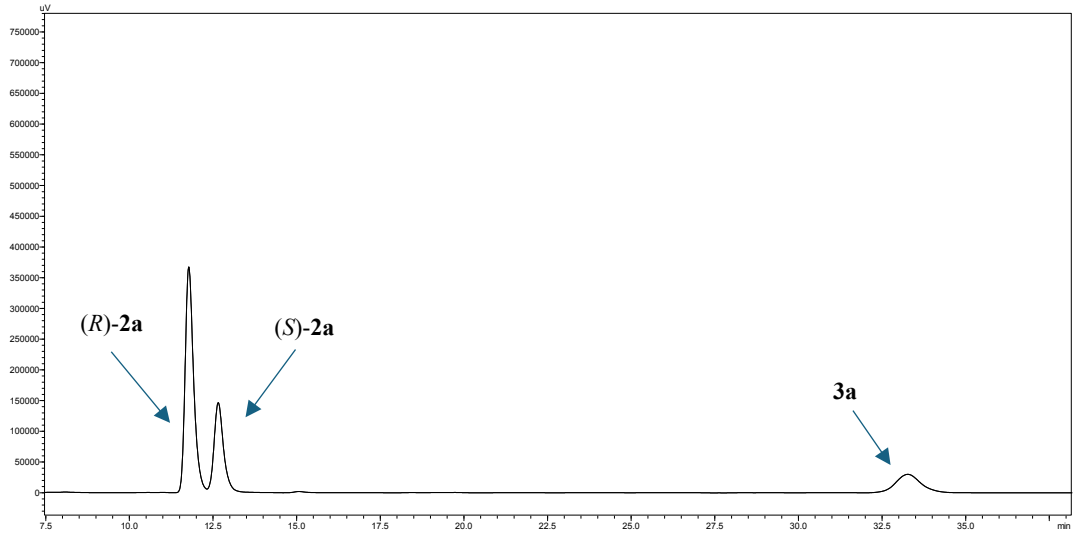

Figure S53. HPLC chromatograms of 3-(hydroxymethyl)-2-(naphthalen-1-yl) benzaldehyde (**3a**) produced by ADH-R10-catalyzed reaction, 24 h.

.

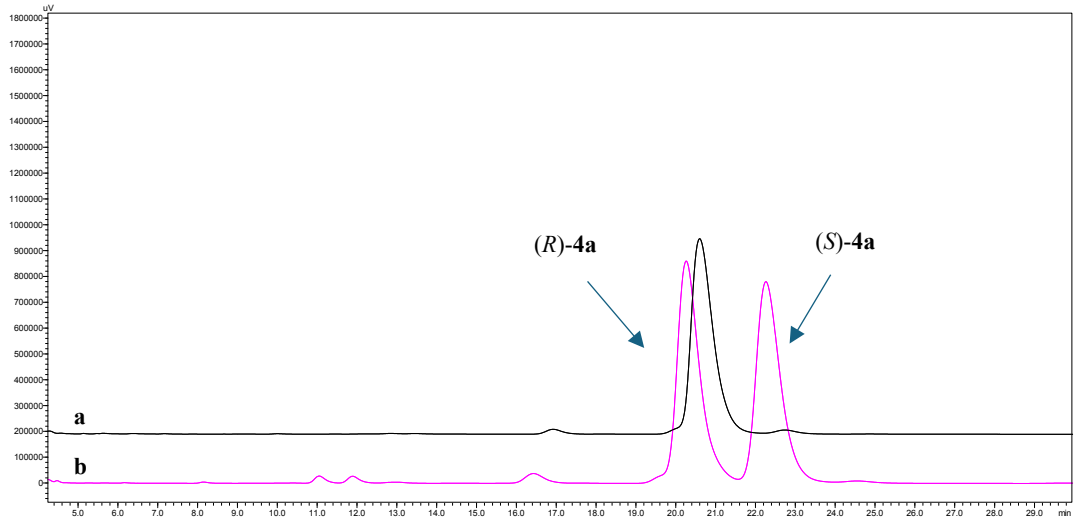

Figure S54. HPLC chromatograms of 3-(hydroxymethyl)-2-(naphthalen-1-yl) benzaldehyde oxime (**4a**) (**a**: product of chiral substrates; **b**: racemic standard) (AD-H, eluents: n-hexane/i-PrOH = 90/10, 254 nm, 30 °C, flow rate: 1.0 mL/min，retention time [min]: 20.261/22.261).

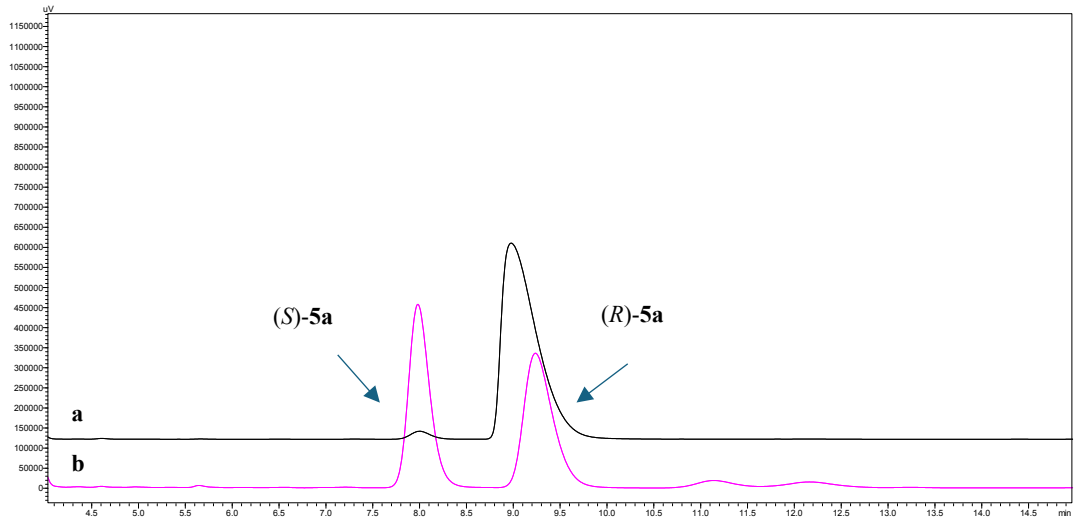

Figure S55. HPLC chromatograms of (2-(naphthalen-1-yl)-3-vinylphenyl) methanol (**5a**) (**a**: product of chiral substrates; **b**: racemic standard) (Chiralcel® OJ-H, eluents: n-hexane/i-PrOH = 90/10, 254 nm, 30 °C, flow rate: 1.0 mL/min，retention time [min]: 7.982/9.236).

.

10. ^{1}H and ^{13}C NMR spectra

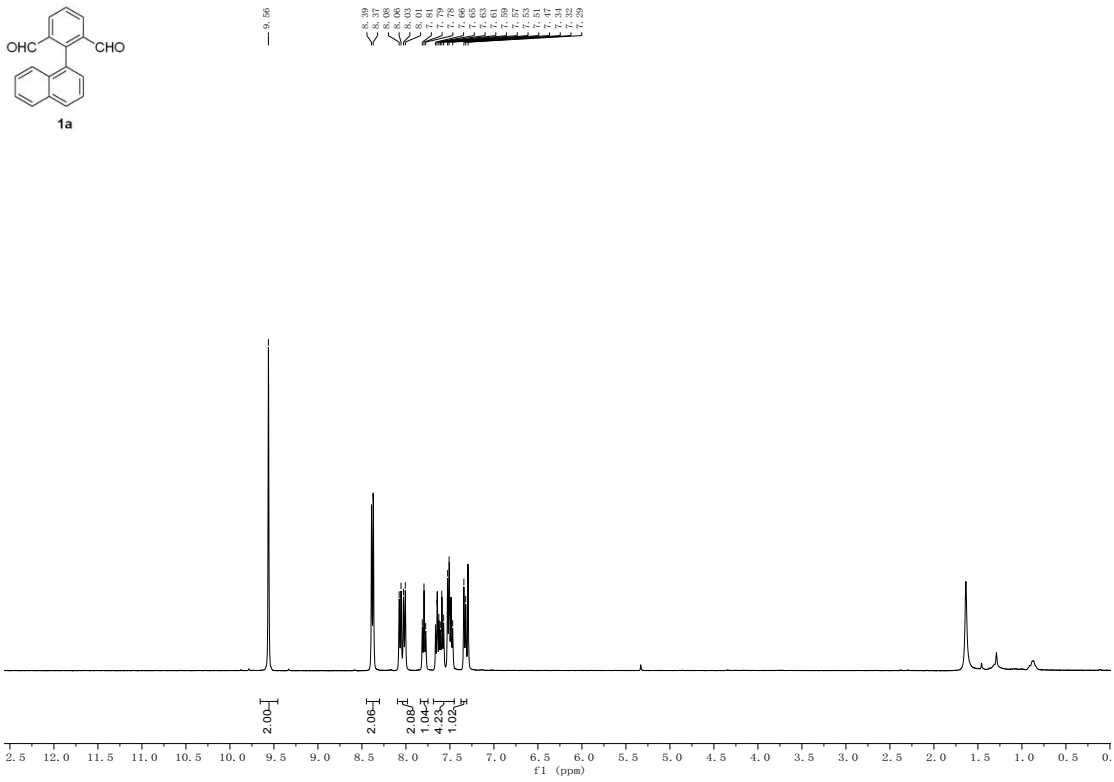

Figure S56. ^{1}H NMR spectra of **1a** in $CDCl_3$.

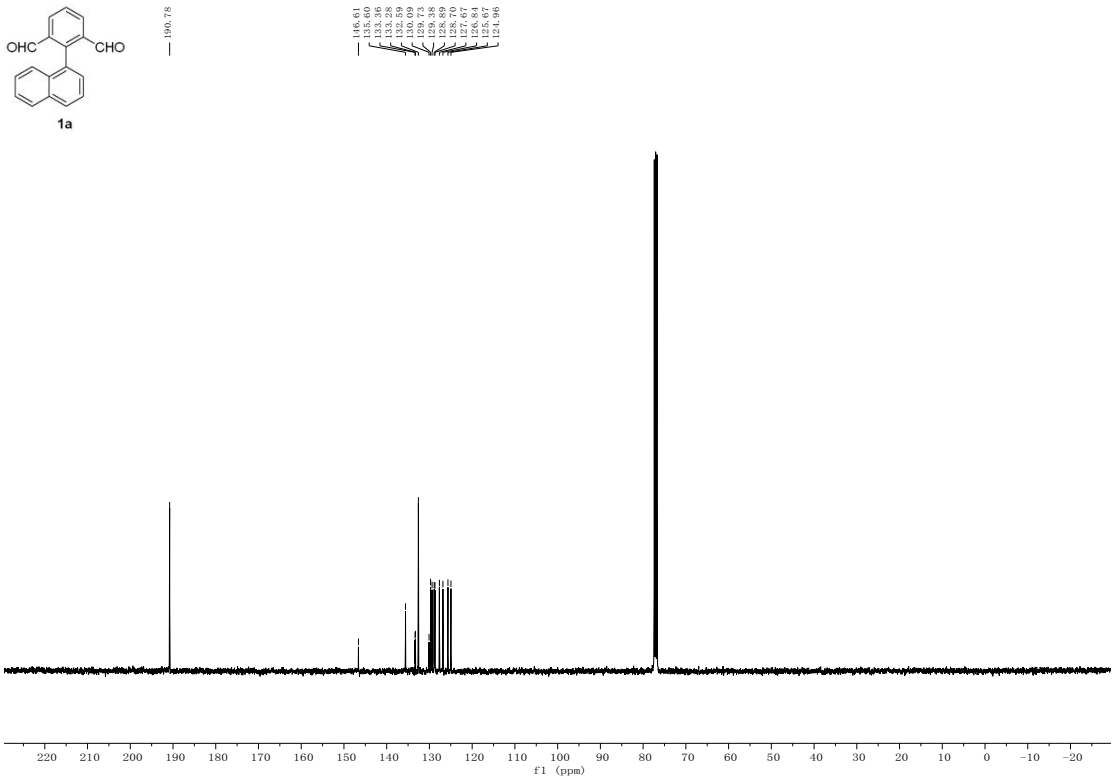

Figure S57. ^{13}C NMR spectra of **1a** in $CDCl_3$.

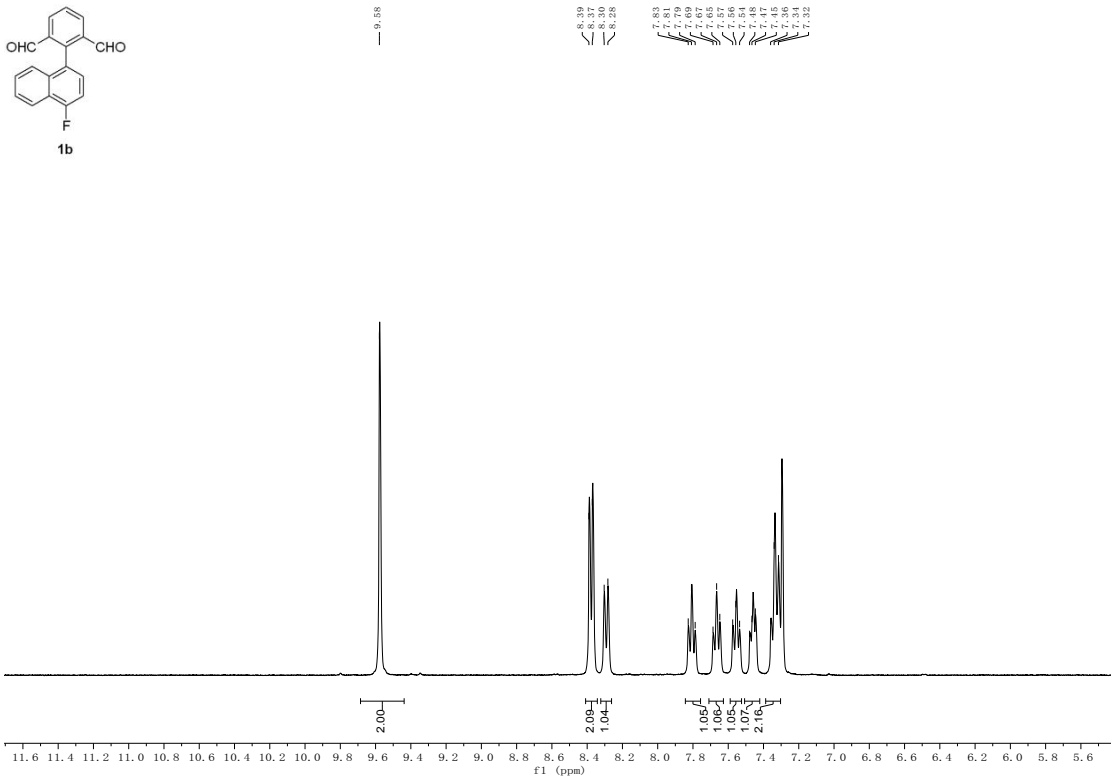

Figure S58. ^{1}H NMR spectra of **1b** in $CDCl_3$.

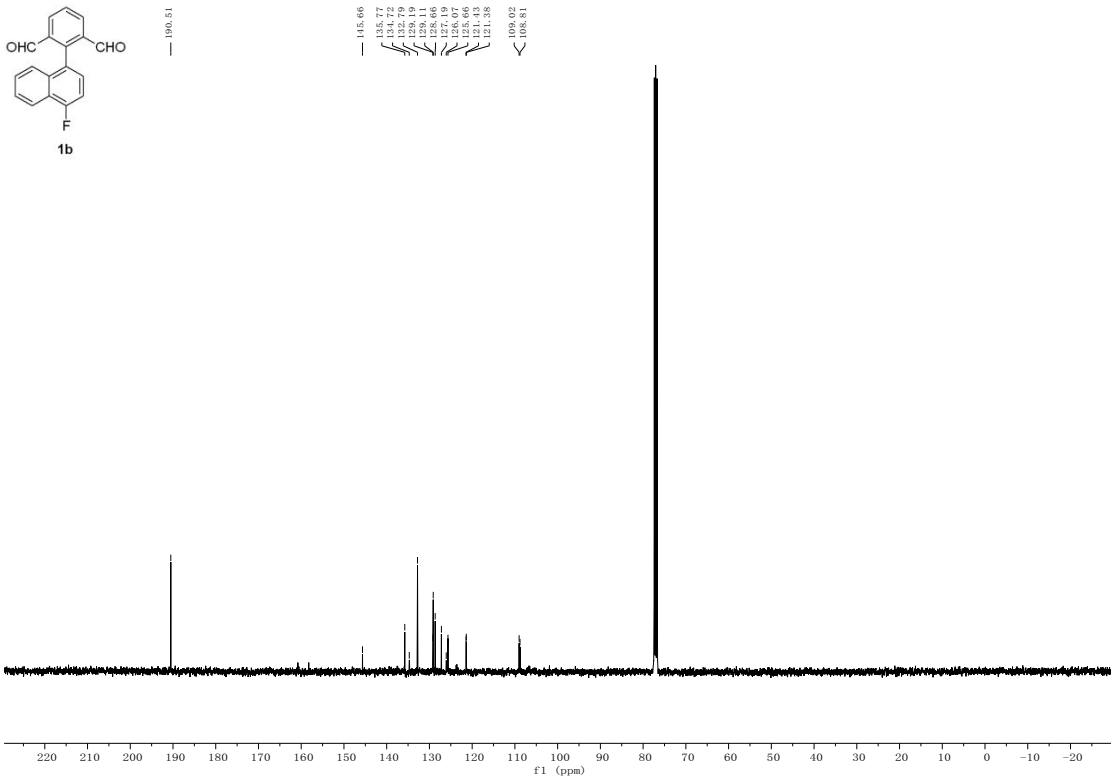

Figure S59. ^{13}C NMR spectra of **1b** in $CDCl_3$.

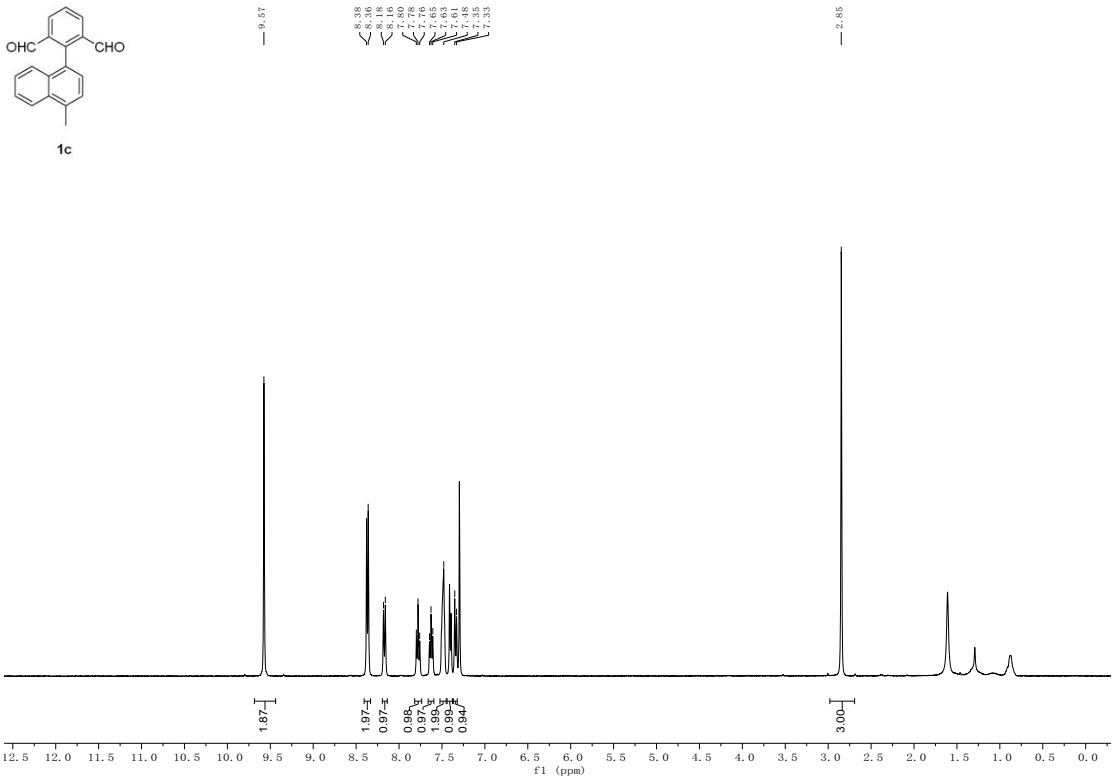

Figure S60. ^{1}H NMR spectra of **1c** in $CDCl_3$.

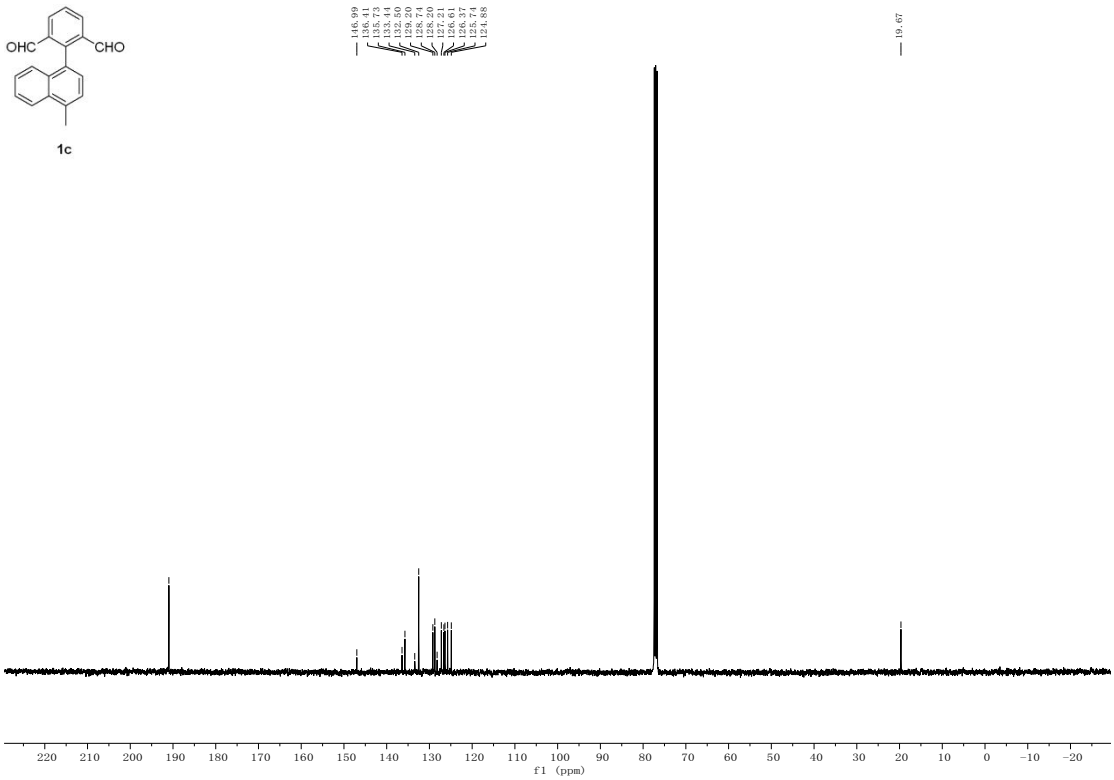

Figure S61. ^{13}C NMR spectra of **1c** in $CDCl_3$.

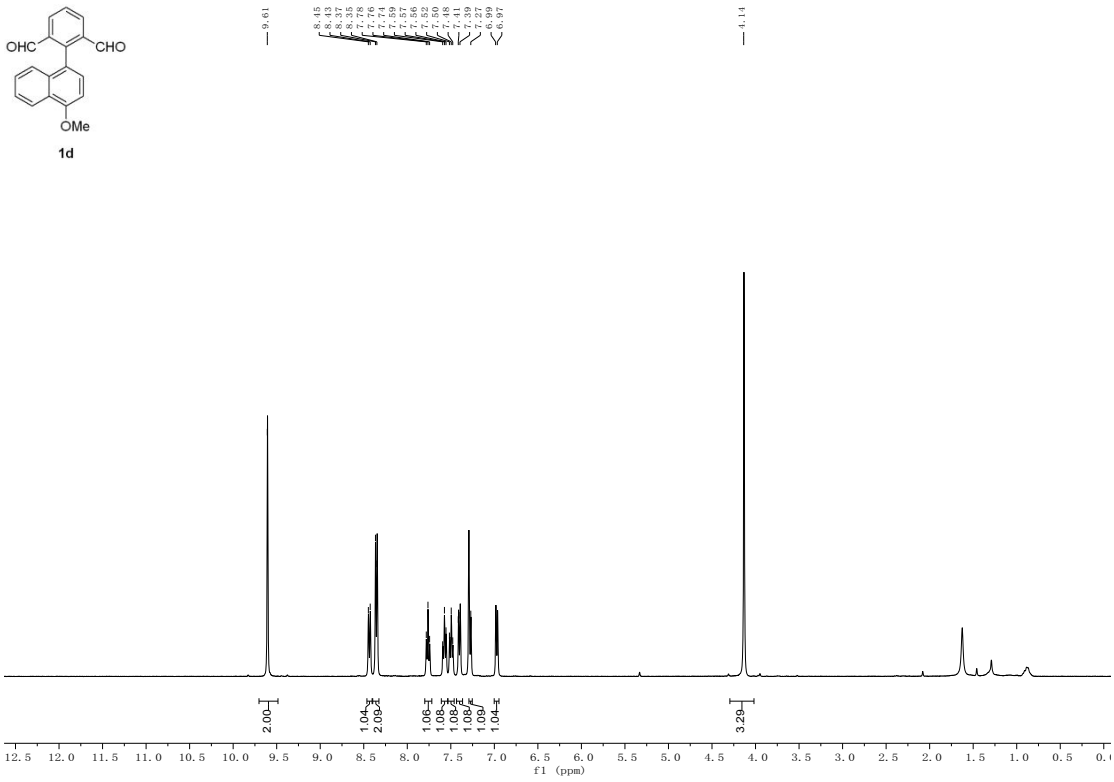

Figure S62. ^{1}H NMR spectra of **1d** in $CDCl_3$.

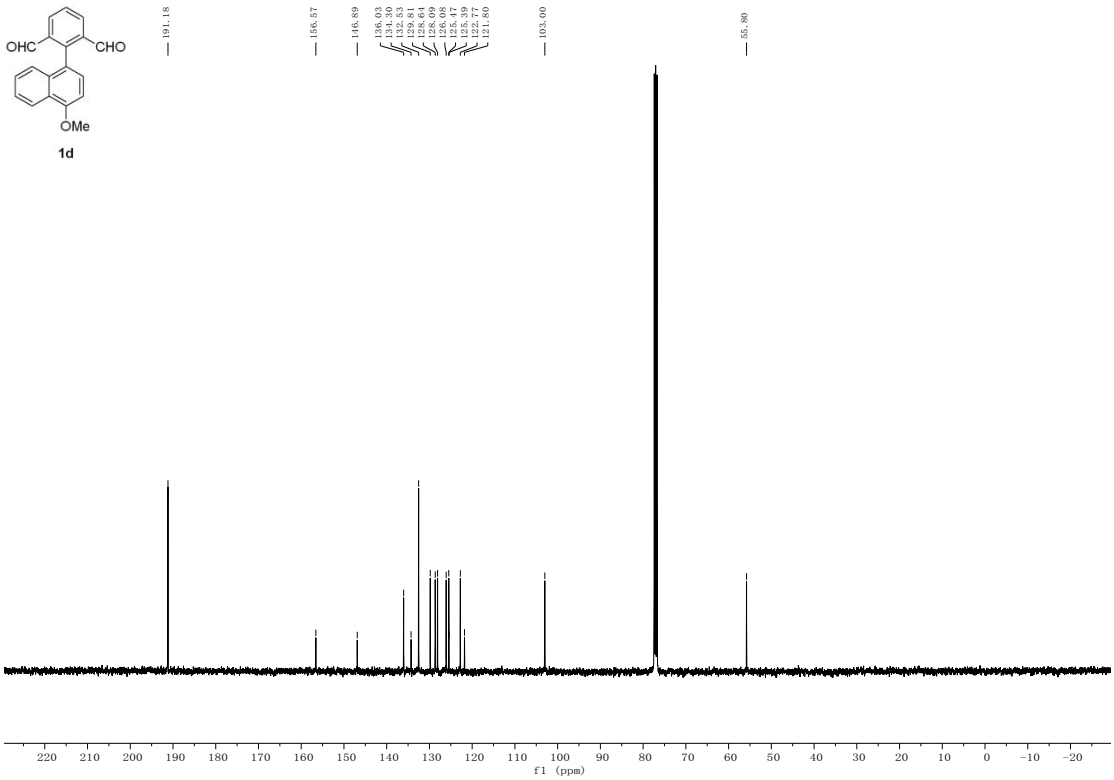

Figure S63. ^{13}C NMR spectra of **1d** in $CDCl_3$.

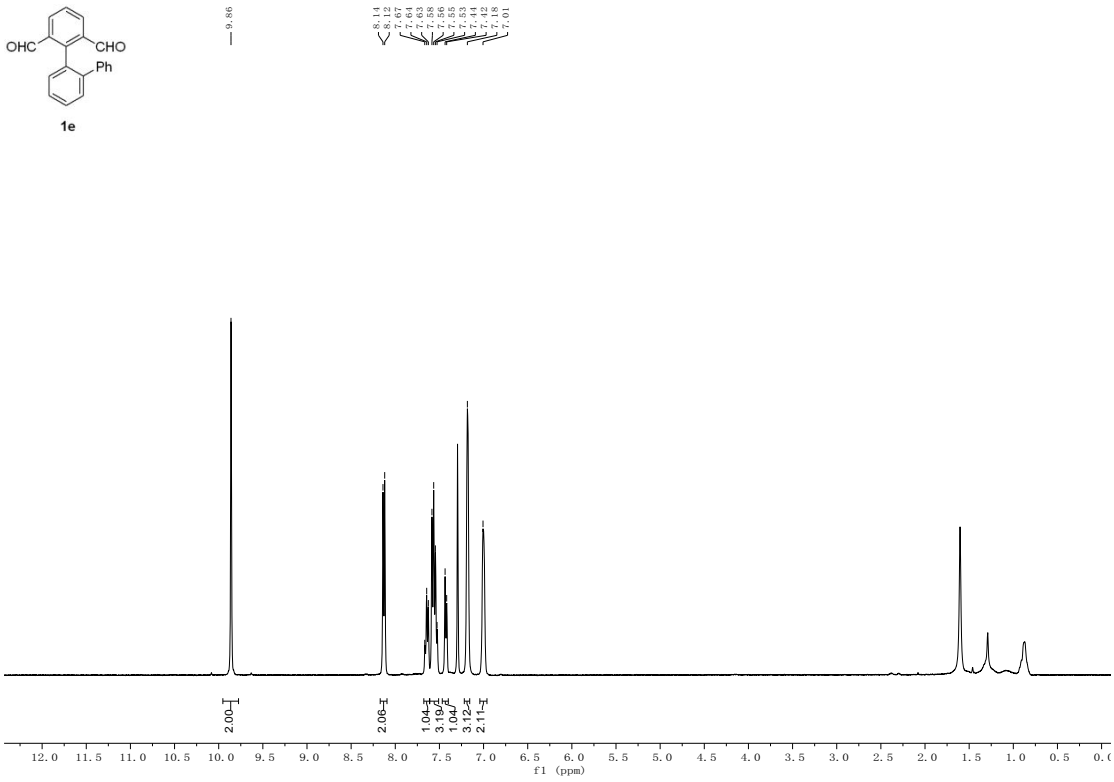

Figure S64. ^{1}H NMR spectra of **1e** in $CDCl_3$.

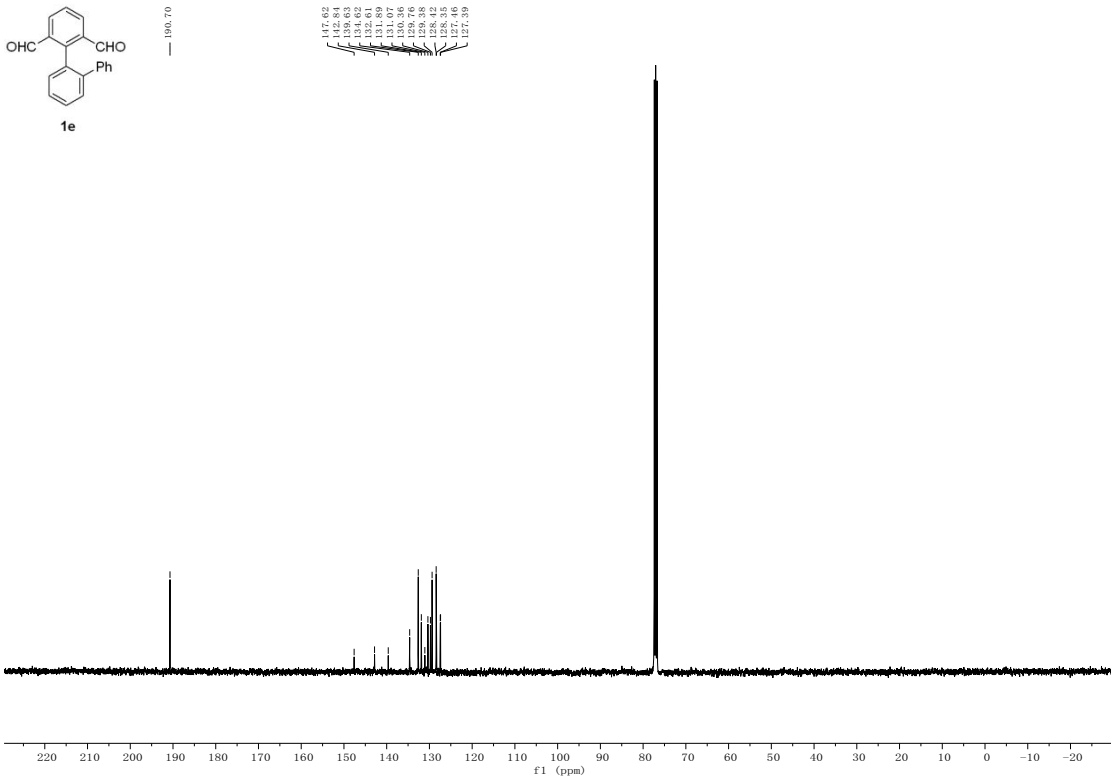

Figure S65. ^{13}C NMR spectra of **1e** in $CDCl_3$.

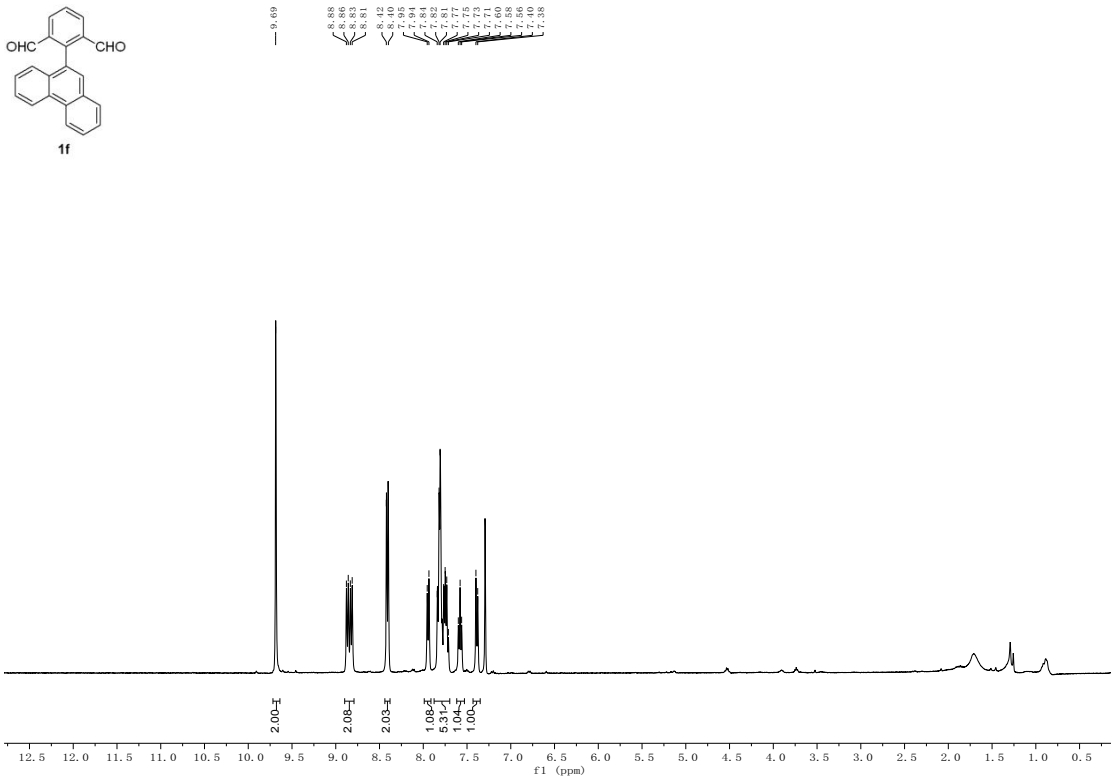

Figure S66. ^{1}H NMR spectra of **1f** in $CDCl_3$.

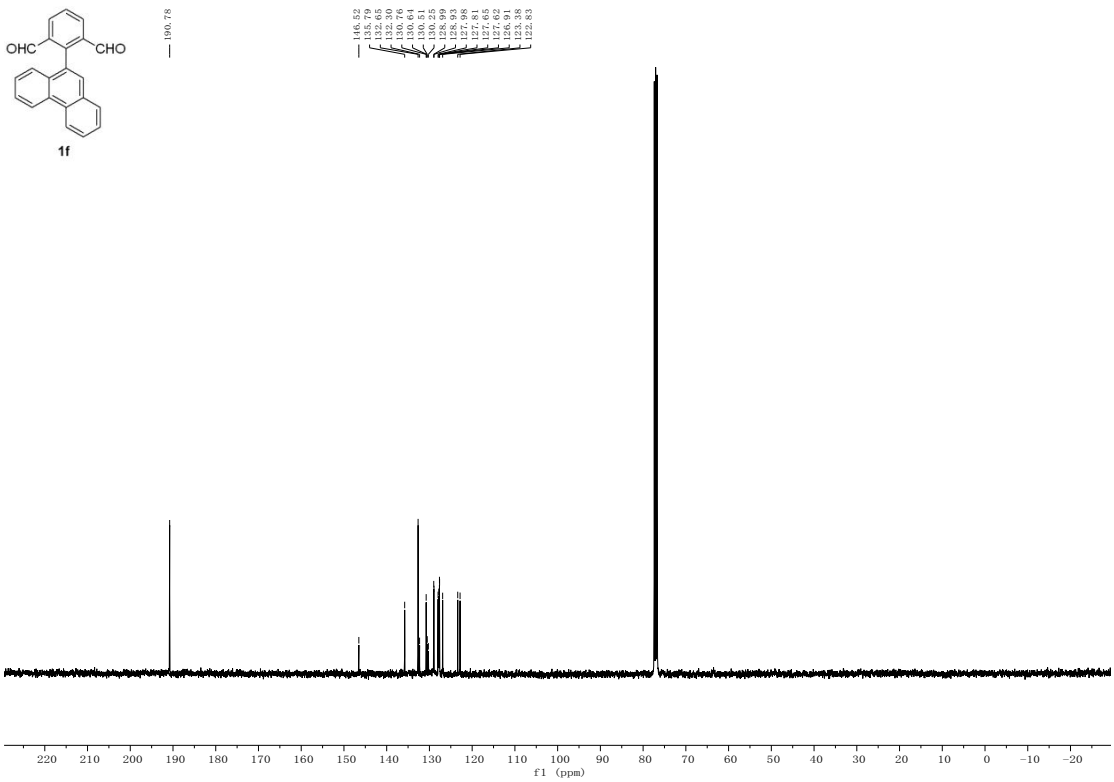

Figure S67. ^{13}C NMR spectra of **1f** in $CDCl_3$.

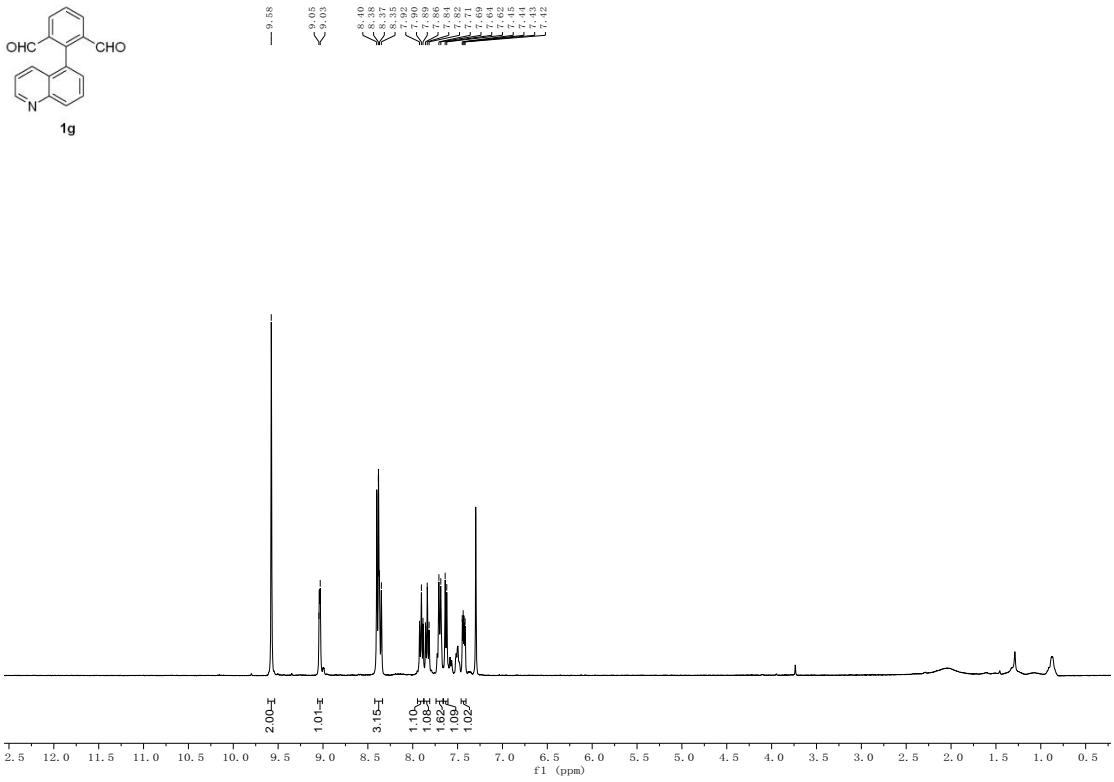

Figure S68. ^{1}H NMR spectra of **1g** in $CDCl_3$.

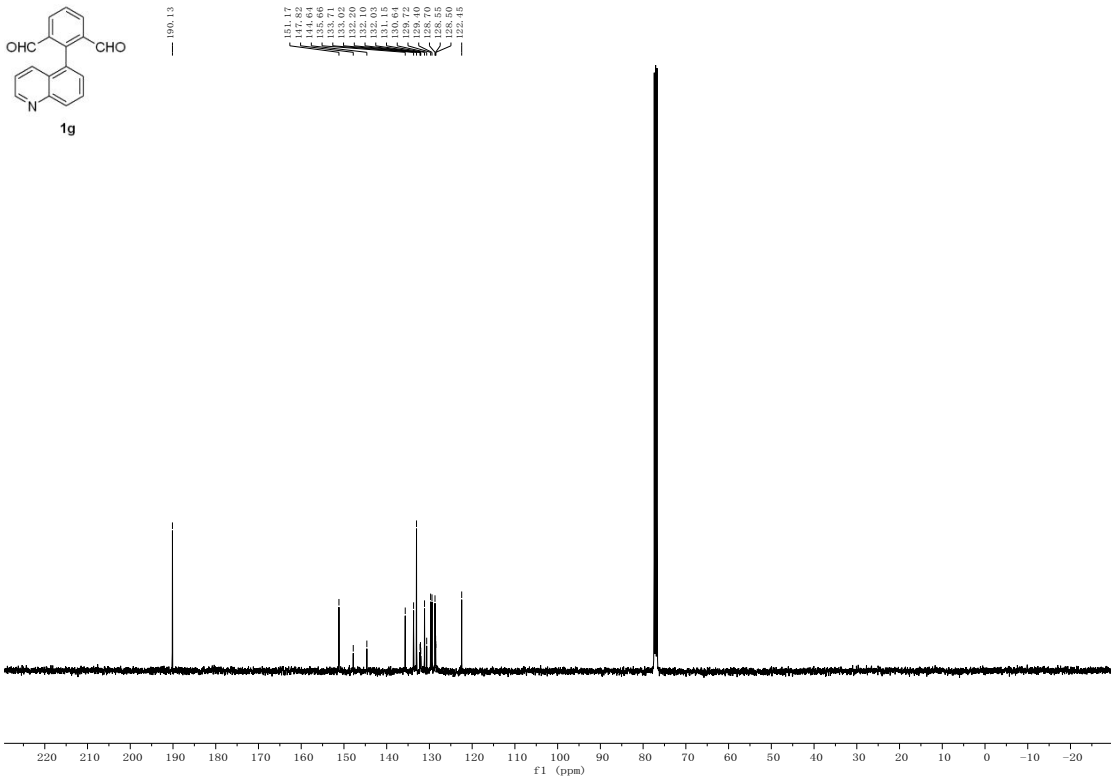

Figure S69. ^{13}C NMR spectra of **1g** in $CDCl_3$.

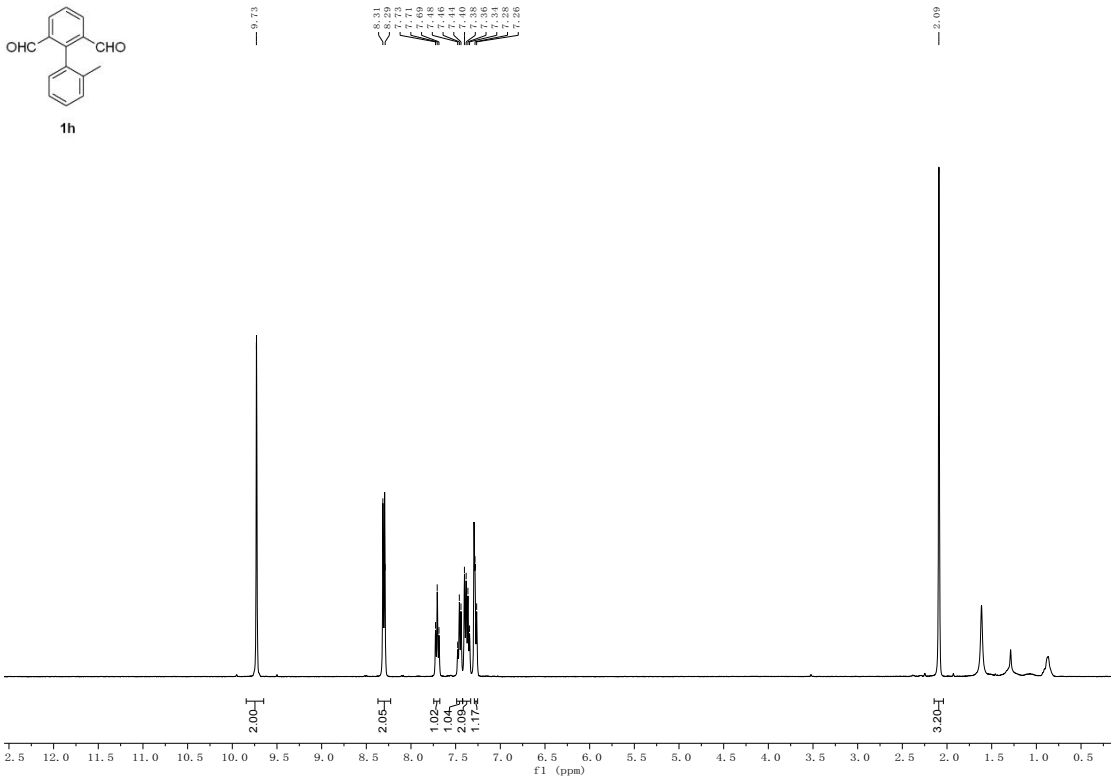

Figure S70. ^{1}H NMR spectra of **1h** in $CDCl_3$.

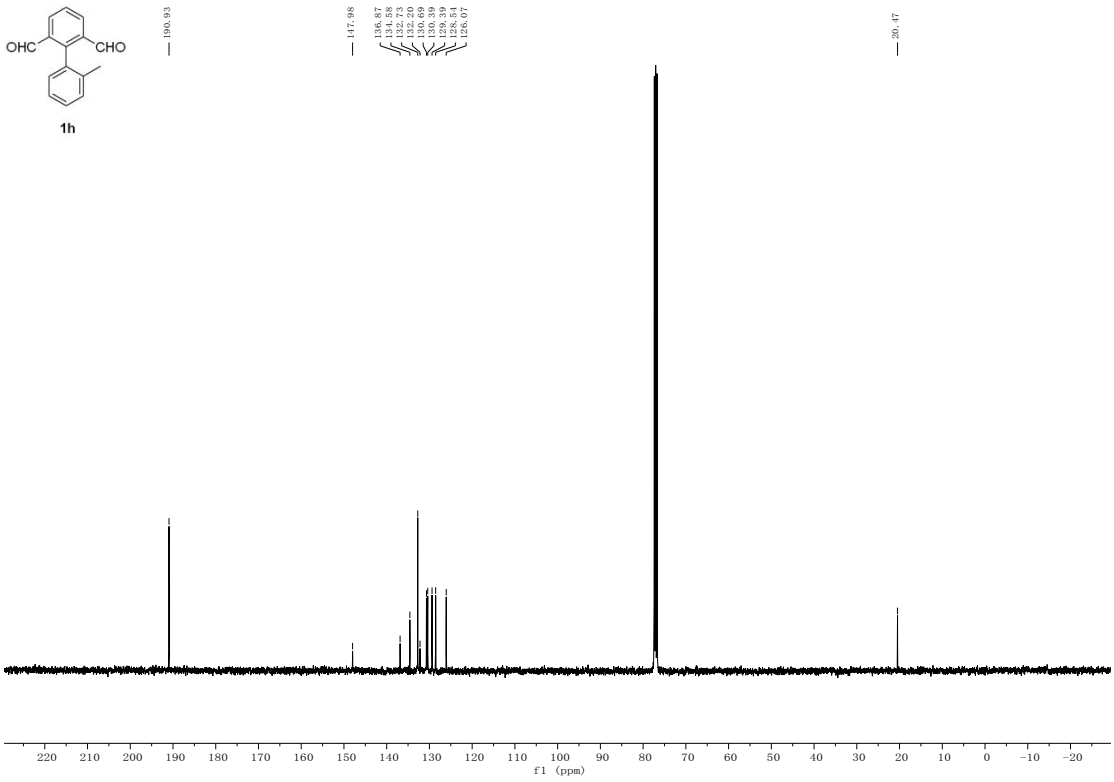

Figure S71. ^{13}C NMR spectra of **1h** in $CDCl_3$.

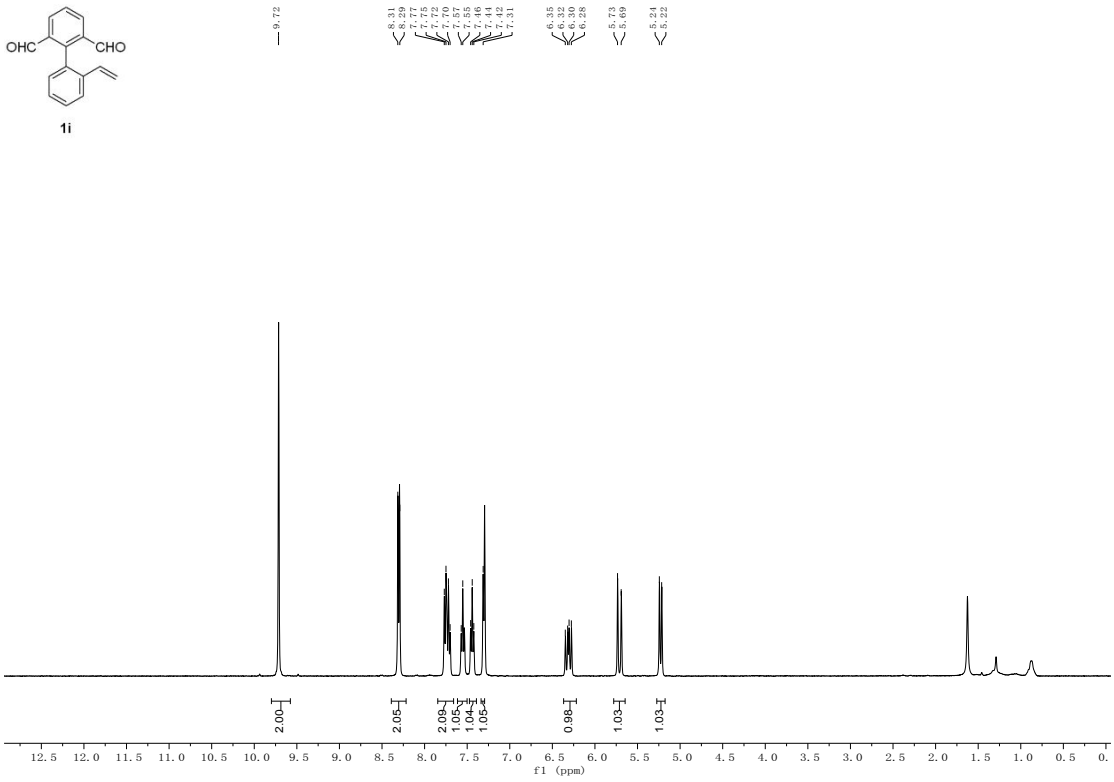

Figure S72. ^{1}H NMR spectra of **1i** in $CDCl_3$.

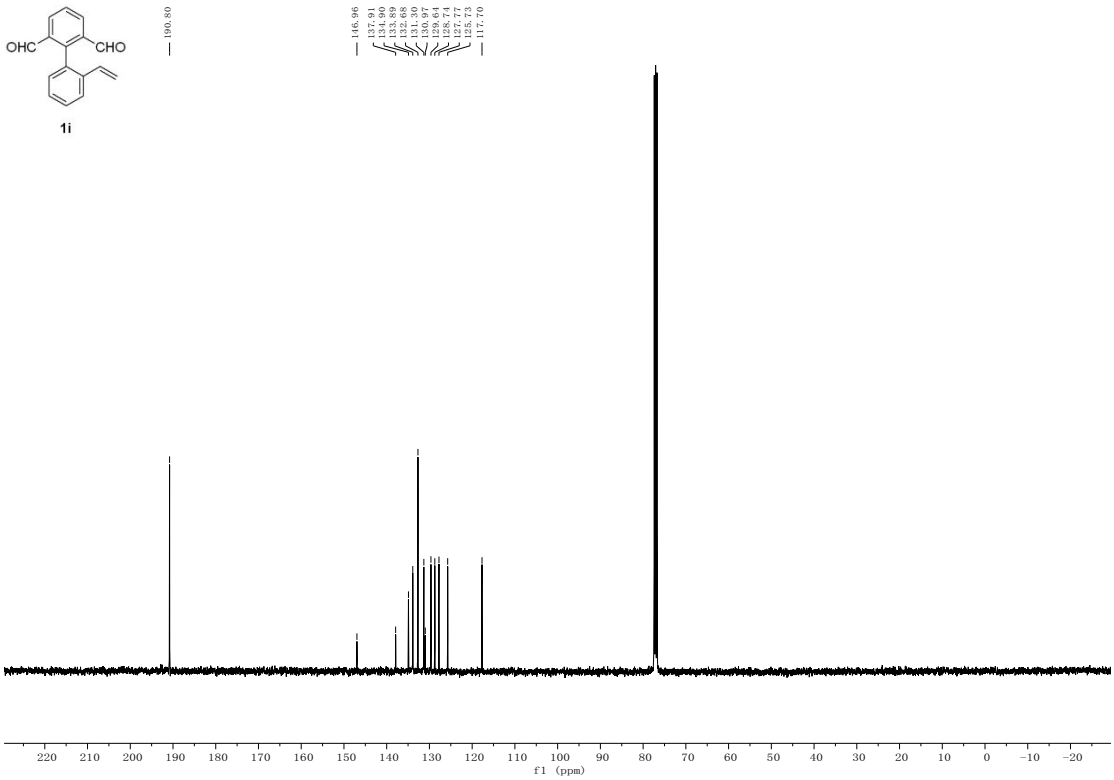

Figure S73. ^{13}C NMR spectra of **1i** in $CDCl_3$.

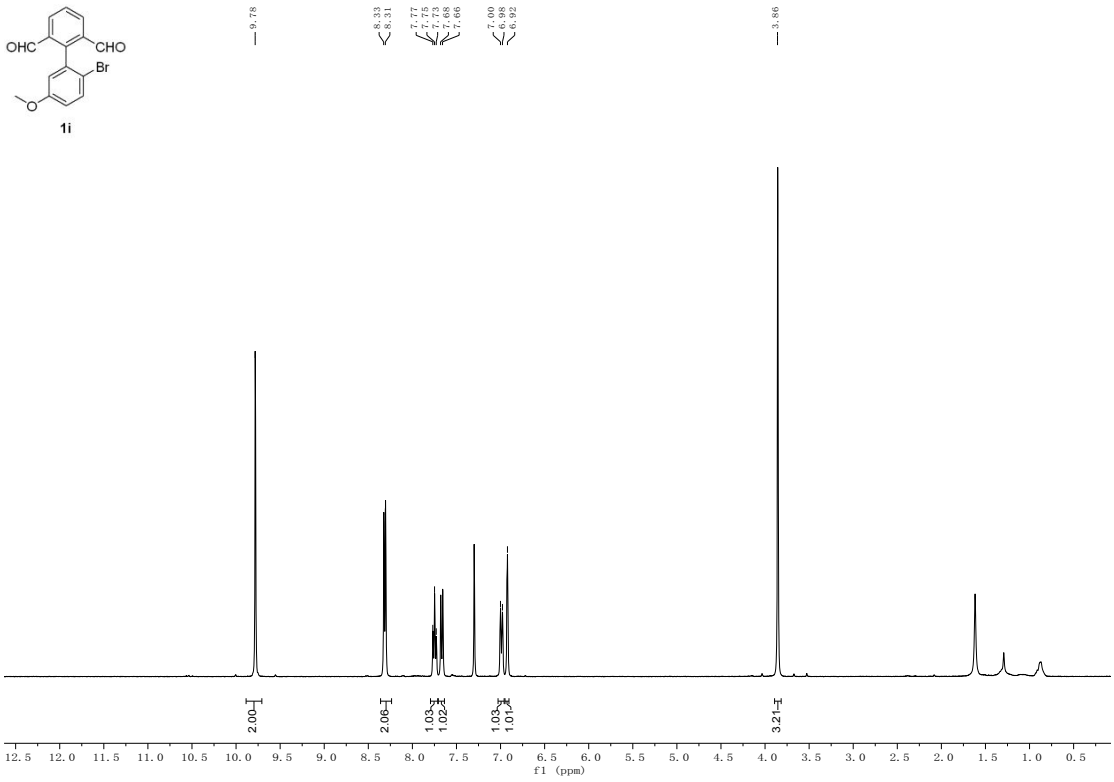

Figure S74. ^{1}H NMR spectra of **1j** in $CDCl_3$.

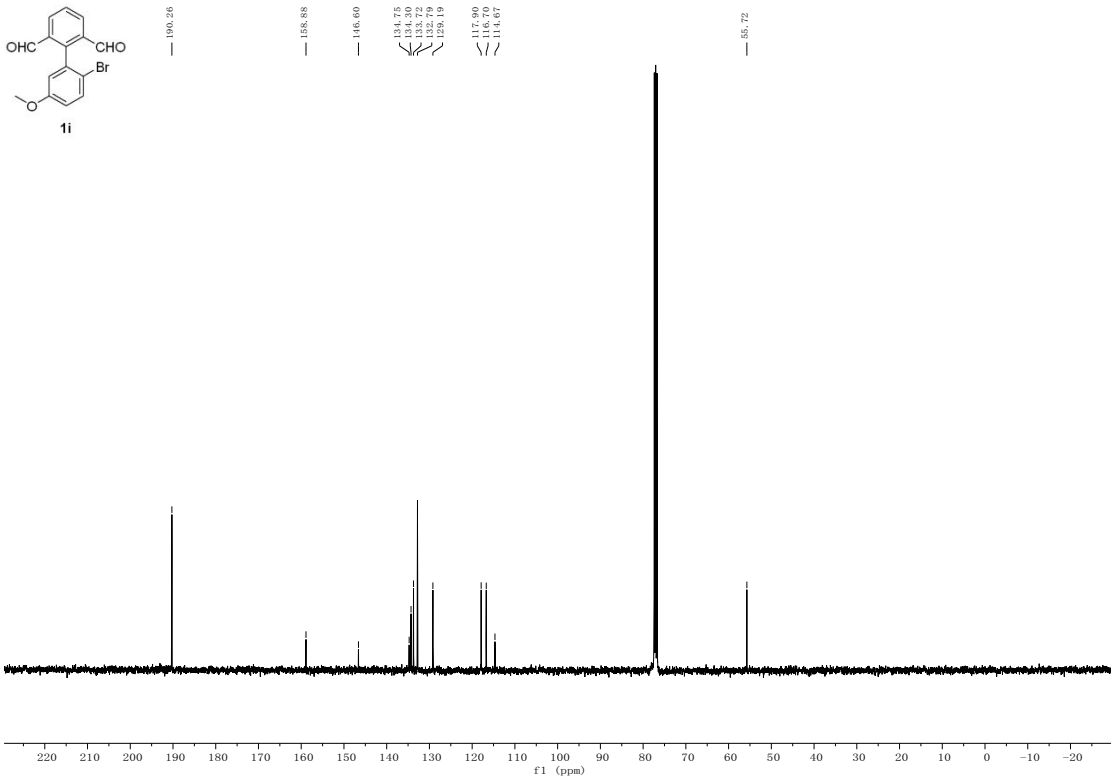

Figure S75. ^{13}C NMR spectra of **1j** in $CDCl_3$.

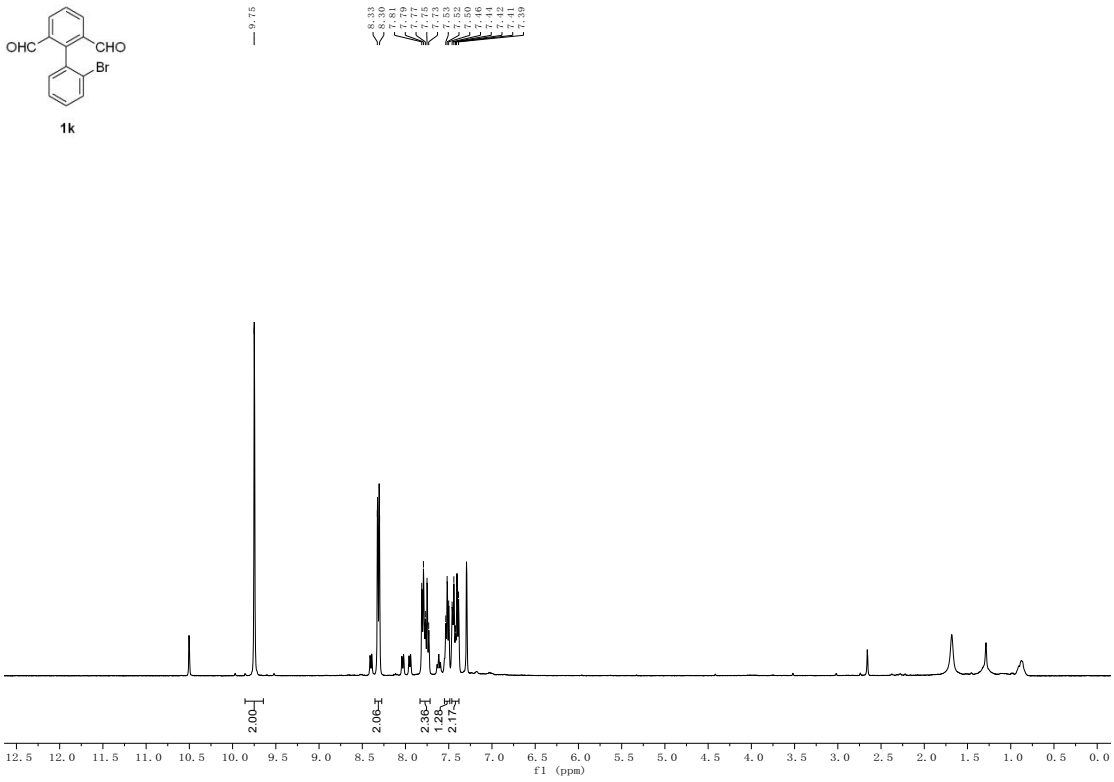

Figure S76. ^{1}H NMR spectra of **1k** in $CDCl_3$.

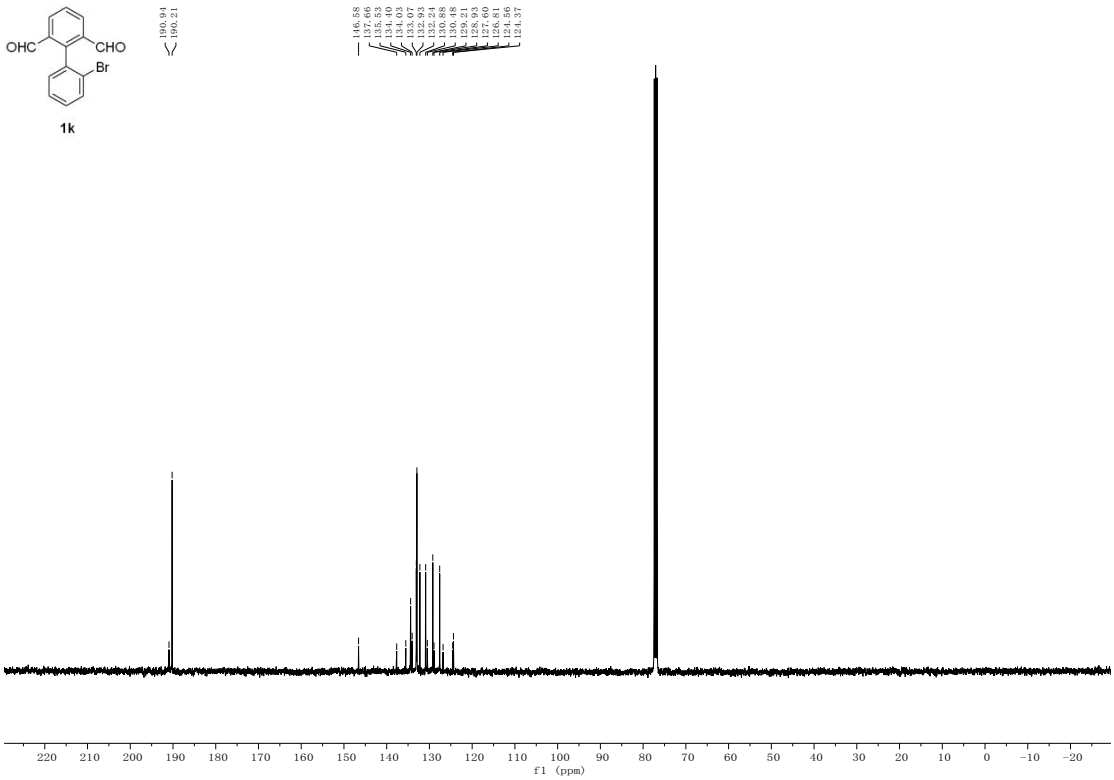

Figure S77. ^{13}C NMR spectra of **1k** in $CDCl_3$.

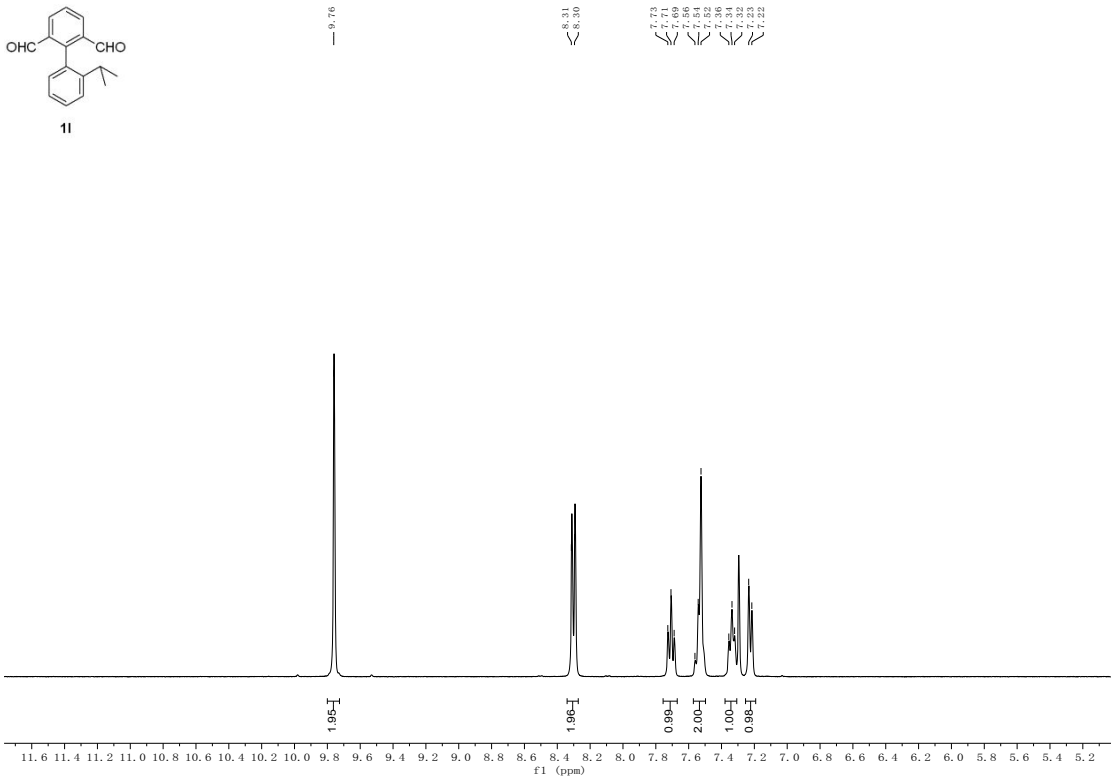

Figure S78. ^{1}H NMR spectra of **1l** in $CDCl_3$.

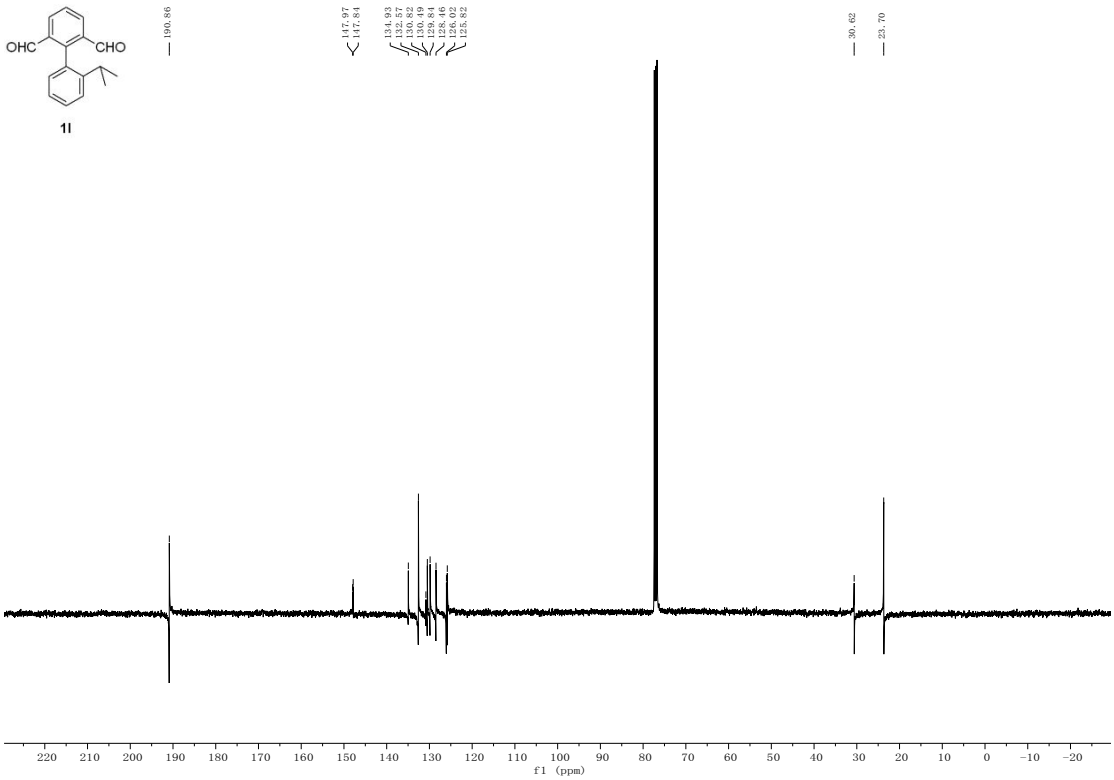

Figure S79. ^{13}C NMR spectra of **1l** in $CDCl_3$.

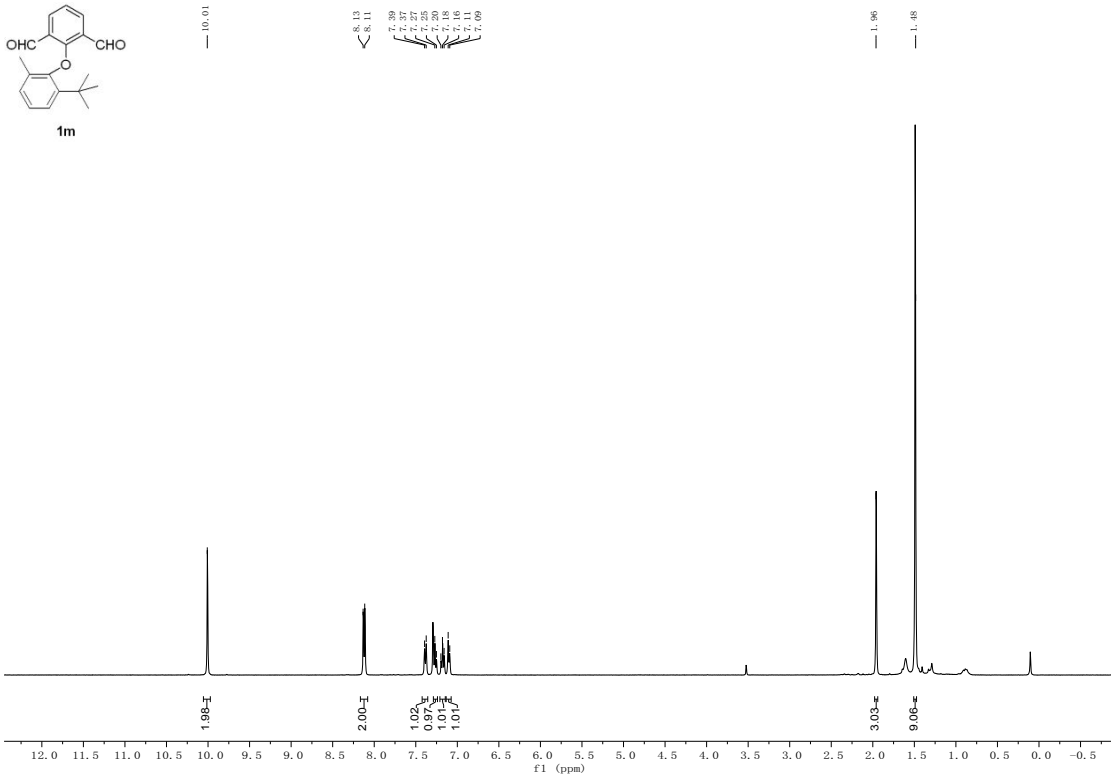

Figure S80. ^{1}H NMR spectra of **1m** in $CDCl_3$.

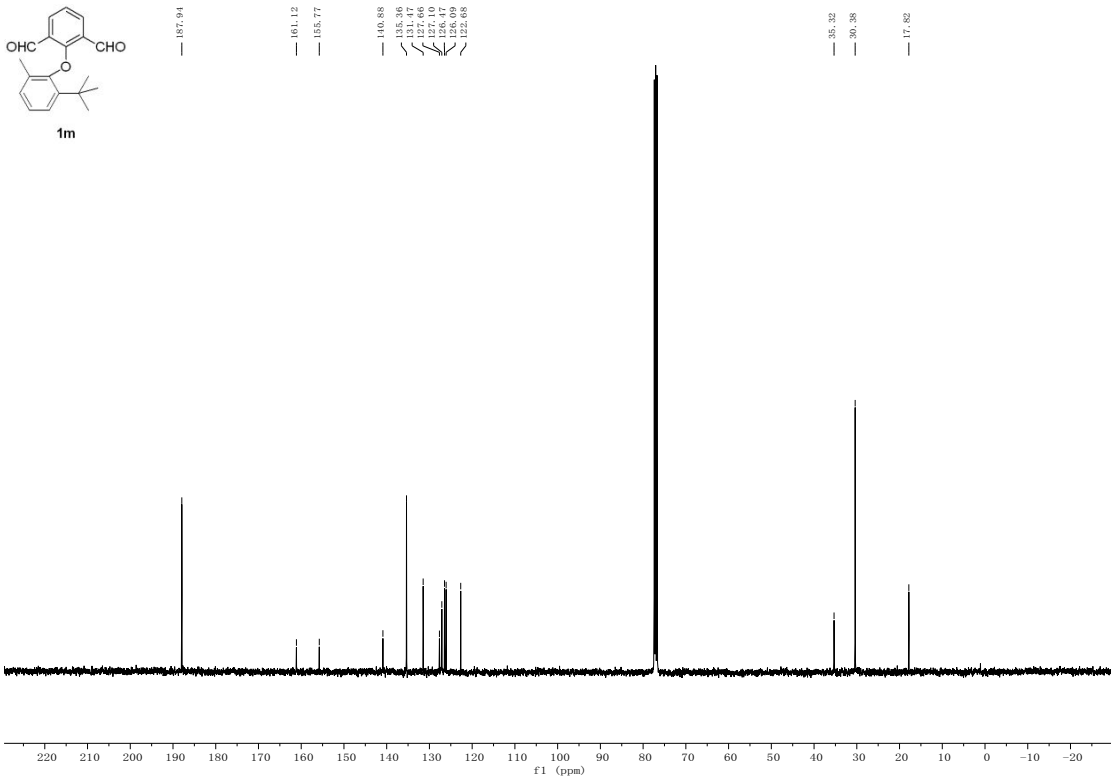

Figure S81. ^{13}C NMR spectra of **1m** in $CDCl_3$.

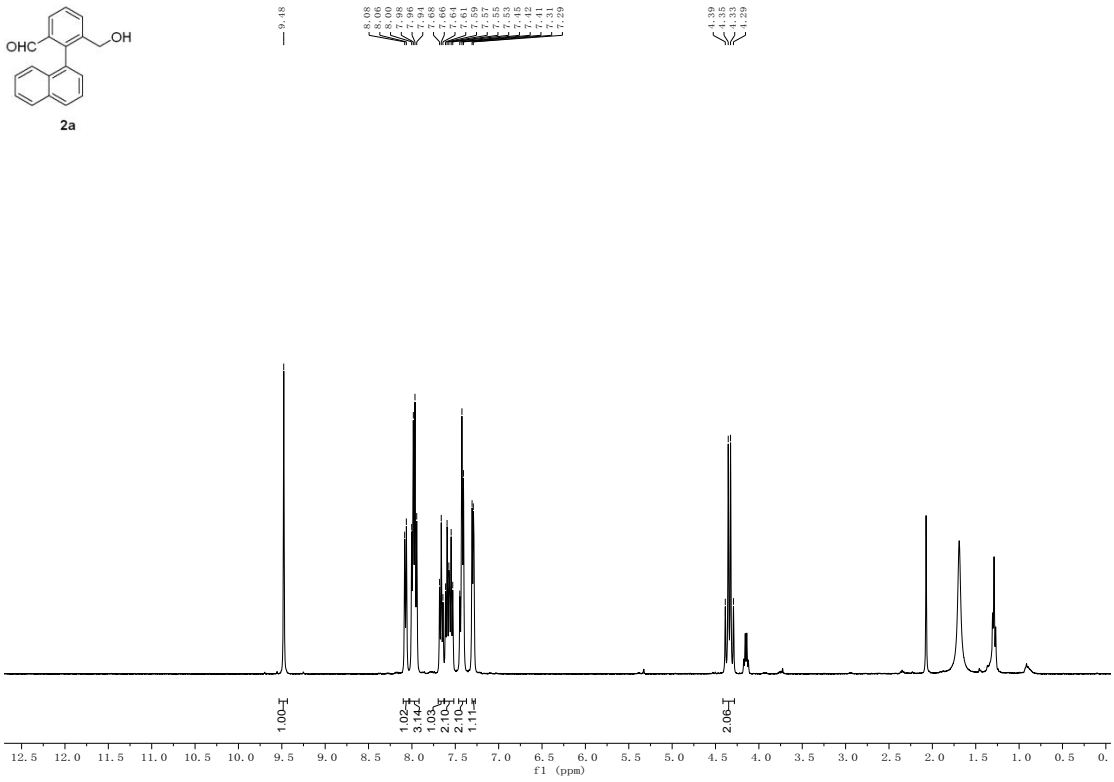

Figure S82. ^{1}H NMR spectra of **2a** in $CDCl_3$.

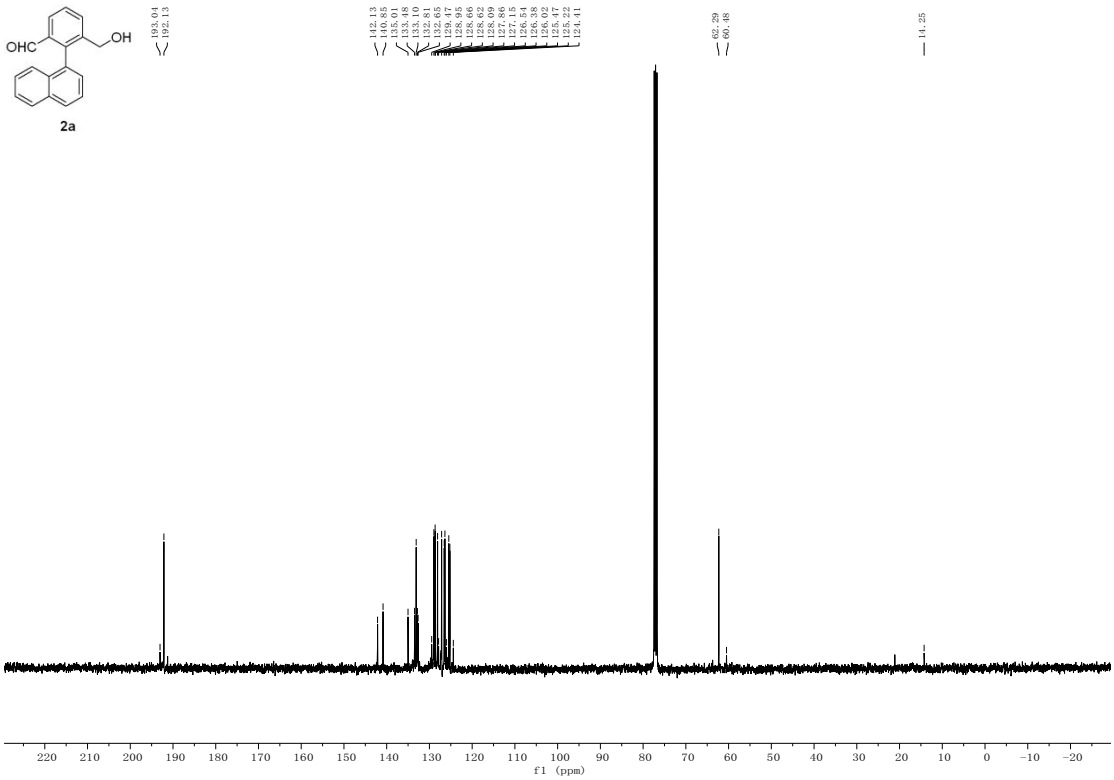

Figure S83. ^{13}C NMR spectra of **2a** in $CDCl_3$.

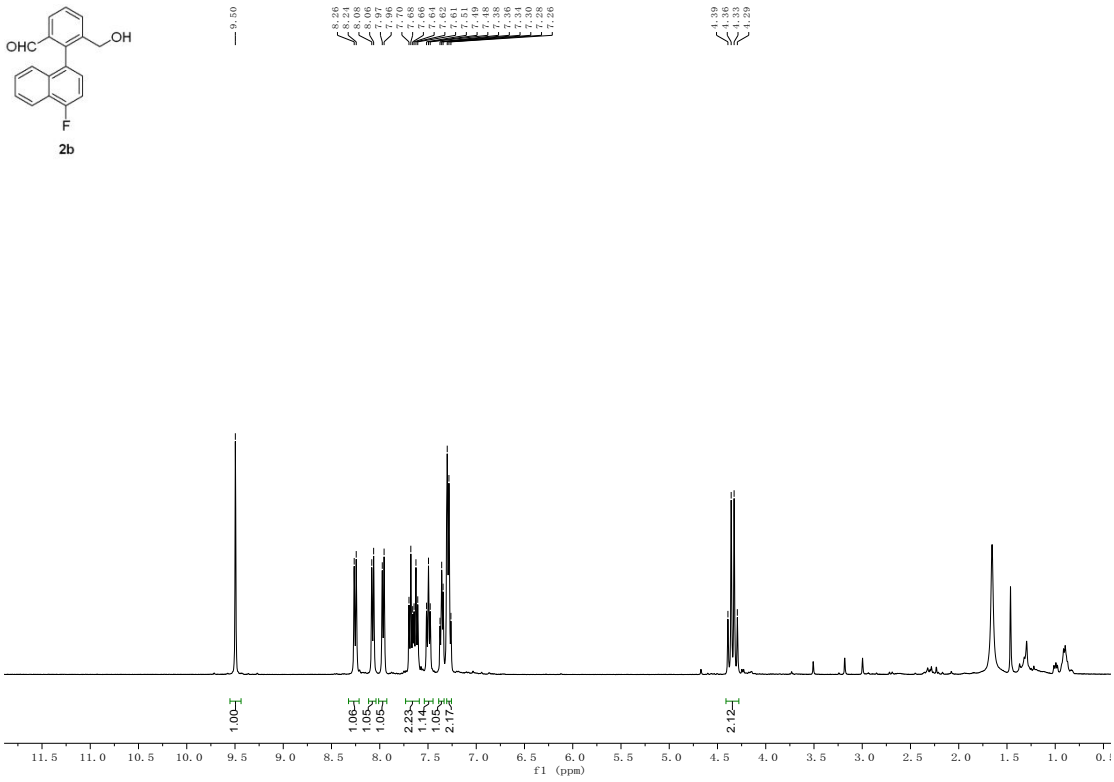

Figure S84. ^{1}H NMR spectra of **2b** in $CDCl_3$.

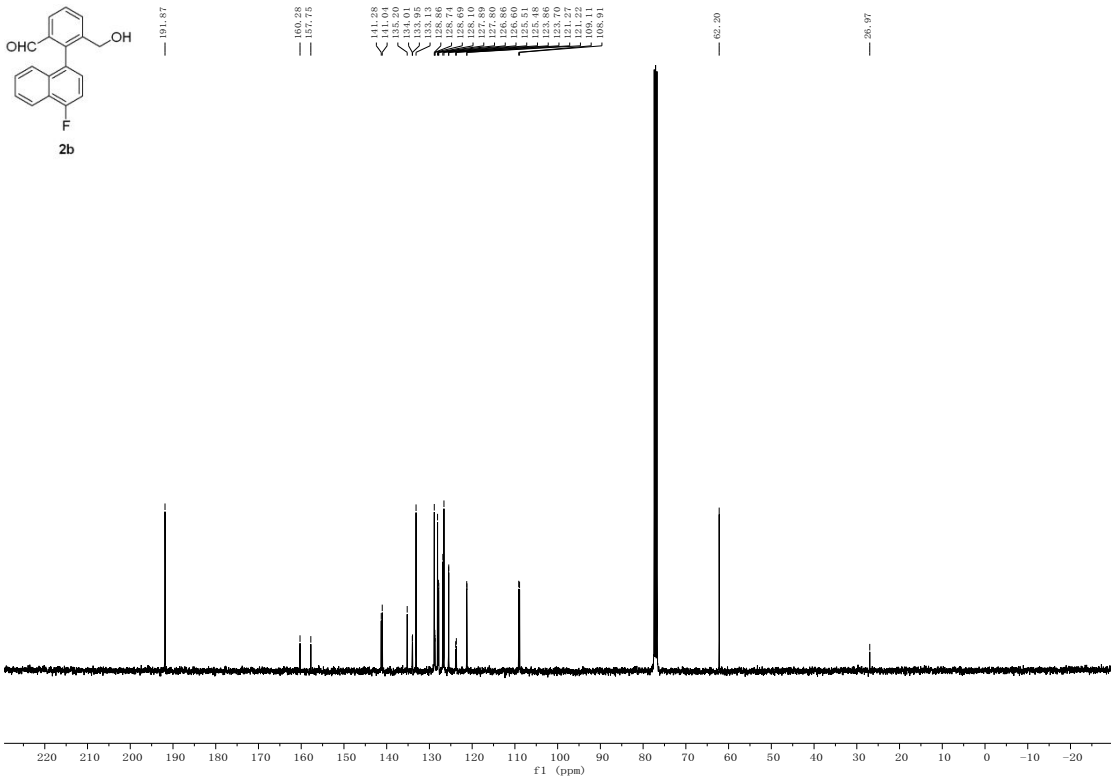

Figure S85. ^{13}C NMR spectra of **2b** in $CDCl_3$.

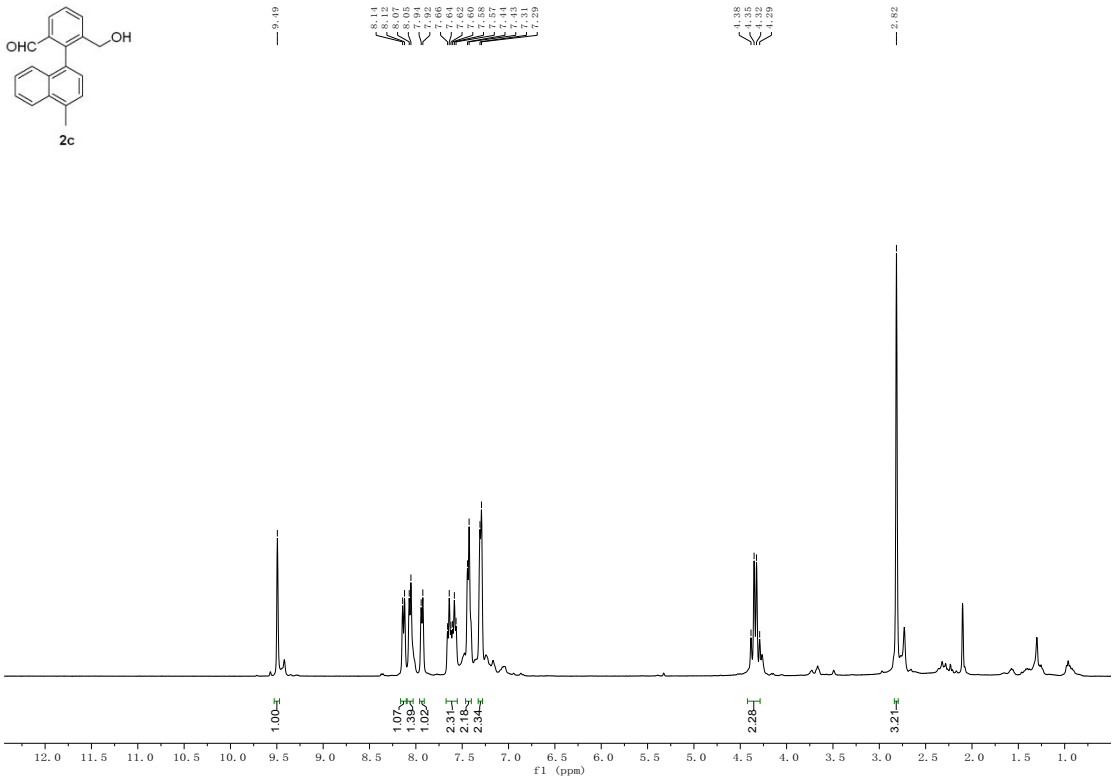

Figure S86. ^{1}H NMR spectra of **2c** in $CDCl_3$.

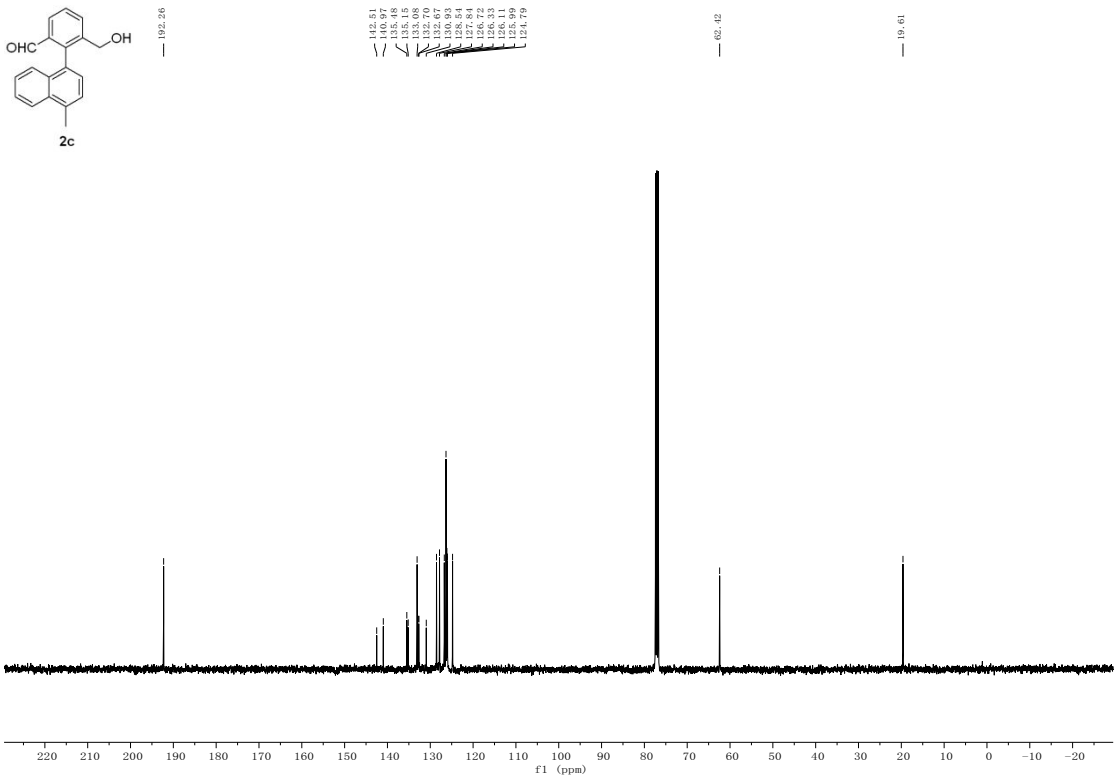

Figure S87. ^{13}C NMR spectra of **2c** in $CDCl_3$.

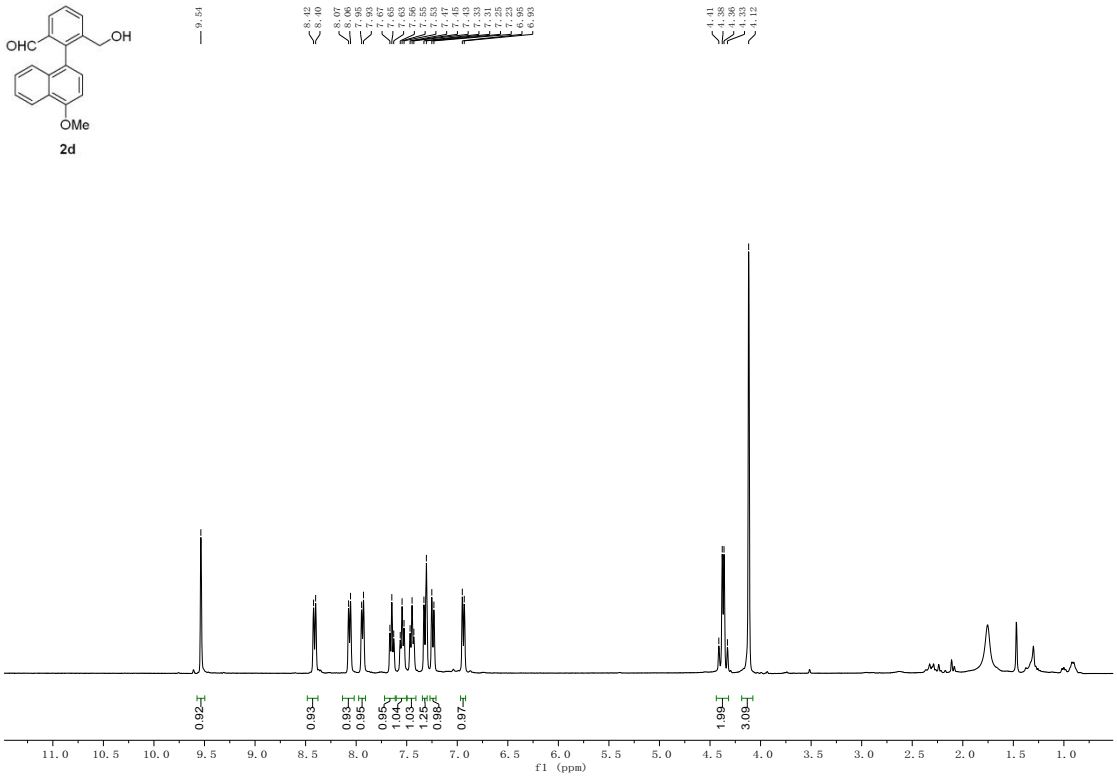

Figure S88. ^{1}H NMR spectra of **2d** in $CDCl_3$.

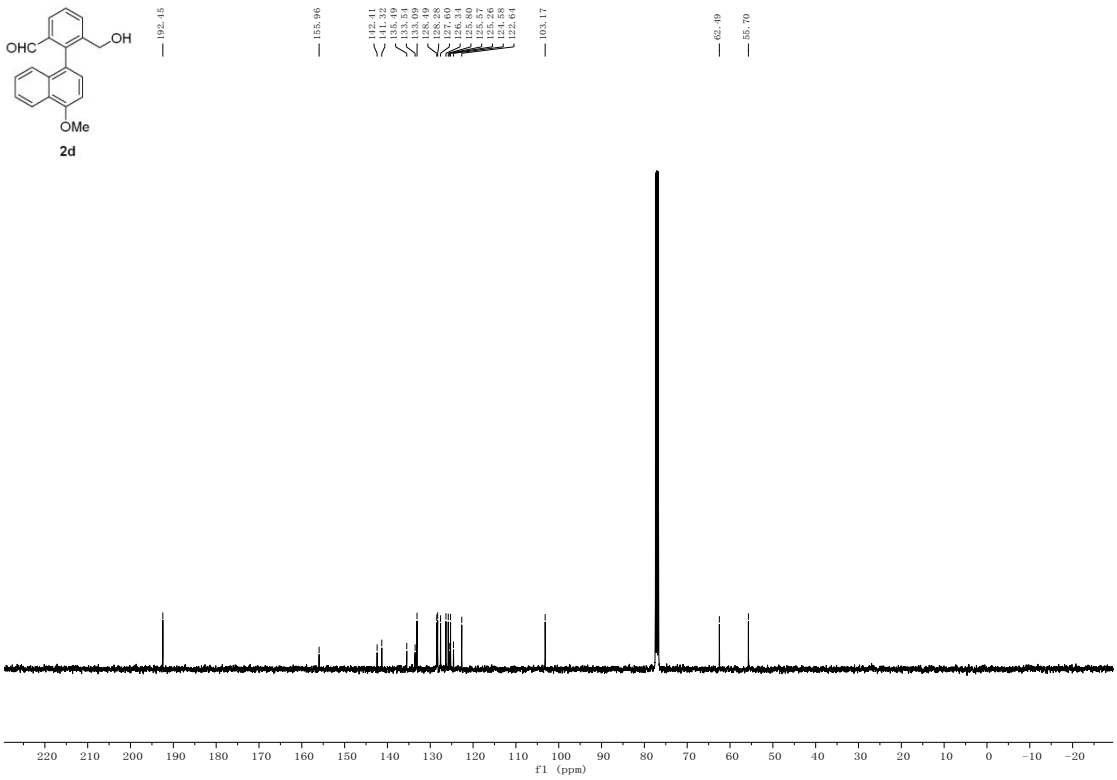

Figure S89. ^{13}C NMR spectra of **2d** in $CDCl_3$.

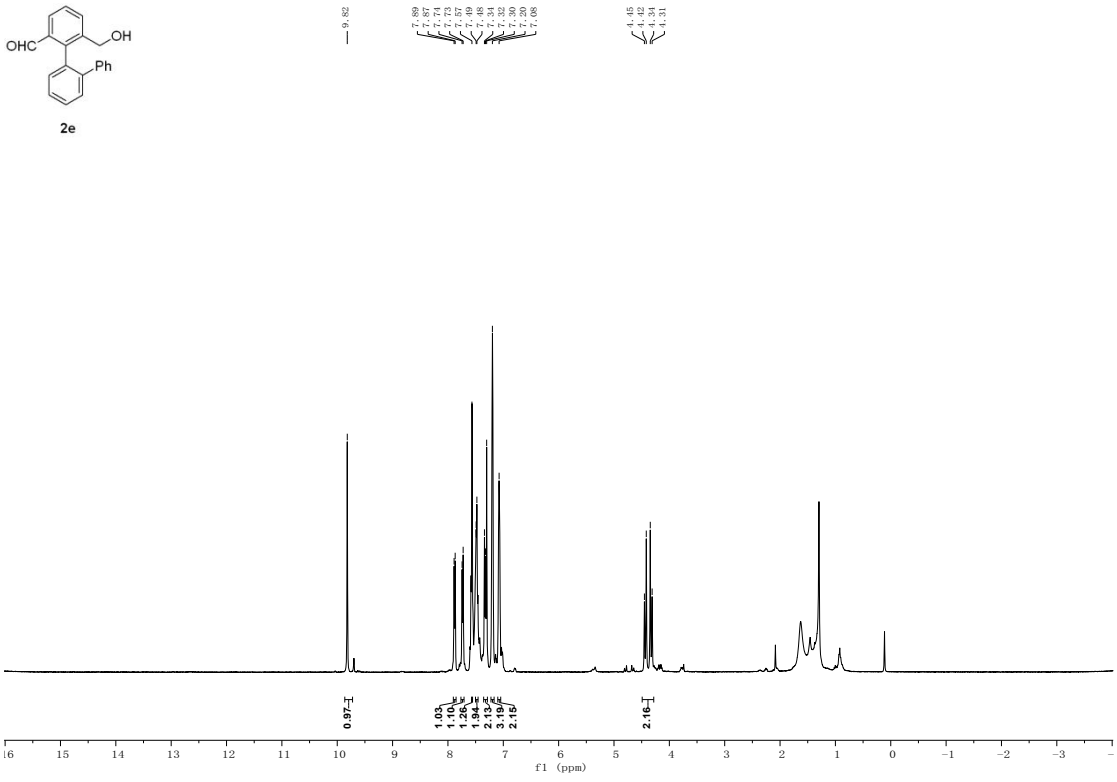

Figure S90. ^{1}H NMR spectra of **2e** in $CDCl_3$.

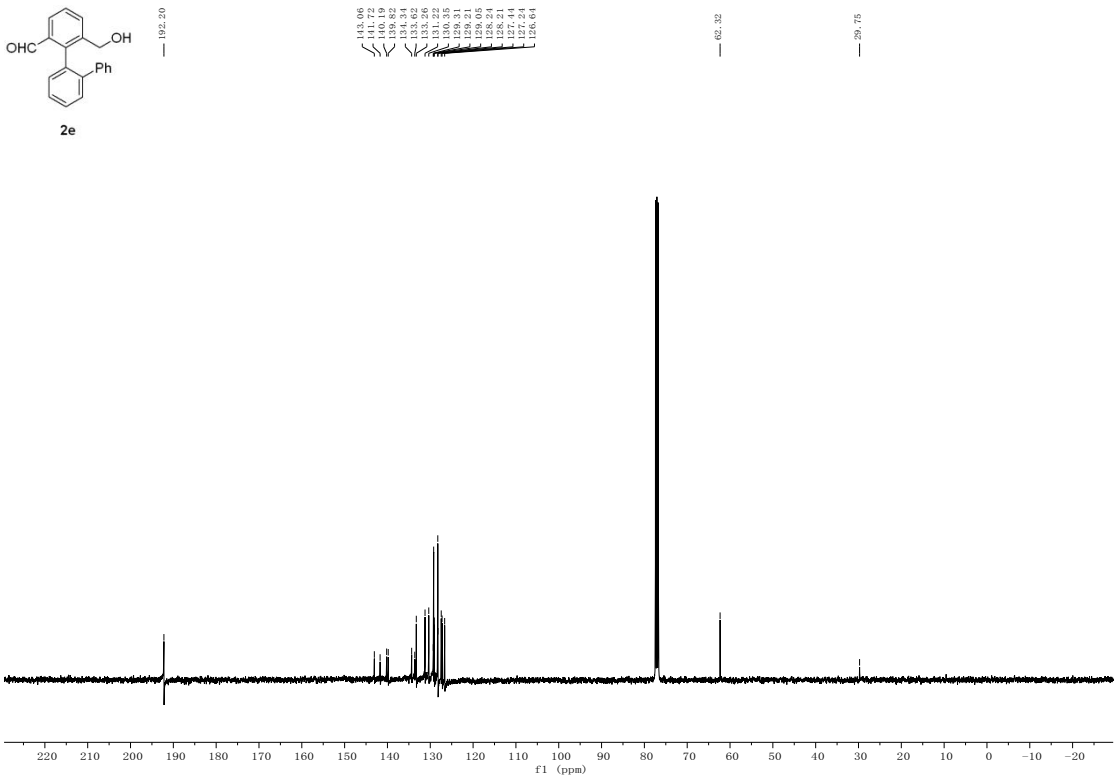

Figure S91. ^{13}C NMR spectra of **2e** in $CDCl_3$.

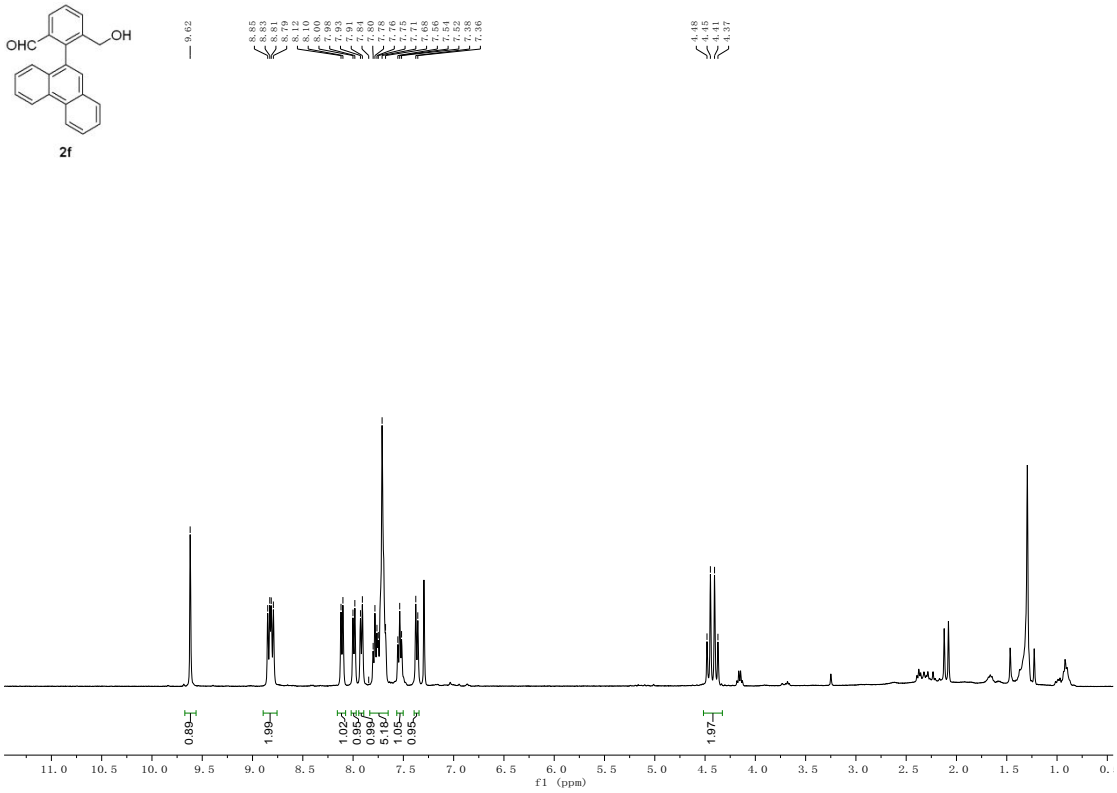

Figure S92. ^{1}H NMR spectra of **2f** in $CDCl_3$.

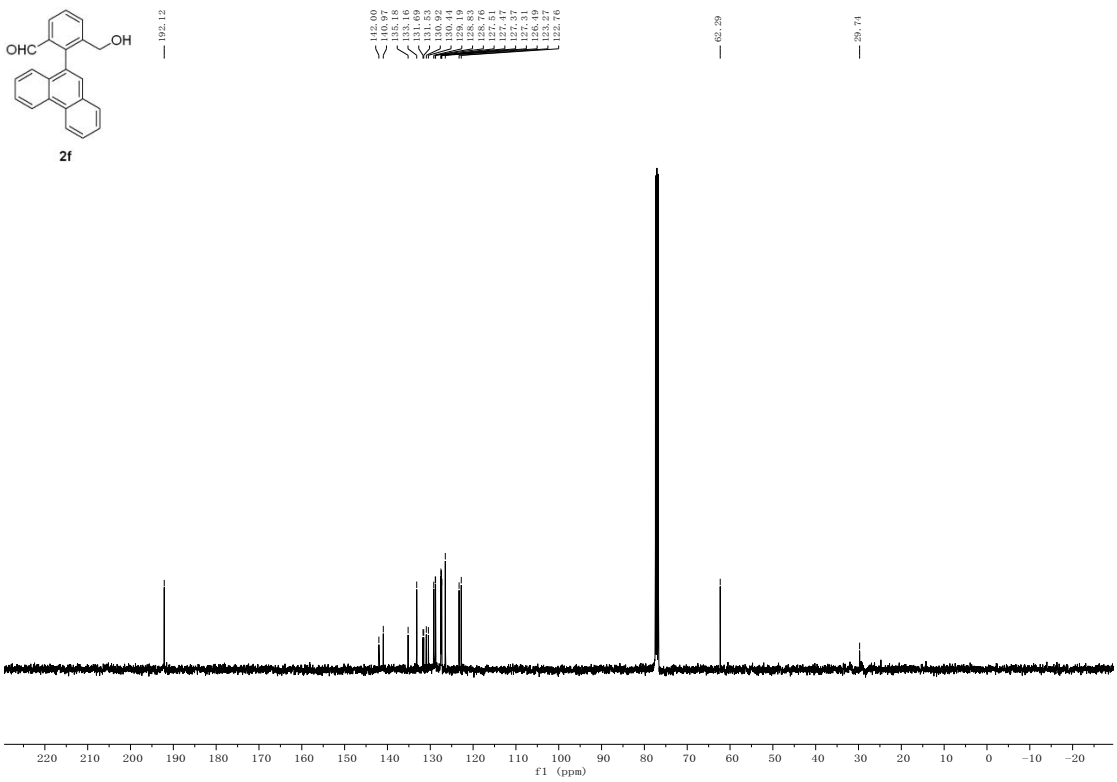

Figure S93. ^{13}C NMR spectra of **2f** in $CDCl_3$.

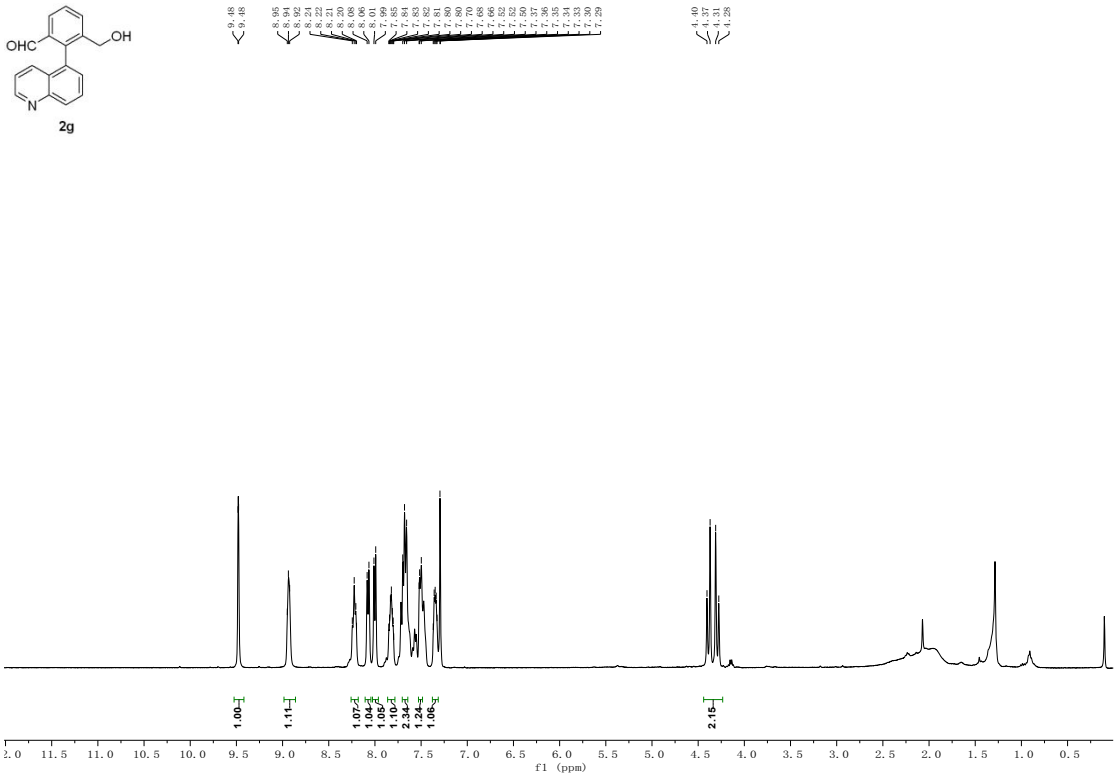

Figure S94. ^{1}H NMR spectra of **2g** in $CDCl_3$.

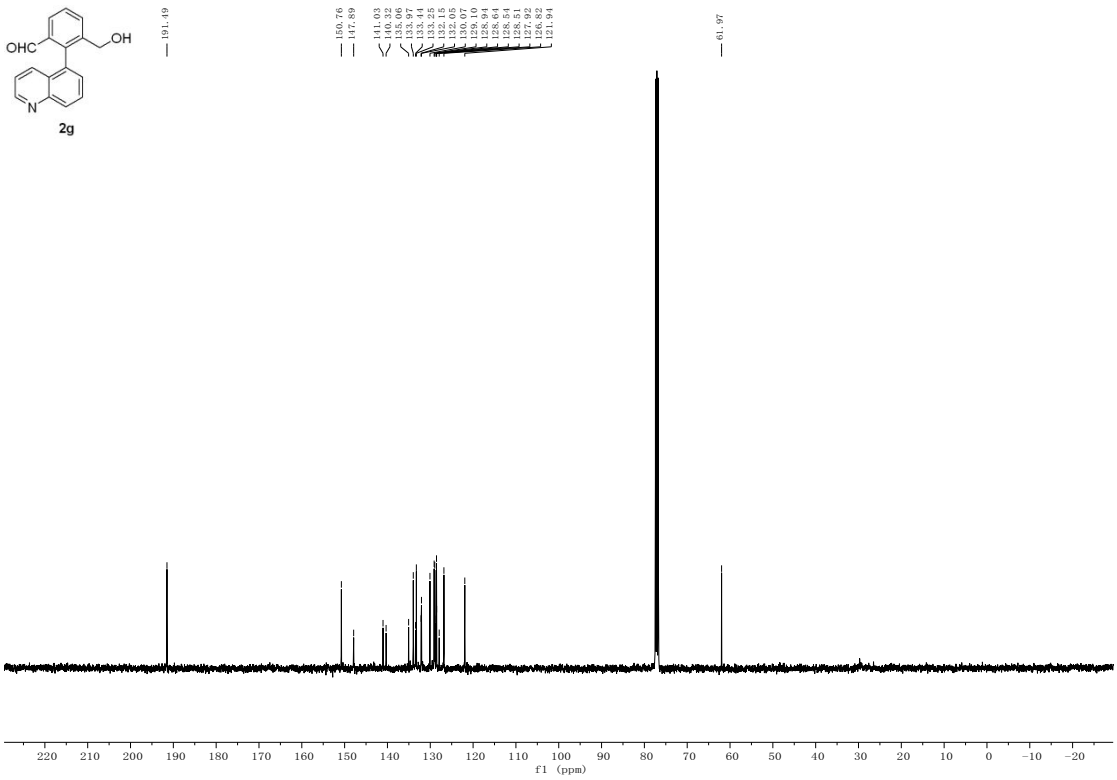

Figure S95. ^{13}C NMR spectra of **2g** in $CDCl_3$.

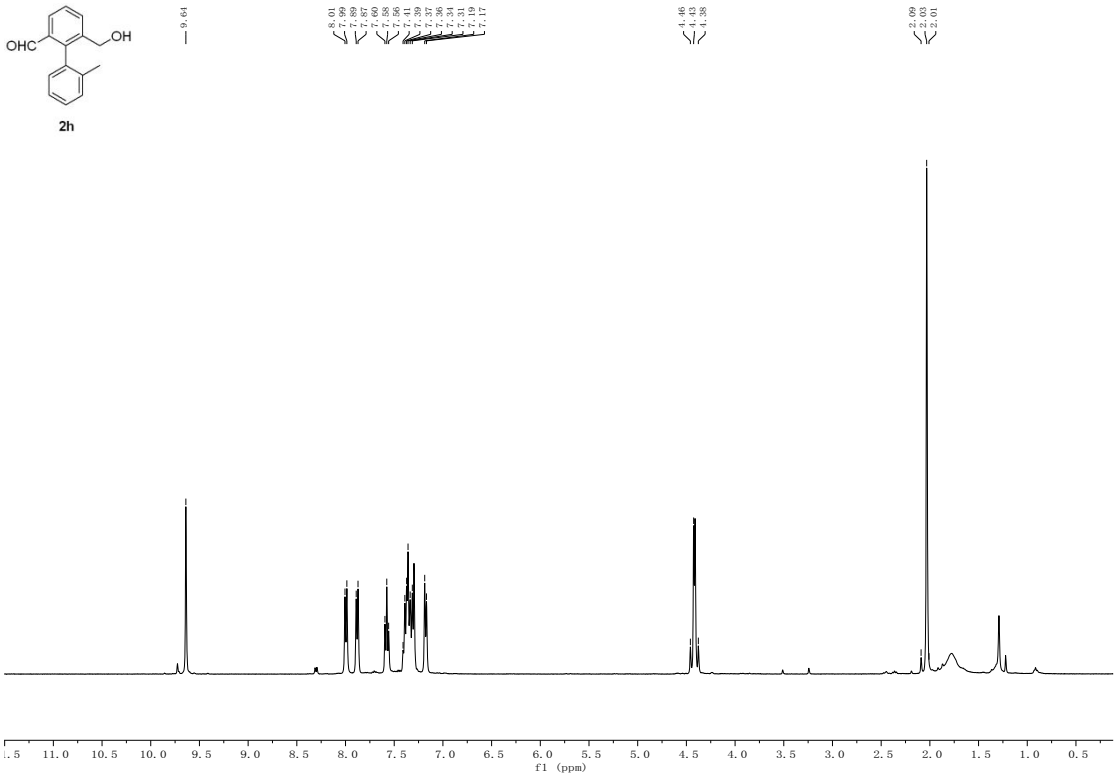

Figure S96. ^{1}H NMR spectra of **2h** in $CDCl_3$.

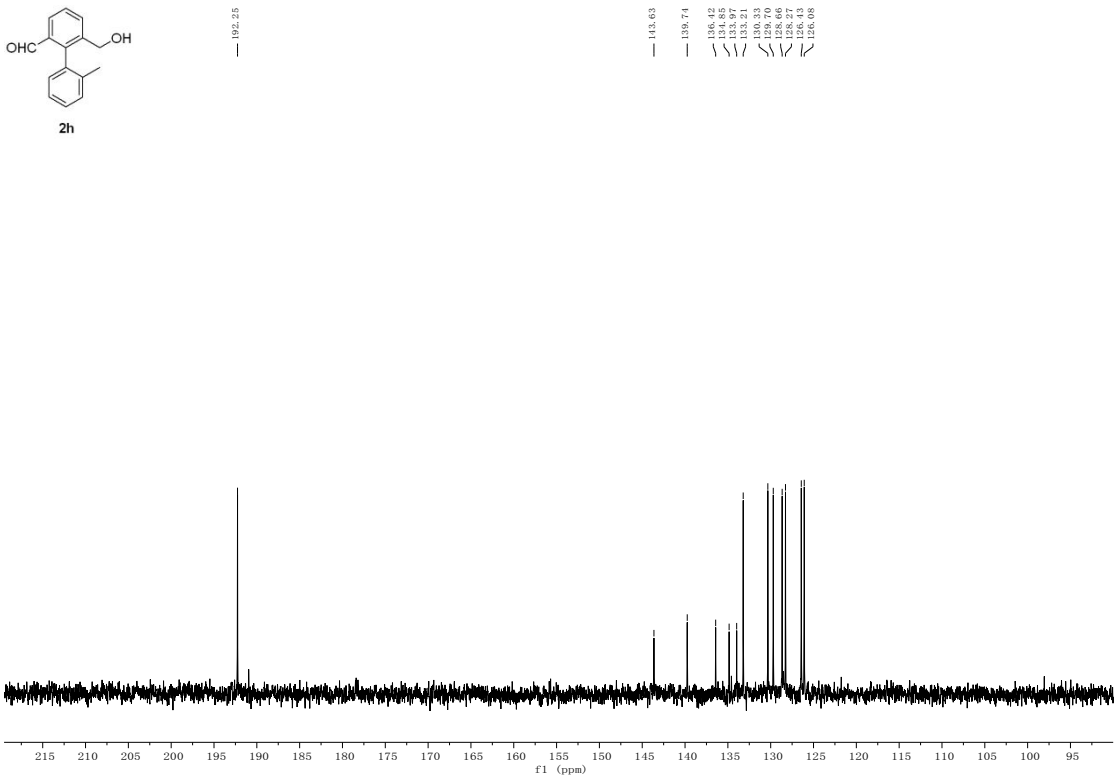

Figure S97. ^{13}C NMR spectra of **2h** in $CDCl_3$.

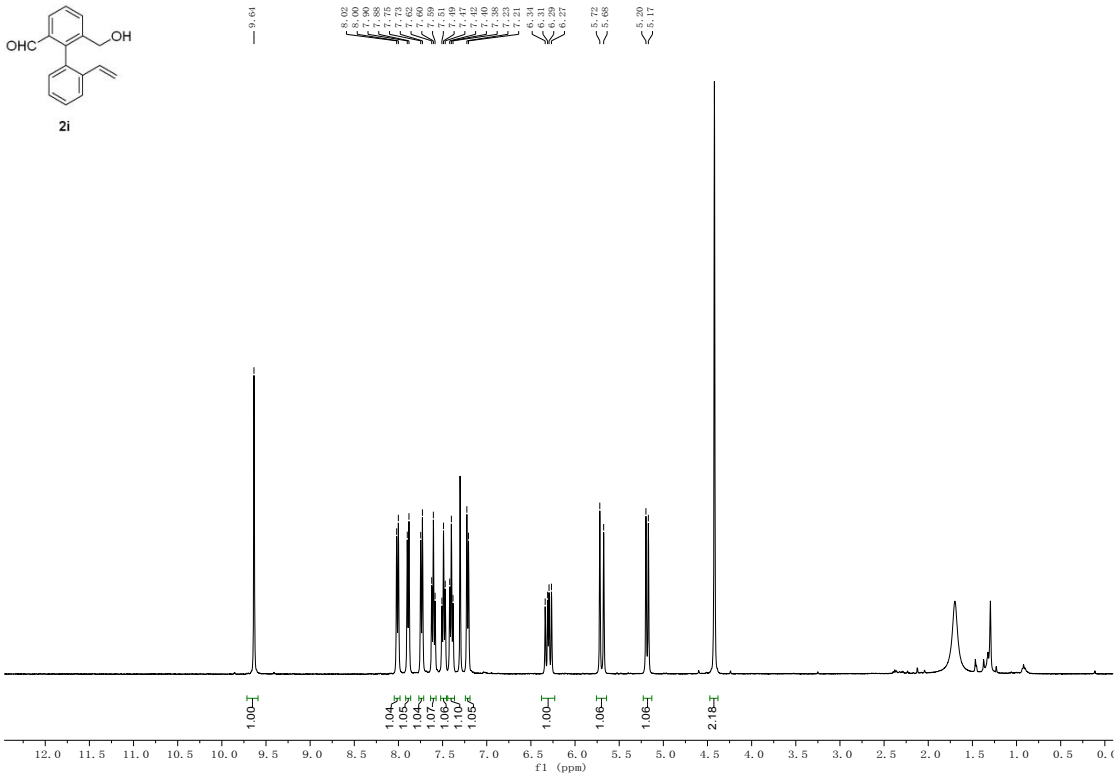

Figure S98. ^{1}H NMR spectra of **2i** in $CDCl_3$.

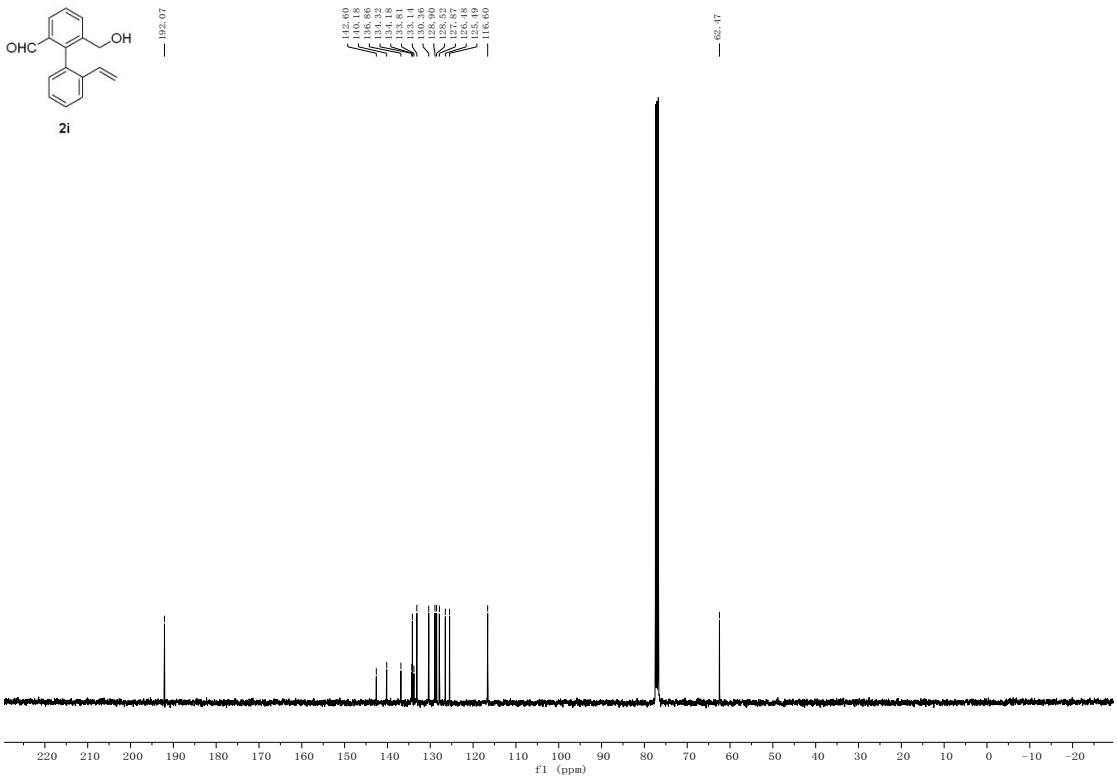

Figure S99. ^{13}C NMR spectra of **2i** in $CDCl_3$.

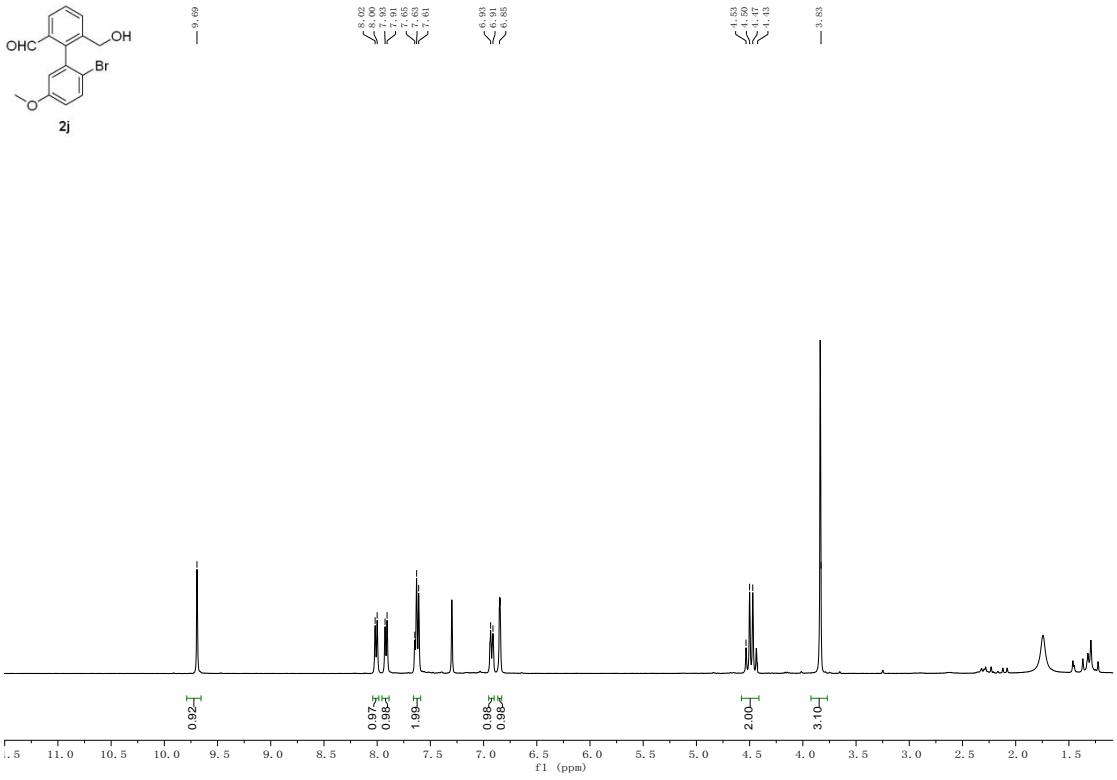

Figure S100. ^{1}H NMR spectra of **2j** in $CDCl_3$.

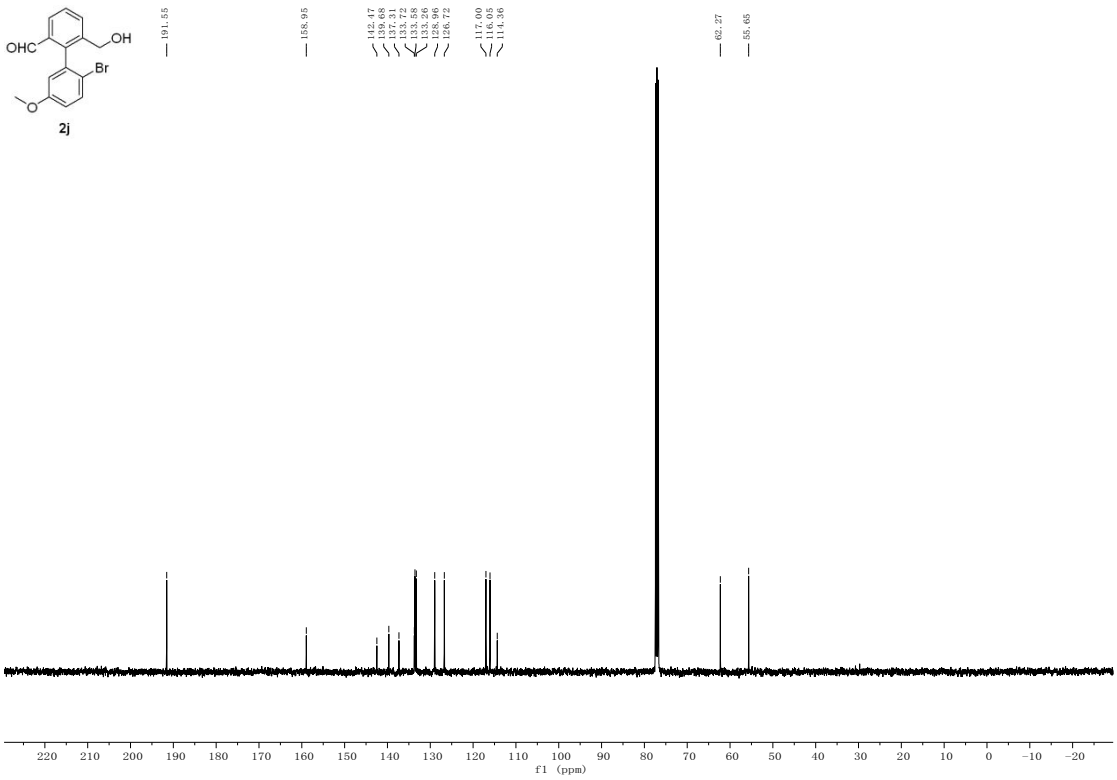

Figure S101. ^{13}C NMR spectra of **2j** in $CDCl_3$.

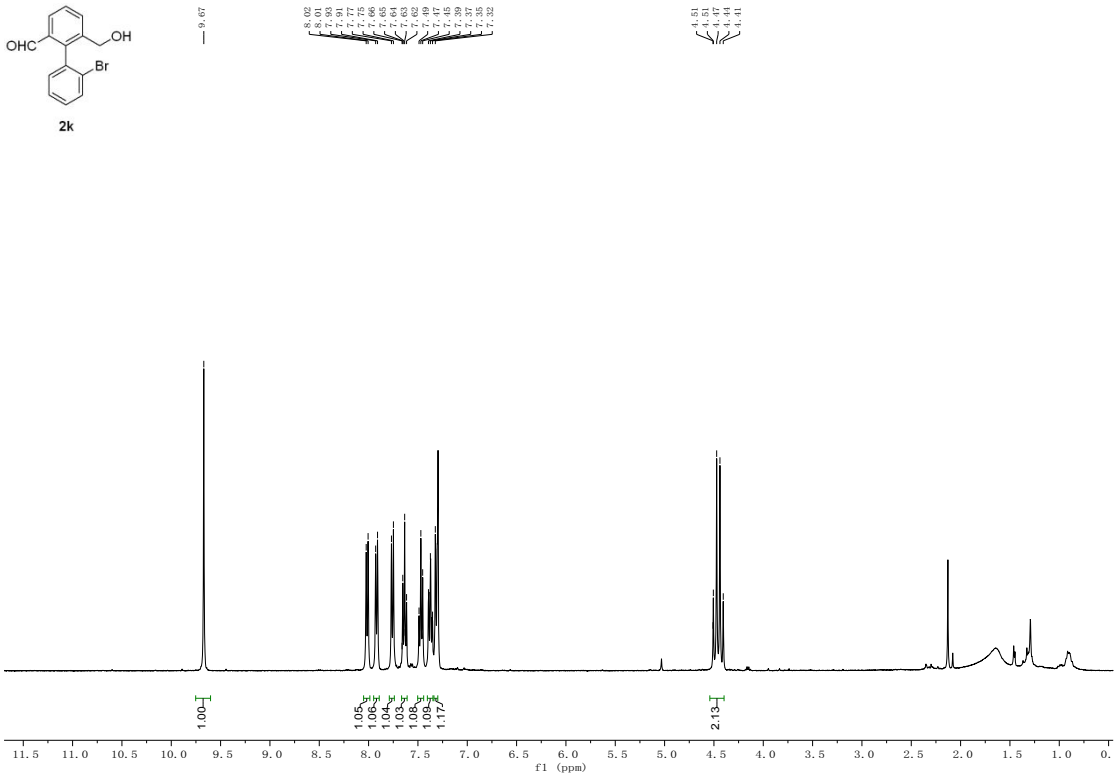

Figure S102. ^{1}H NMR spectra of **2k** in $CDCl_3$.

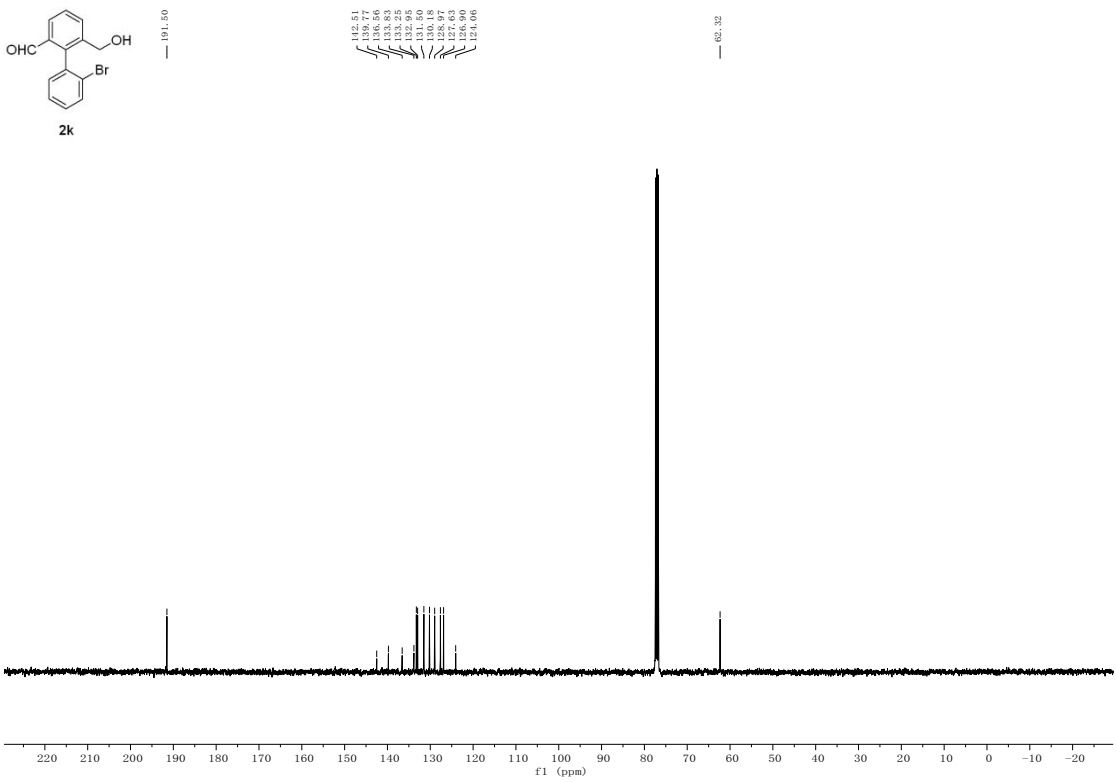

Figure S103. ^{13}C NMR spectra of **2k** in $CDCl_3$.

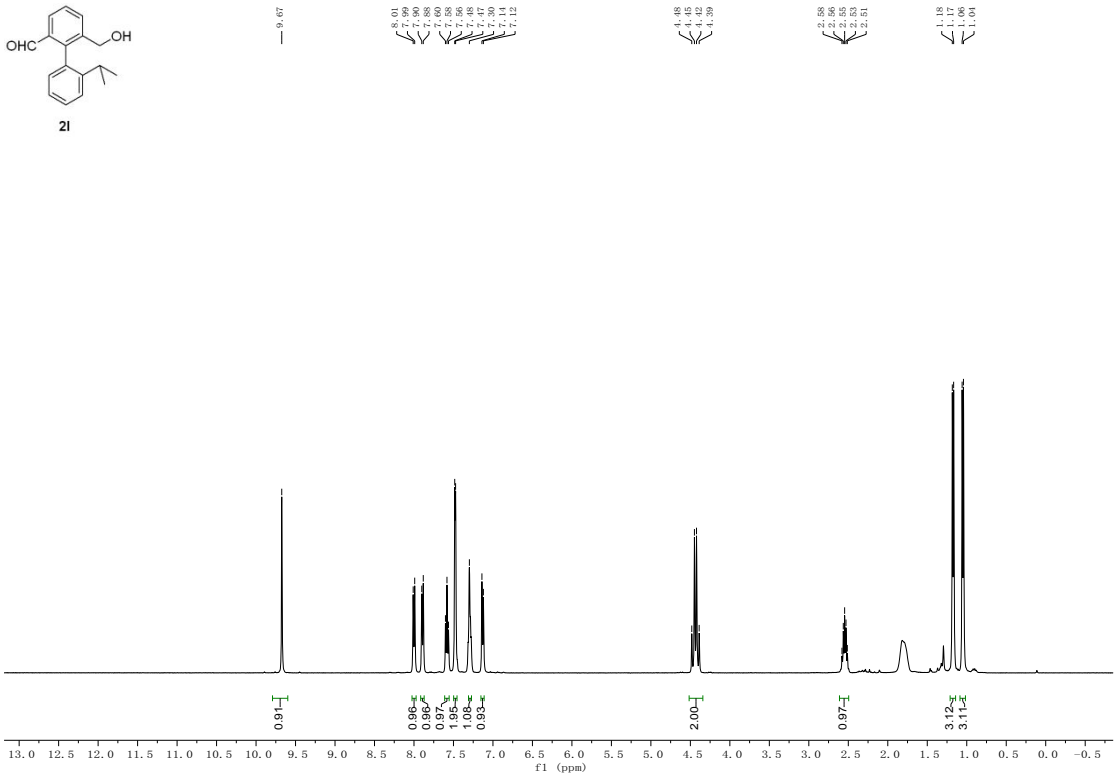

Figure S104. ^{1}H NMR spectra of **2l** in $CDCl_3$.

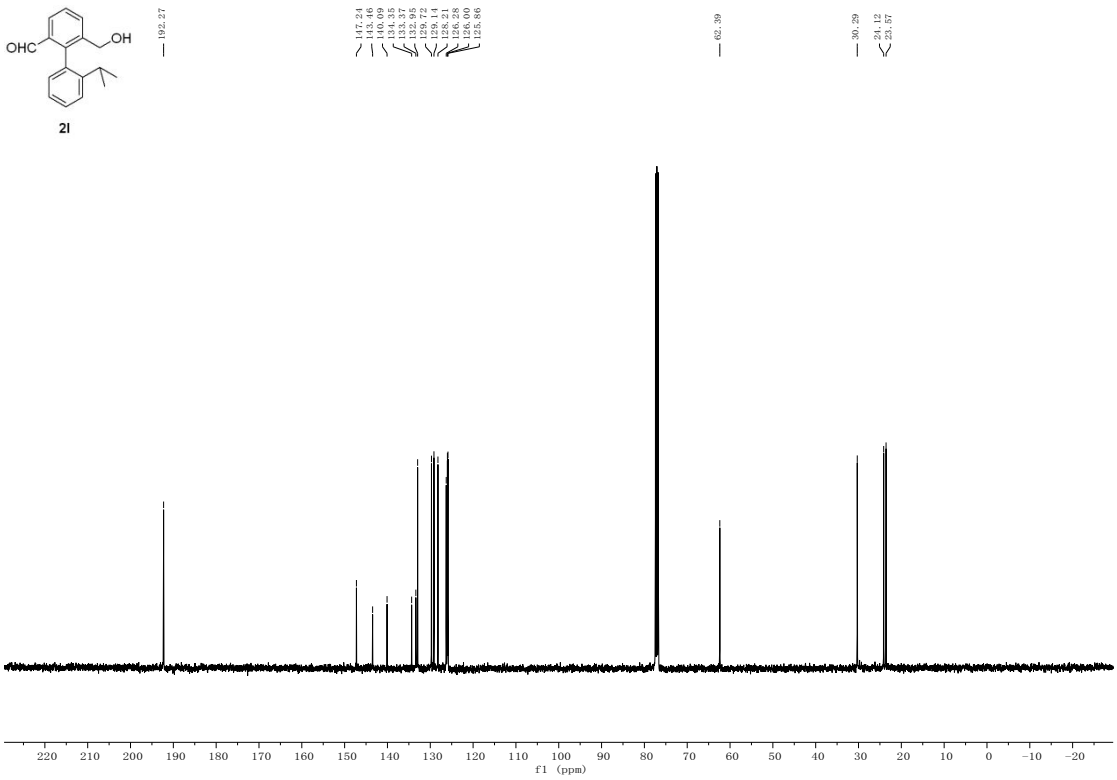

Figure S105. ^{13}C NMR spectra of **2l** in $CDCl_3$.

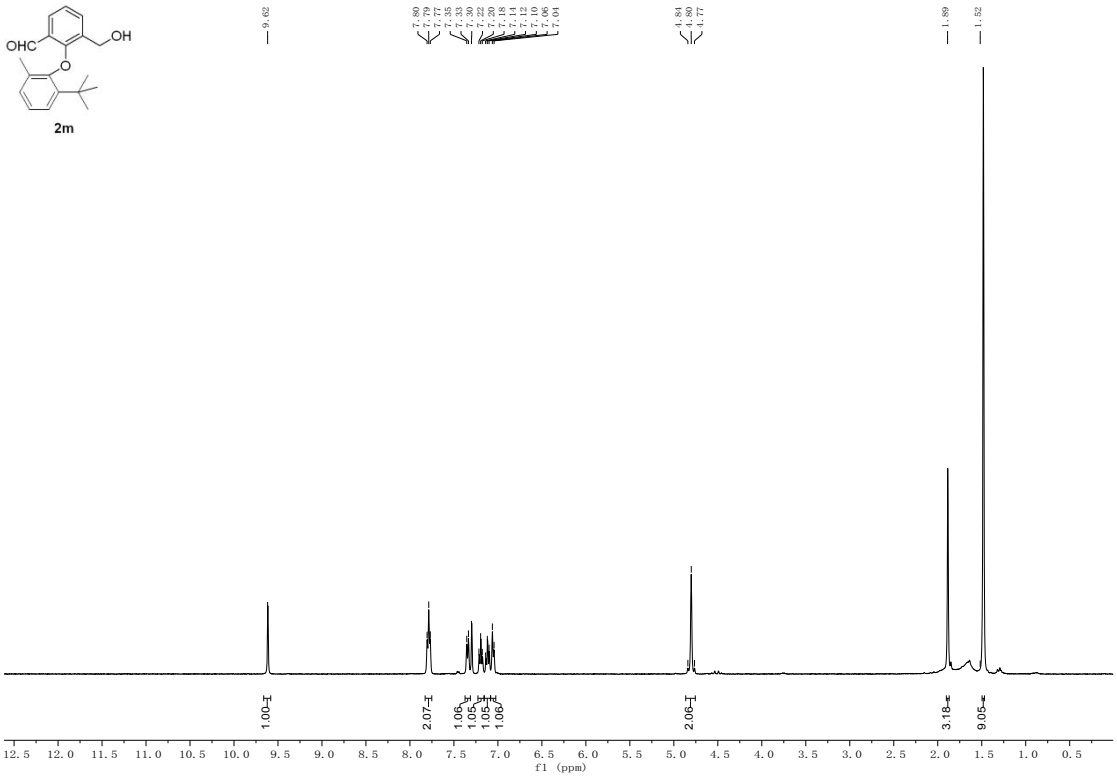

Figure S106. ^{1}H NMR spectra of **2m** in $CDCl_3$.

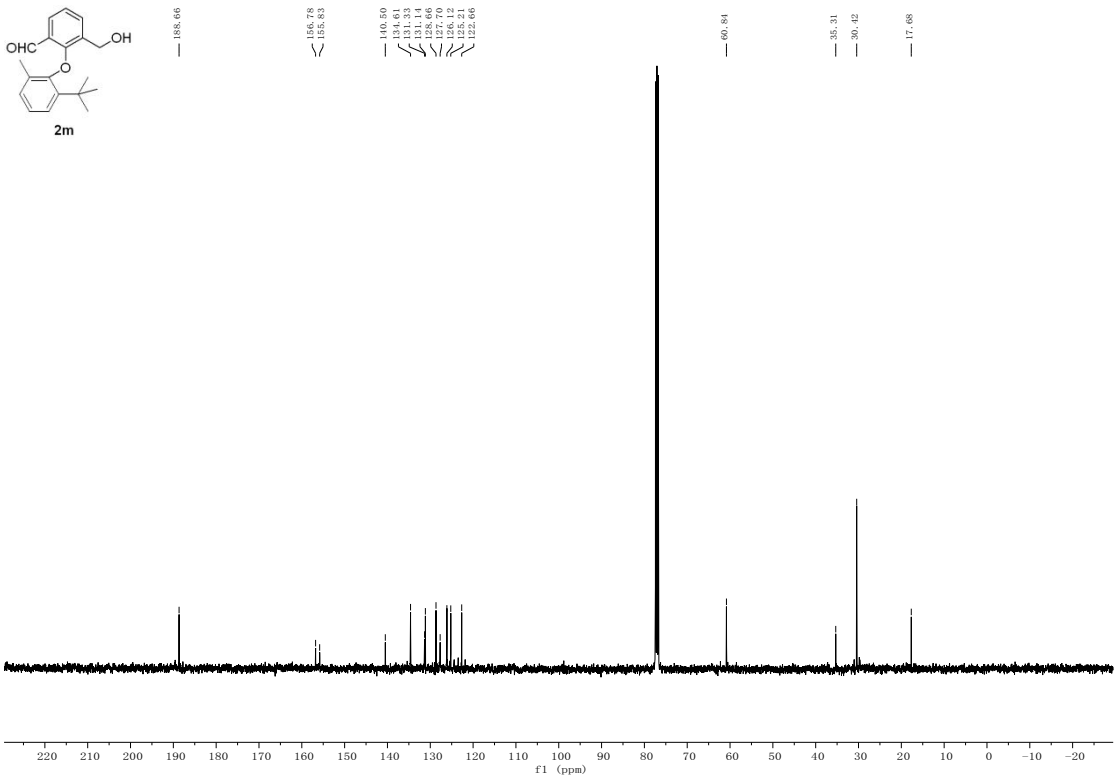

Figure S107. ^{13}C NMR spectra of **2m** in $CDCl_3$.

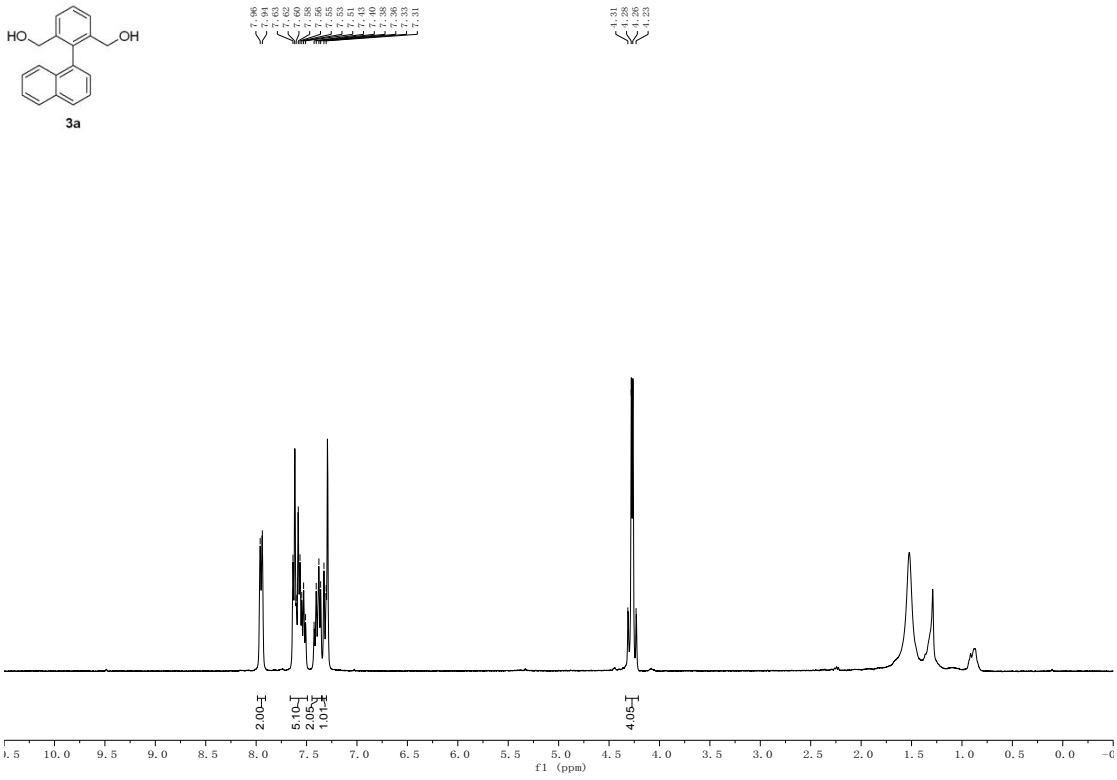

Figure S108. ^{1}H NMR spectra of **3a** in $CDCl_3$.

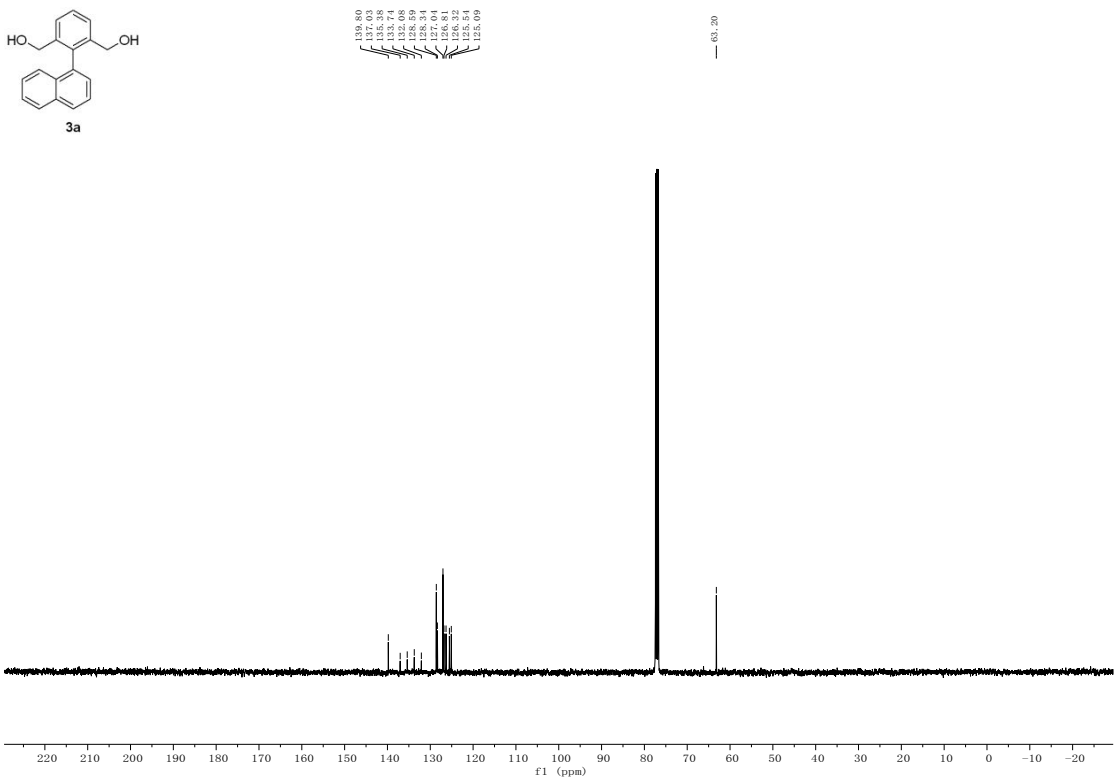

Figure S109. ^{13}C NMR spectra of **3a** in $CDCl_3$.

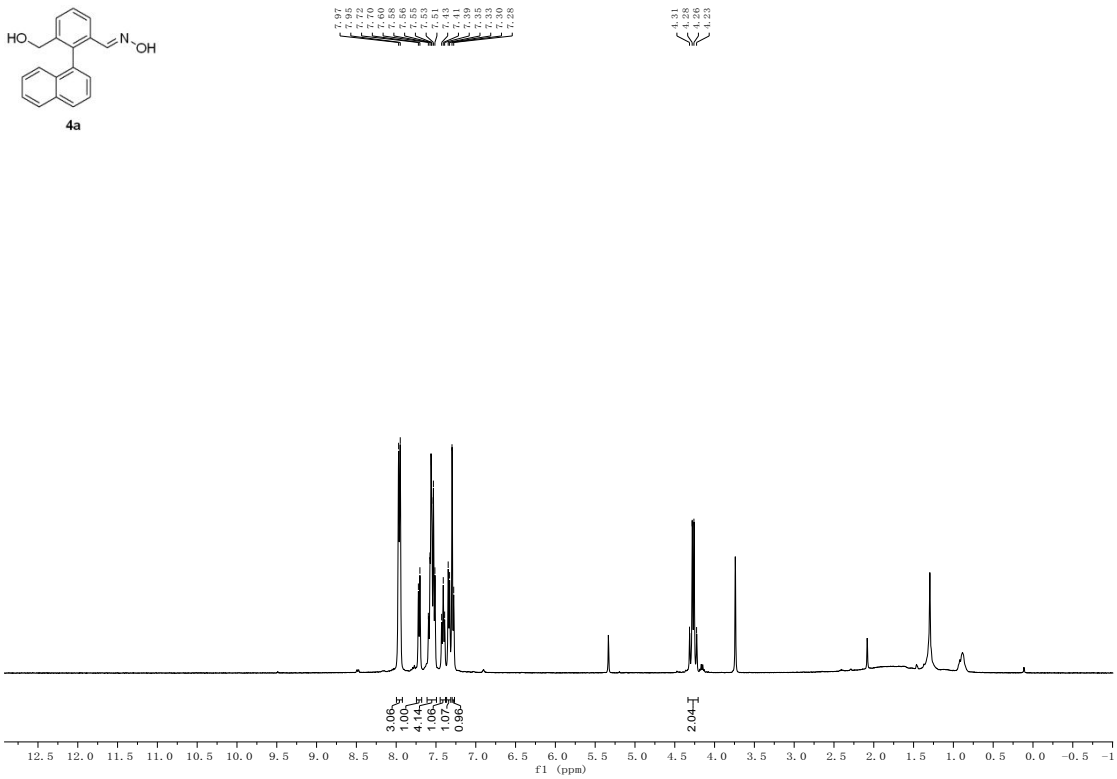

Figure S110. ^{1}H NMR spectra of oxime in $CDCl_3$.

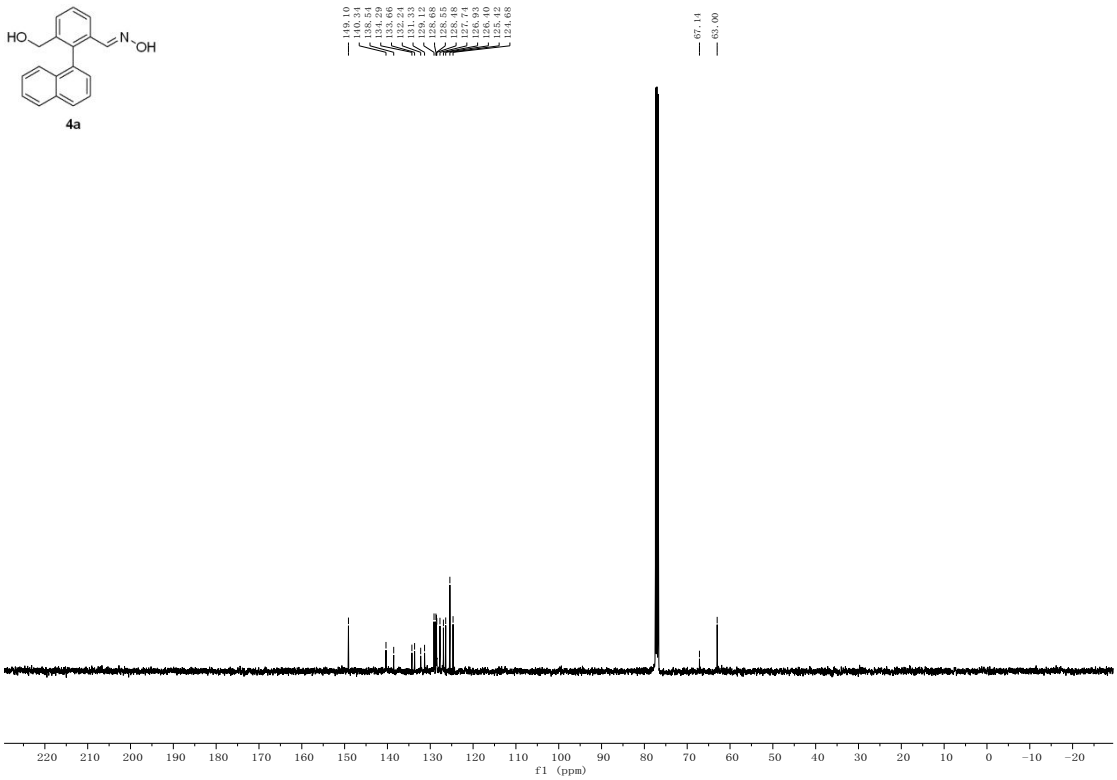

Figure S111. ^{13}C NMR spectra of oxime in $CDCl_3$.

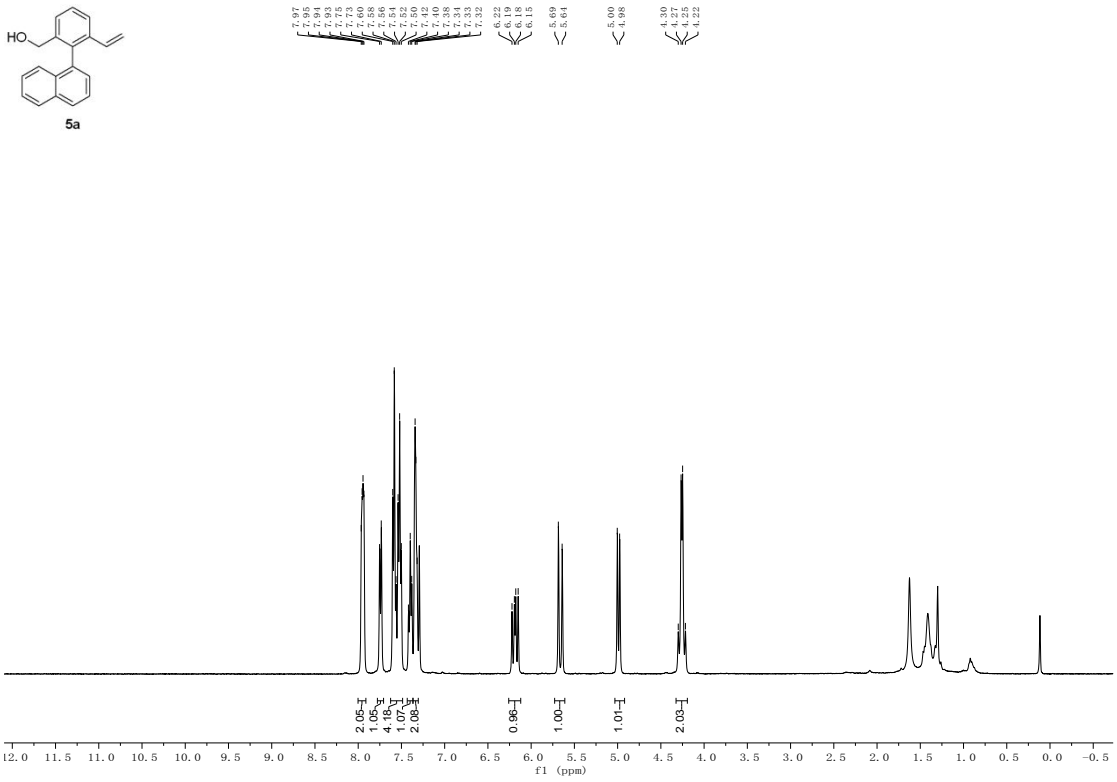

Figure S112. ^{1}H NMR spectra of wittig product in $CDCl_3$.

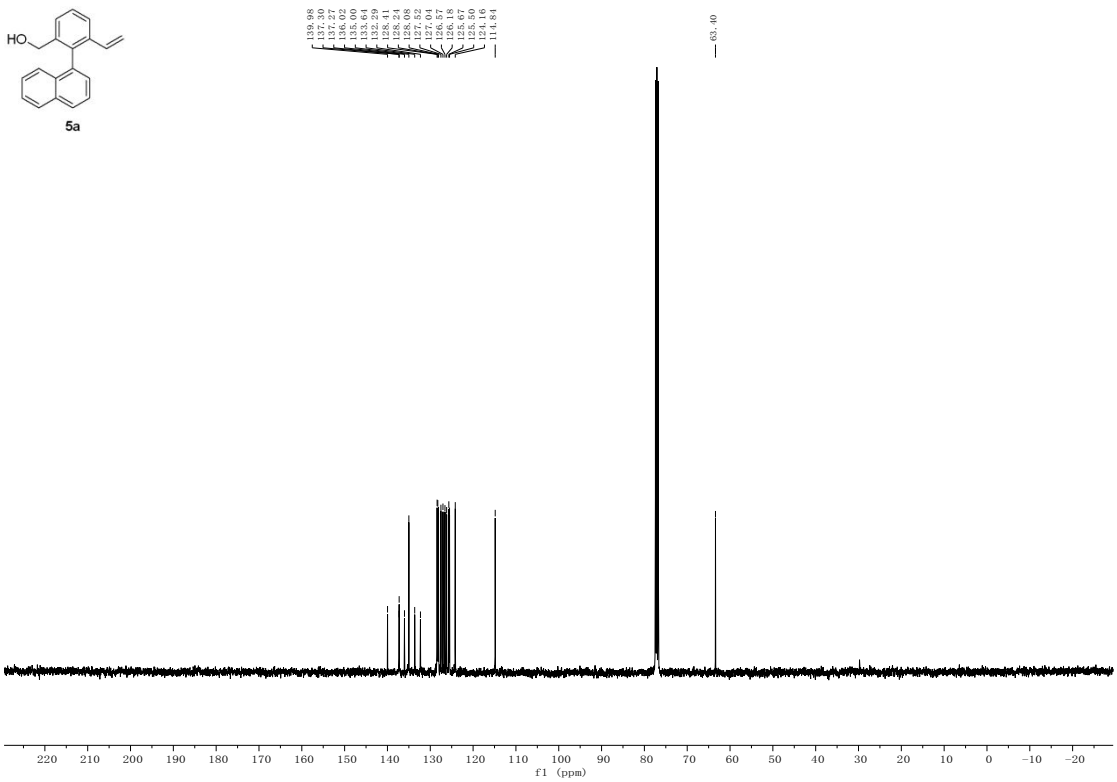

Figure S113. ^{13}C NMR spectra of wittig product in $CDCl_3$.

11. References

(1) Su, B.; Y. Wang; C. Sun. Response adaptive mechanisms of three mangrove (Avicennia marina, Aegiceras corniculatum, and Bruguiera gymnorrhiza) plants to waterlogging stress revealed by transcriptome analysis. *Front. Mar. Sci.* **2022**, *9*.

(2) Lavandera, I.; Kern, A.; Resch,V.; Ferreira-Silva, B.; Glieder, A.; Fabian, W. M.; de Wildeman, S.; Kroutil, W. One-way biohydrogen transfer for oxidation of sec-alcohols. *Org. Lett.* **2008**, 10, 2155-2158.

(3) Weckbecker, A.; Hummel, W. Cloning, expression, and characterization of an (R)-specific alcohol dehydrogenase from Lactobacillus kefir. *Biocatal. Biotransform.* **2009**, *24* (5), 380-389.

(4) Badotti, F.; Moreira, A. P.; Tonon, L. A.; de Lucena, B. T.; Gomes Fde, C.; Kruger, R.; Thompson, C. C.; de Morais, M. A., Jr.; Rosa, C. A.; Thompson, F. L. Oenococcus alcoholitolerans sp. nov., a lactic acid bacteria isolated from cachaca and ethanol fermentation processes. *Antonie Van Leeuwenhoek*. **2014**, *106* (6), 1259-67.

(5). Keshav, K. F.; Yomano, L. P.; An, H.; Ingram, L. O. Cloning of the Zymomonas mobilis structural gene encoding alcohol dehydrogenase I (adhA): sequence comparison and expression in Escherichia coli. *J. Bacteriol.* **1990**, 172, 2491-2497.

(6) Kim, M.; Jang, B.; Ahn, Y. J. Enhanced production of recombinant alcohol dehydrogenase using the genetically engineered escherichia coli Strain that heterologously expresses carrot heat shock protein 70. *Curr. Microbiol.* **2019**, *76* (11), 1338-1344.

(7) Pace, V.; Cabrera, Á. C.; Ferrario, V.; Sinisterra, J. V.; Ebert, C.; Gardossi, L.; Braiuca, P.;

Alcántara, A. R. Structural bases for understanding the stereoselectivity in ketone reductions with ADH from *Thermus thermophilus*: a quantitative model. *J. Mol. Catal. B-Enzym.*, **2011**, *70* (1-2), 23-31.

(8) Kuvaeva, T. M.; Katashkina, J. I.; Kivero, A. D.; Smirnov, S. V. Novel NADPH-dependent L-aspartate dehydrogenases from the mesophilic nitrogen-fixing bacteria Rhodopseudomonas palustris and Bradyrhizobium japonicum. *Appl. Biochem. Microbiol.* **2013**, *49* (2), 136-143.

(9) González, V.; Santamaría, R.I.; Bustos, P.; Hernández-González, I.; Medrano-Soto, A.; Moreno-Hagelsieb, G.; Janga, S.C.; Ramírez, M.A.; Jiménez-Jacinto, V.; Collado-Vides, J.; et al. The partitioned *Rhizobium etli* genome: genetic and metabolic redundancy in seven interacting replicons. *Proc. Natl. Acad. Sci. U. S. A.* **2005**, 103 (10) 3834-3839.

(10) Groen, B.; Frank, J.; Jzn. and Duine, J. A. Quinoprotein alcohol dehydrogenase from ethanol-grown Pseudomonasaeruginosa. *Biochem. J.* **1984**, 223 (3): 921-924.

(11) Schrödinger, L.; DeLano, W. 2020. PyMOL, Available at: http://www.pymol.org/pymol.

(12) Accelrys Software Inc., Discovery Studio Visualizer v21.1.0. Available online: https://discover.3ds.com/discovery-studiovisualizer-download. Accessed November 20, 2020.

(13) Staniland, S.; Yuan, B.; Gimenez-Agullo, N.; Marcelli, T.; Willies, S. C.; Grainger, D. M.; Turner, N. J.; Clayden, J. Enzymatic desymmetrising redox reactions for the asymmetric synthesis of biaryl atropisomers. *Chem.-Eur. J.***2014,** *20* (41), 13084-8.

(14) Wu, Y.; M. Li; J. Sun; G. Zheng, and Q. Zhang. Synthesis of axially chiral aldehydes by N-Heterocyclic-Carbene-Catalyzed desymmetrization followed by kinetic resolution. *Angew. Chem., Int. Ed.* **2022**, 61, e202117340.